UNIVERSITY OF OKLAHOMA

GRADUATE COLLEGE

TOP-DOWN THERMAL PROTEOME PROFILING USING MASS SPECTROMTERY ON HUMAN PLASMA PROTEINS

A THESIS

SUBMITTED TO THE GRADUATE FACULTY

in partial fulfillment of the requirements for the

Degree of

MASTER OF SCIENCE

By

JI KANG
Norman, Oklahoma
2022

TOP-DOWN THERMAL PROTEOME PROFILING USING MASS SPECTROMTERY ON HUMAN PLASMA PROTEINS

A THESIS APPROVED FOR THE
DEPARTMENT OF CHEMISTRY AND BIOCHEMISTRY

BY

Dr. Si Wu, Chair

Dr. Zhibo Yang

Dr. Shanteri Singh

Acknowledgements

Firstly, I would like to appreciate all the support and guidance from my principal investigator, Dr. Si Wu. She is the first person who led me to have interest in research and grow up as a scientist. She gave me the opportunity to be involved in our lab, and being a part of the lab was the best experience I have had in my life. Dr. Wu is one of the people who I admire for so many aspects including her passion for research, kindness to people, positive mindset, and considerate guidance to students. Being with her always inspires and motivates me to be a better person. I will never forget everything that she offered me and will try my best to spread the love that I have gotten from her.

I deeply appreciate all my lab member's support: Kellye, Yanting, Mulin, Zhitao, Jiaxue, Trishika, Anju, Samin, Joel, Walter, and Oliver. Dr. Kellye A Cupp Sutton, my mentor, provided countless supports and affections throughout all my stay in OU. She led me whenever I feel lost not only during the research, but also when I make important life decisions. Yanting and Mulin, my dear friends, were always next to me both inside and outside of the lab, no matter I am happy or sad. All the time that we spent together are precious memories that I will treasure forever. Again, I would like to express my deep gratitude to all my lab members. Without everyone's support, I would never made it so far.

I also would like to thank my committee members. Dr. Singh was there for me whenever I need help. She gave me helpful advice not only regarding research, but also how I could become a decent person. Dr. Yang offered me a lot of support and considerations inside and outside of the classroom. His courses helped me a lot to grow my knowledge in the analytical chemistry field.

Finally, I would like to thank the University of Oklahoma and the department of Chemistry and Biochemistry for the opportunity to be in the program and conduct the research.

Table of Contents

List of Tables

List of Figures

Abstract

Proteins play vital roles in biological systems; hence, the characterization of protein function is crucial for better understanding of complex cellular systems. The study of biological function of proteins at the proteome level is called functional proteomics. One way to probe functionality of proteins is to measure stability via the measurement of protein unfolding as a result of chemical or thermal denaturation. My research is focused on developing and applying novel thermal proteome profiling (TPP) technologies to measure protein thermal stability by heating proteins using a temperature gradient.

Traditionally, TPP is conducted using a bottom-up approach in which proteins are enzymatically digested into peptides for mass spectrometry (MS) analysis. Here, a top-down TPP approach was applied to analyze the stability of intact proteoforms and observe the effect of protein modifications that might be obscured due to protein digestion. We applied this top-down TPP method to human plasma to observe the stability of functional proteoforms of low-abundance, clinically relevant proteins. However, it is challenging to elucidate such proteins in human plasma because high-abundant proteins often mask the detection of low-abundant proteins. We systematically evaluated and optimized a depletion protocol to efficiently remove high-abundant proteins in human plasma samples prior to proteomics analysis. Overall, my research illustrates the feasibility of studying functional proteomes in human plasma through a novel platform that integrates the depletion of high-abundant proteins and top-down TPP applications.

Chapter 1: Elucidation of Protein Functionality using Mass Spectrometry-based Stability Proteomics

1.1 Abstract

Functional proteomics aims to elucidate biological functions, mechanisms, and pathways of proteins and proteoforms at the molecular level to examine complex cellular systems and disease states. A series of stability proteomics methods have been developed to examine protein functionality by probing protein stability under different conditions. One of the most widely used stability proteomics methods has been thermal proteome profiling (TPP) which utilizes thermal denaturation to measure protein structural stability. TPP has been successfully applied to measure the thermal stability of thousands of proteins in complex biological samples such as cell lysate and recent application of TPP has allowed the study of proteome-wide thermal stability to characterize structural changes in proteins such as those caused by post-translational modification (PTM), mutations, and protein-protein interactions (thermal coaggregation). Here, we review the application of TPP methods to observe the effect of protein structure and protein structural changes on protein stability. This includes application of traditional TPP methods to observe proteome wide thermal stability of proteins and adaptation of these method such as Hotspot Thermal Profiling (HTP) and phospho-TPP to examine the effect of PTMs on protein stability and mutation-TPP (mTPP) to study the effect of protein mutation on thermal stability. We also discuss some future perspectives TPP application such as utilization of top-down proteomics approaches to observe proteoform stability at the proteome level to help better understand the functions of protein modifications.

1.2 Introduction

Elucidating protein functionality is very important for understanding biological systems[1]. Proteomics is the study of gene expression and protein impact on cellular function on a large scale[2]. The study of protein structure, function, and interactions has typically been done using traditional biochemical methods including protein Nuclear Magnetic Resonance (NMR)[3], protein crystallography[4], cryogenic electron microscopy (cryo-EM)[5]. These traditional methods are robust, widely used, and high resolution; however, despite these advantages, they usually require a relatively large amount pure protein, so time consuming protein expression and purification are often required. Furthermore, sample preparation and data analysis are often complicated[6] and it can be challenging to express proteoforms with functional modifications such as posttranslational modifications (PTMs) that are relevant to protein function. These critical drawbacks have stimulated the search for further proteomics techniques. Hence, mass-spectrometry (MS)-based proteomics methods have been developed that provide high-throughput analysis of complex samples in native or native-like environtments[7].

Original MS-based proteomics techniques include protein footprinting methods (e.g., Hydrogen-Deuterium exchange coupled to mass spectrometry (HDX-MS)[8], Fast Photochemical Oxidation of Protein (FPOP)[9], and Hydroxyl Radical Foot printing (HRF)[10]). Protein footprinting methods generally chemically label specific amino acid residues (or, in the case of HDX-MS, the amide backbone) that are solvent accessible of a protein in its native state to probe the protein composition, structure, and binding.[11] Footprinting methods can acquire considerable resolution when combined with MS, but still remain low throughput as, generally, the protein or protein complex must be pure.[12]

Recently, a series of MS-based 'stability proteomics' methods have been introduced that analyze the thermodynamic stability of proteins under different experimental conditions to probe protein functionality. [13] These stability proteomics methods are high throughput and can be applied to analyze complex protein systems such as lysates and, in some cases, even intact cells and tissues. Analysis of proteins in the context of these native or native-like environments results in a 'bird's eye view' of protein functionality to observe the effect of experimental conditions more completely on cellular response. Stability proteomics fall general into two categories: proteolysis-based methods (e.g., Drug Affinity Responsive Target Stability (DARTS)[14] and Limited Proteolysis coupled with Mass Spectrometry (LiP-MS)[15]) and denaturation-based methods (e.g., Pulse Proteolysis (PP)[16], Semi Tryptic peptide Enrichment strategy for Proteolysis Procedures (STEPP)[17], Stability of Proteins from Rates of Oxidation (SPROX)[18], Thermal Proteome Profiling (TPP)[19], Chemical denaturation and Protein Precipitation (CPP))[20], and ion-based protein precipitation with Proteome-Integrated Solubility Alteration (i-PISA)[21]. Proteolysis-based methods utilize the resistance of a protein to proteolysis to probe protein stability, and denaturation-based methods probe the protein stability by studying tendency of a protein to denature when exposed to a denaturation (chemical or thermal) gradient[22].

This review will focus on TPP, which is unique among the stability proteomics methods as a thermal gradient is used for protein denaturation. When a protein is exposed a temperature gradient, it will denature and subsequently aggregate[19]. These aggregate proteins can be removed from the solution and the precipitate or the supernatant can be analyzed using quantitative bottom-up MS to determine the melting temperature of each protein[23]. The use of thermal denaturation allows TPP methods to be applied to native environments such as intact cells, tissues, and blood/serum in addition to cell lysates for a more accurate representation of protein functionality.

TPP is capable of studying the overall thermal stability of proteins or the change in thermal stability of a protein under various conditions such as interaction with ligand or protein or change in chemical environment[24].

TPP has been previously reviewed in conjunction with other label-free drug binding methods[25,26] and structural biology methods[22]; furthermore, TPP and related methods have been reviewed independently by Mateus et al.[27,24,19] In this review, will focus on the TPP as a tool to investigate the thermal stability of proteins without environmental perturbations such as addition of ligand; these methods include post-translational modification TPP (PTM-TPP or hotspot thermal profiling), mutant TPP (mTPP), and protein thermal co-aggregation (TPCA) **(Figure 1.1, Table 1.1)**

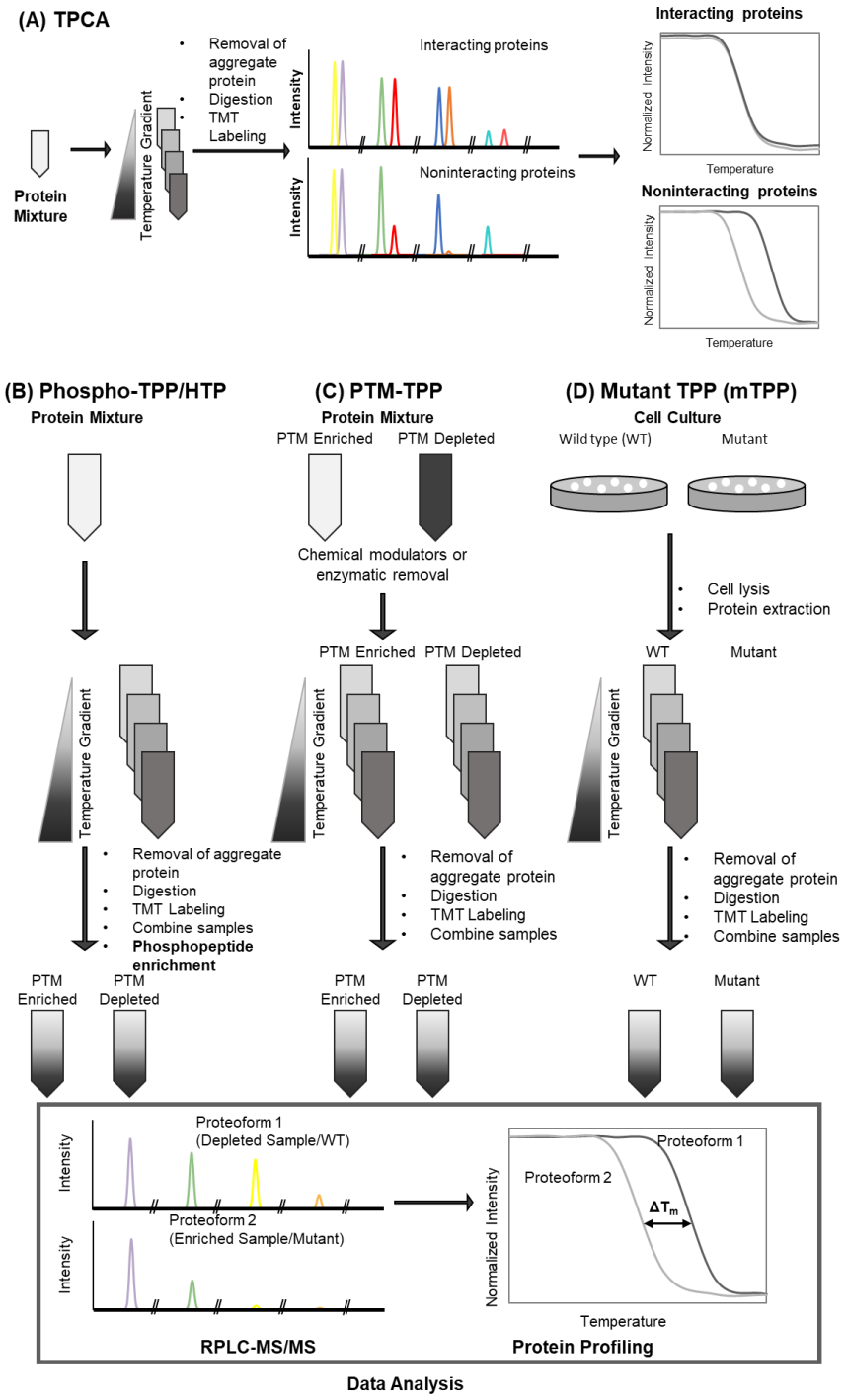

Figure 1.1 - Workflow for (A) thermal proximity coaggregation (TPCA); (B) phospho-TPP/hotspot thermal profiling (HTP); (C) post translational modification TPP (PTM-TPP); (D) mutant TPP (mTPP)

Table 1.1- Advantages and limitations of TPP techniques

Method	*Description*	*Advantages*	*Limitations*	*Application*
PTM-TPP (post-translational modification TPP)	TPP applied under the impact of post-translational modification	• Can identify post-translational modification site on a proteome-wide scale • Avoid requirement of the mapping specific PTM • Enable a greater depth of coverage	• Poor reproducibility may occur	Phosphorylation site identification, O-GlcNAcylation effect identification
m-TPP (mutant TPP)	Conjunction of TPP with temperature sensitive (TS) mutations	• Can examine the effect of mutations on proteins' thermal stability and associated PPI	• Process to make TS mutants may cause multiple mutations, making it difficult to know which mutations are causative of specific structural/stability and PPI changes	Elucidation of mutant protein thermostability and identification of associated PPI
Thermal co-aggregation	Interacting proteins tend to have the similar melting behavior signature	• Can be applied both cell lysate and intact cell, even can be extended to vivo specimen (e.g., tissue, blood) • Requires neither antibody nor epitope tagging	• Existing interaction data must be incorporated with graph/network clustering algorithms to identify novel protein complexes	Study the dynamics of known or predicted protein complexes across cellular states and physiological conditions

1.3 Probing Protein-Protein Interaction using Thermal Proximity Coaggregation (TPCA)

The human interactome commonly refers to the network of interacting proteins that are the basis for functional pathways within a cell.[28] As protein-protein interactions (PPIs) can be disturbed or influenced by changes in protein structure such as mutation[29] or PTMs[59], high throughput methods of monitoring PPIs are particularly important. Interacting proteins have been shown to have a tendency toward simultaneous denaturation and aggregation when exposed to a thermal gradient. Thermal proximity coaggregation (TPCA), introduced first by Tan et al.[32] examined this behavior to lead to discoveries regarding how proteins interact and what structural aspects of the proteins facilitate the interaction. Initially, TPCA was applied to K562 lysate and found 7,693 human proteins to demonstrate that interacting protein pairs generally have higher melting curve similarity compared to non-interacting proteins[32]. They benchmarked the TPCA method to observe protein complexes across growth phase and in multiple cell lines[32]. This impressive work demonstrated the utility of TPCA to observe PPIs in complex systems such as cell lysates and intact cells.

Further application of TPCA was demonstrated by Hashimoto et al. to study the effect of human cytomegalovirus (HCMV) infection on host-host, virus-host, and virus-virus PPIs[33]. They found that viral immediate-early proteins IE1 and IE2 which are known to interact with pUL84 to inhibit immune responses show similar aggregation profiles. They further revealed that virus-host interactions could also be observed by demonstrating that some melting curves, such as pUL38 the TSC1/2 complex, became more consistent later in the infection. Mateus et al.[34] performed TPP experiments on 121 *E. coli* mutants and found again that known functionally related proteins were co-regulated. Additionally, they used gene ontology on highly correlated proteins and found 140 proteins without annotated function could be linked with biological function. Justice et al. (2021)

utilized TPCA to elucidate PPI of DNA sensor IFI16 and DNA-dependent protein kinase (DNA-PK) under infection of herpes simplex virus 1[35].

1.4 Post-translational Modification Thermal Proteome Profiling (PTM-TPP)

PTMs are covalent modifications of proteins that can alter protein function and ultimately increase the functional diversity of the proteome[36]. Functionally relevant PTMs can affect protein function in a variety of ways. For example, as discussed above, PTMs can participate importantly in PPIs as they can modulate interactions via variation of structural or ionic properties.[31,37] Phosphorylation has been commonly referred to as a 'molecular switch' to activate or deactivate enzymes and signaling proteins and is also involved in production of ATP.[38] Glycosylation refers generally to many types of PTMs that are commonly found on cell surface and extracellular proteins and are implicated in human disease such as cancer and autoimmune disease.[39] As such, high-throughput examination of PTM functionality has been a focus for advancement of TPP methods; the methods that have been adapted to examine PTM functionality are review here and include phospho-TPP/hotspot thermal profiling (HTP) and post translational modification TPP (PTM-TPP) .

1.4.1 Phospho-Thermal Proteome Profiling (Phospho-TPP) or Hotspot Thermal Profiling (HTP)

A subsect of TPP techniques, phospho-TPP or HTP, have been develop and applied to examine the effects of endogenous phosphorylation on thermal stability and protein functionality[40]. Phosphorylation is of particular interest because it is an extremely common transient PTM that influences protein binding, stability, and dynamics[41,42]. Combination of phospho-proteomics and TPP has been first introduced by Azimi et al. in 2018 to determine the

effect of protein phosphorylation on thermal stability by comparing the thermal stability of the phosphoproteome of SK-Mel 24 and SK-Mel 28 human carcinoma cells. This study identified a series of proteins involved in the progression of the cell cycle that may be targeted to counteract the drug resistance of the SK-Mel 28 cell line[43]. Phospho-TPP differs from traditional TPP by the addition of phosphopeptide enrichment after isotopic labeling. Phosphopeptide enrichment allows this method to be applied to determine the effect of phosphorylation on thermal stability and study the effect of phosphorylation on protein function[40].

As a further application of phospho-TPP, Huang et al. examined the stability of the proteome and phosphoproteome of HEK293T and identified 2,883 proteins that were expressed endogenously with and without phosphorylation[40]. While Huang et al. did not report a significant difference in the T_m of the proteome and phosphoproteome, they did report significant changes in the melting behavior for 25% of phosphorylated sites[40]. However, it should be noted that re-analysis of Huang's data by Smith et al. revealed that 20% of co-enriched unmodified peptides had significant stability effects which suggests that independent labeling and mass spectrometry analysis may have caused substantial error for the unmodified proteome and the phosphoproteome[44].

More recently, Potel et al. optimized the phospho-TPP method and examined *HeLa* cell lysate to conclude that phosphorylation affected the proteoform stability to a lesser extent than previously reported[45]. Similarly, Lenz et al. (2022) showed that phosphorylation or dephosphorylation has no effect on the thermal stabilization of for MAPKAPK2 protein and concluded that only 1.5-3% of phosphosites significantly impact thermal protein stability[46]. Additionally, there has been a development in methodology that Stein et al. (2021, preprint) presented an improved HTP workflow which involves high-pH reverse phase fractionation prior

to phosphopeptide enrichment, label-fractionate-enrich (LFE)-HTP method[47]. LFE-HTP shows more precise proteoform coverage compared to the original HTP methodology. Live HEK293T cells were analyzed using this method and it led to the deeper phosphoproteome coverage that contains novel phosphorylation sites which significantly impact the thermal stability[47].

1.4.2 Investigation of Other Post-translational Modification using PTM-TPP

TPP methods have also been applied to observe the effect of PTMs other than phosphorylation. King et al. studied the effect of O-GlcNAcylation on melting behavior such as change in thermostability[48]. O-GlcNAcylation is a PTM that involves the attachment of O-linked N-acetylglucosamine(O-GlcNAc) moieties to Serine (Ser) and Threonine (Thr) residues of proteins[49].

As proteoforms with PTMs are often expressed at low abundance, two methods were used to observe the effect of O-GlcNAc on protein stability. Enzymatic removal TPP (erPTM-TPP) and chemical modulators TPP (cmPTM-TPP). erPTM-TPP utilized bacteroides thetaiotaomicron (BtGH84) glycoside hydrolase to enzymatically remove O-GlcNAc to generate O-GlcNAc-deficient and enriched samples[48]. Alternatively, as erPTM-TPP could not be applied *in vivo*, the authors also used cmPTM-TPP by introducing thiamet-G (TMG) and 2-acetamido-2-deoxy-5-thio-α-D-glucopyranose (5SG) to increase and decrease O-GlcNAc, respectively. 40 proteins which show O-GlcNAc dependent thermal stability changes were revealed; 10 proteins displayed stabilization and 30 displayed destabilization[48]. Even though O-GlcNAc has often been reported to stabilize proteins[50], the authors found that O-GlcNAc more often tended to destabilize proteins; destabilization was attributed to O-GlcNAc interference with protein-protein interactions.

Variation in stabilization effect of O-GlcNAc on proteins may also be influenced by the tendency of O-GlcNAc to compete with and modulate protein phosphorylation.[51]

1.5 Mutant Thermal Proteome Profiling (m-TPP)

When studying essential gene function, it is often useful to interrupt standard gene activity via genetic techniques in order to gain a better understanding of the fundamental mechanisms that drive organic processes.[52] One of these genetic methodologies is the use of conditional mutants — mutants which display either a wild-type or defective phenotype based on their environmental conditions.[52] Commonly used variants are temperature-sensitive (TS) mutants, as their protein function may be downregulated without requiring the alteration of the transcriptional context of a gene, the addition of specialized chemicals, or the changing of media.[52] To alter phenotypic effect, the incubation temperature at which the cells are grown is changed so that the protein retains function at a permissive temperature, loses function at a non-permissive temperature, or maintains partial function at a semi-permissive temperature.[1] The missense mutations caused by genetic methodologies modify protein structure, leading to alterations in protein stability as well as protein-protein interactions (PPIs).[52] Such changes in protein structure and protein-protein interactions could affect the thermal stability of either the particular protein or the PPI network as a whole.[52] In this context, the TPP method can be used in conjunction with TS mutations to examine the effect of mutations on proteins' thermal stability and associated PPI, leading to the development of mutant thermal proteome profiling (mTPP).

While large-scale MS-based PPI analysis can be used to study the effects of missense mutations, the requirement of a large amount of protein sample which necessitates purification of the protein of interest along with its interaction components limits the wider application of this

method.[52] An untargeted, proteome-wide MS method to measure how mutations in a protein can alter PPI networks has great value in identifying global effects of a genomic change.[52] mTPP uses TS mutations to study the effect of missense mutations on protein structure and the associated changed in PPIs.[52] m-TPP works as mutations affect both the thermal stability of the protein of interest as well as the PPI network due to structural changes in protein interfaces.[52]

Savitski et. al. (2014) first developed the TPP method and then adapted it to analyze and compare the thermal stability of wild-type *E. coli* with *tolC* knockout strain.[53] This mutation resulted in the change of abundance of 38 proteins (11 down-regulated, 27 up-regulated) , as well as the change in thermostability of 55 proteins (17 destabilized, 38 stabilized).[53] Additionally, they found that deletion of *tolC* causes the destabilization of multiple efflux pumps, inducing periplasmic stress and metabolic changes.[53]

Viéitez et. al. (2019, preprint) created 474 phospho-deficient yeast strains and screened their fitness in 102 different conditions in order to study the functional relevance of phosphorylation.[54] From the mutated strains, changes in thermal stability were able to be measured in 8 phospho-mutants, with one exhibiting an increase and one demonstrating a decrease that were not statistically significant.[54]

Justice et. al. (2020) extended TPP's application into studying the effects of missense mutations on the whole proteome, terming it mutant thermal proteome profiling (m-TPP). Using wild-type and as mutated strands of *Saccharomyces cerevisiae* as well as an isobaric affinity-purified protein complex trigger channel, it was determined that no major changes of T_m were observed.[55]

Banzhaf et. al. (2020) studied the effect of an NlPI mutant on lipoproteins, finding that the deletion of NlPI altered both protein abundance as well as thermal stability.[56] Double mutants on

NlPI and mepS behaved similar to the single mutants, slightly affecting the width of the cells, and therefore the thermal stability.[56]

Though m-TPP is helpful to understand protein stability and structure, the processes which produce TS mutants often lead to many mutations, which makes it difficult to determine which mutations cause which changes in protein structure, stability, and protein-protein interactions.[52]

1.6 Perspectives and Future Applications

Overall, the original TPP method has seen an astonishing number of modifications and developments to make the technique extremely versatile and applicable for a wide variety of purposes. The TPP related methods reviewed here including TPCA, phospho-TPP/HTP, PTM-TPP, and mTPP are unique in their goal to target protein structural changes and the effect on protein stability. Further adaptations of these techniques may, however, improve the investigation of how structural and functional changes such as PPIs, PTMs, and mutations may change protein stability.

1.6.1 Top-down Thermal Proteome Profiling

Bottom-up proteomics techniques such as those applied to the TPP related methods reviewed here are robust, widely used, and above all, benefit from high resolution and low limits of detection[57]. However, the bottom-up proteomics approach has significant drawbacks including the loss of site specific information such as PTMs.[57] This loss of site specific information is particularly detrimental to the TPP methods reviewed here as proteins with multiple mutations, PTMs, or PTM cross-talk is difficult to analyze using bottom-up methodology. Top-down proteomics approaches, however, analyze intact proteins directly so that functional proteoforms

can be examined[58]. Application of top-down proteomics methods would allow examination into how protein stability relates unique protein proteoforms and would result in more detailed information regarding how PTMs are involved in PPIs and PTM crosstalk.

The primary impediment to the application of top-down proteomics methods to TPP is challenge of applying quantitation methods to intact proteins. As metabolic labeling cannot be applied to TPP, top-down quantitation is limited to label-free quantitation or isobaric chemical tag labeling.[59] Label-free quantitation may be applied to top-down, however, the throughput would be very low as an individual run must be completed for every temperature condition. Additionally, proteome coverage is limited using label-free quantitation due to high sample complexity and dynamic range; label-free quantitation is not compatible with multidimensional label-free quantitation. Recently, a method for intact protein TMT labeling for complex protein mixtures has been optimized that allows for isobaric chemical tag labeling and multiplexing for top-down proteomics.[60–62] Application of this intact protein TMT labeling method for top-down TPP methods would allow high-throughput TPP analysis and application of multidimensional separation techniques such as high-pH/low-pH RPLC-MS/MS[63] for deeper TPP analysis of intact proteomes.

1.6.2 Human Plasma Thermal Proteome Profiling

Plasma is a rich source of biomarkers, which is most widely used in clinical sample for disease categorization and treatment support[64]. Perrin et al. (2020) introduced the possibility of conducting TPP experiments on human whole blood[65]. Likewise, there is a possibility that plasma can be analyzed through TPP experiments. Since the percentage of human serum albumin (HSA) is 52~60% of total protein[66], enrichment of lower abundant protein prior to the TPP will be required

to get the full analysis of the whole proteoform. The enrichment step might be possible with TiO_2 resin prior to digestion, if needed, prior to TMT labeling[67]. We would like to learn target and off-target engagement directly in human plasma through human plasma TPP.

1.6.3 Stability Proteomics coupled with Two-dimensional Separation

Stability proteomics can be coupled with two-dimensional separation for deeper and more precise analysis. Two-dimensional separation is a technique that samples are displaced orthogonally to improve the coverage and dynamic range[68]. This technique are generally applied to bottom-up approach, but also can be applied to top-down approach[69].

1.7 Dissertation synopsis

This dissertation presents the development, evaluation, and application of novel top-down thermal proteome profiling (TPP) technologies to measure proteoform thermal stability in human plasma samples. This research was completed in two steps, given here in Chapter 2 and Chapter 3.

In Chapter 2, I evaluated depletion methods for high abundance plasma proteins that hinder the observation of low abundance proteins. Since the biomarkers are known to be existent in low-abundant proteins[70], the development of plasma depletion contributes to the discovery of plasma biomarkers.Three depletion methods including proteominer™, organic precipitation, and gel-eluted liquid fraction entrapment electrophoresis (GELFrEE) were evaluated to determine the efficiency of high abundance protein depletion. All three methods effectively depleted high abundance proteins such as HSA, however, GELFrEE was chosen to pair with TPP in Chapter 3 due to its ability to enrich low molecular weight proteins appropriate for top-down MS methods

In Chapter 3, I adapted and optimized TPP sample preparation methods for top-down plasma protein analysis. I applied GELFrEE low molecular weight sample enrichment and top-down TPP methods to human plasma to quantify and identify intact proteoforms and determine proteoform stability. The results demonstrated the melting behavior of intact, low abundance plasma proteoforms. This work resulted in a proof-of-concept for a top-down TPP platform for the high-throughput functional proteomics analysis of intact human plasma.

Overall, my research illustrates the feasibility of studying functional proteomes in human plasma through a novel platform that integrates the depletion of high-abundant proteins and top-down TPP applications.

Chapter 2: Optimization of Depletion for Intact Human Plasma Proteins

2.1 Introduction

Plasma is a complex body fluid which contains a rich source of biomarkers and is widely used in clinical field for diagnostic process[64,71]. Despite the advantages of being easily accessible and minimally invasive, it is challenging to study the human plasma proteome due to the complexity of the sample and a wide dynamic range of protein abundances[11,72]. The top ten most abundant proteins make up 90% of the total composition of plasma and a wide dynamic range of protein concentrations, more than 10 orders of magnitude, obscures analysis of low abundance proteins[73]. These low abundance proteins may be biomarkers, so it is crucial to deplete high-abundance proteins[70]. As such, many methods have been utilized to deplete high abundant proteins including immunoaffinity depletion, combinatorial peptide ligand library, molecular weight-based separation, and chemical precipitation[74].

Mass spectrometry (MS) based proteomics methods can be divided into two categories: bottom-up (BU) and top-down (TD)[2]. BU proteomics requires protein digestion and, hence, may obscure information regarding the intact proteoform such as location of post-translational modifications[57]. TD proteomics analyze intact proteoforms, which provides a "bird's eye" view of intact proteoform[58]. TD analysis is challenging because of the relatively high dynamic range of protein in complex solutions and limitation in the size of proteoforms that can be analyzed using modern high resolution mass spectrometers. As a few high abundance proteins make up 90% of plasma protein composition[75], depletion of high abundance and large molecular weight proteoforms from plasma improves TD plasma analysis.

I have evaluated three methods for depletion of high abundance plasma proteins including Proteominer™, organic precipitation, and gel-eluted liquid fraction entrapment electrophoresis (GELFrEE). Proteominer™ is a spin column functionalized with a highly diverse library of combinatorial hexapeptide ligands; this provides extensive fractionation between high abundant proteins and medium-low abundant proteins without immunodepletion[76]. Organic precipitation uses organic solvents such as methanol (MeOH), ethanol (EtOH), acetone, acetonitrile (ACN), and isopropanol (IPA) as well as additives such as formic acid (FA) and trifluoro-acetic acid (TFA) to precipitate the high-abundant proteins[74]. Organic precipitation techniques are easy to utilize and cost-friendly, however, low specificity causes loss of some low abundance proteins. GELFrEE is a gel column that consist of sodium dodecyl-sulfate (SDS) which is used for separation based on molecular size[77]. GELFrEE is a highly reproducible and effective technique, however, it is limited by relatively low separation resolution.

Here, evaluation and optimization of plasma depletion was conducted using Proteominer™, organic precipitation, and Gel-eluted liquid fraction entrapment electrophoresis (GELFrEE).

2.2 Proteominer™

2.2.1 Materials

Proteominer™ kit, sodium dodecyl-sulfate polyacrylamide gel electrophoresis (SDS-PAGE) kit, acrylamide (AA)/Bis solution, ammonium persulfate (APS), and tetramethyl ethylenediamine (TEMED) were purchased from BioRad (Hercules, CA). LC/MS CHRAMASOLV® grade HPLC water, isopropanol (IPA), acetonitrile (ACN), methanol (MeOH) and ACS reagent acetic acid (HAc) were purchased from Sigma-Aldrich (St. Louis, MO). Ethanol (EtOH), phosphate buffered saline (PBS), 2-(4-(2-hydroxyethyl)-1-piperazinyl)-ethanesulfonic

acid (HEPES), sodium chloride (NaCl), glycine, ethylene glycol, tris-HCl, SDS, formamide, and Stains-all powder were also purchased from Sigma-Aldrich (St. Louis, MO). Pierce™ Bicinchoninic acid (BCA) protein assay kit, Pierce™ trifluoro-acetic acid (TFA), human plasma, and Coomassie protein assay reagent were purchased from Thermo Scientific (Hanover Park, IL).

2.2.2 Proteominer™

Elution and wash buffers were prepared: 1X PBS (pH 7.4) for wash buffer, 1 M NaCl solution mixed with 20 mM HEPES (pH 7.4) for the first elution buffer, 200 mM glycine (pH 2.4) solution for the second elution buffer, 60% ethylene glycol in Milli-Q water for the third elution buffer, and Milli-Q water with 33.3% IPA, 16.7% ACN, 0.1% TFA for the fourth elution buffer.

The Proteominer™ column was centrifuged for 30-60 seconds to remove storage material and the flowthrough was discarded. 120 µL of wash buffer was added to the column and rotated end-over-end for 5 minutes by rotator from VWR (Radnor, PA), followed by centrifuging for 1 minute (4°C) using an Eppendorf Centrifuge 5804 R with S-4-72 rotor (Enfield, CT). The flowthrough was discarded. The column washing steps were repeated twice. For sample binding, plasma (50 µg/µL) was diluted 25X with 1X PBS (pH 7.4) and 1mL of diluted plasma was added to the column. The column was rotated for 2 hours at room temperature. Then, 120 µL of wash buffer was added, rotated for 5 minutes (4°C), centrifuged for 30-60 seconds and the wash buffer was pipetted out without removing the beads. The sample washing steps were repeated three times. For sequential elution, 40 uL of wash buffer was added to the column, the column was centrifuged for 30-60 seconds (4°C), and the wash buffer was discarded. Then, 40 µL of first elution buffer was added and the tube was rotated for 10 minutes. Eluent was collected and the elution was repeated twice more with the first elution buffer. For second, third and fourth elution, previous

steps were repeated, and the eluents were collected. Eluents were analyzed with BCA assay *(1. BCA assay)* and SDS-PAGE *(3. Sodium Dodecyl-Sulfate Polyacrylamide Gel Electrophoresis (SDS-PAGE)).* **Figure 2.1** shows the proteominer workflow (this figure was created with Biorender).

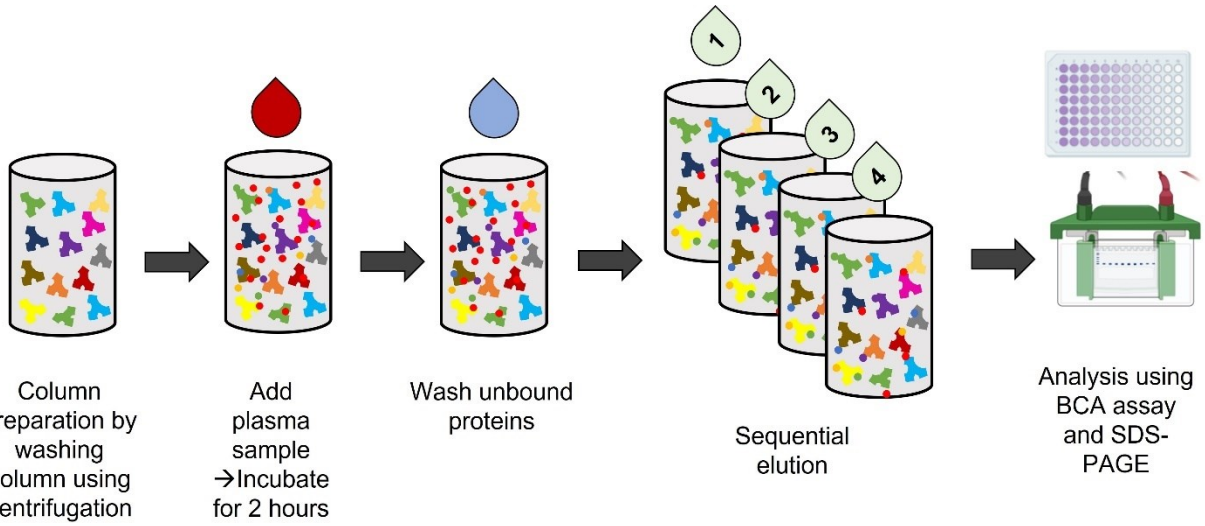

Figure 2.1 - Proteominer^{TM} workflow for plasma abundant proteins depletion

2.2.3 Proteominer™ results

Proteominer™ utilizes a combinatorial library of hexapeptides bound to beads to deplete high-abundance proteins and enrich low-abundance proteins in complex biological samples such as plasma[76]. When the sample is added to the column, the proteins bind to their specific ligands until the library is saturated. The high-abundance proteins saturate their ligands relatively quickly, meanwhile low-abundant proteins continue to bind throughout the incubation[78]. Excess protein is eluted which will primarily consist of high abundance proteins[79]. Subsequently, a series of elutions (using salt, organic, and aqueous buffers) are performed to collect the proteins bound to ligands based on interaction motif. Resulting eluents accordingly have decreased dynamic range[80].

To evaluate the plasma protein depletion efficiency of the Proteominer™ column, sequential elution, which consists of four elution steps, was conducted. As described in *2.2.2 ProteominerTM*, each elution step consists of three fractions. Two fractions were collected for the first elution and three fractions were collected for the second elution. Three fractions were also collected for the third and fourth elution, and these fractions were combined for further analysis. The original plasma (50 μg/μL) was 25X diluted with 1X PBS (pH 7.4) and loaded onto an SDS-PAGE gel for comparison before and after depletion.

The result of protein depletion of plasma is shown in the SDS-PAGE **(**3. Sodium Dodecyl-Sulfate Polyacrylamide Gel Electrophoresis (SDS-PAGE)**).** Human serum albumin (HSA) is the highest abundance protein in human serum and has a mass of approximately 67 kDa. Disappearance of the band between 50 and 75 kDa indicates that HSA has been depleted. Additionally, in the first fraction of the first elution (1-1), HSA obscures other protein bands, but from the second fraction of the first elution (1-2), HSA concentration has decreased, and low abundance proteins can be observed. Very little protein is eluted from the fourth fraction. The

BCA assay indicates that the concentration decreases as sequential elution proceeds **(Table 2.1)**. Still, we will continue to optimize the elution conditions as well as sample loading amounts in future study.

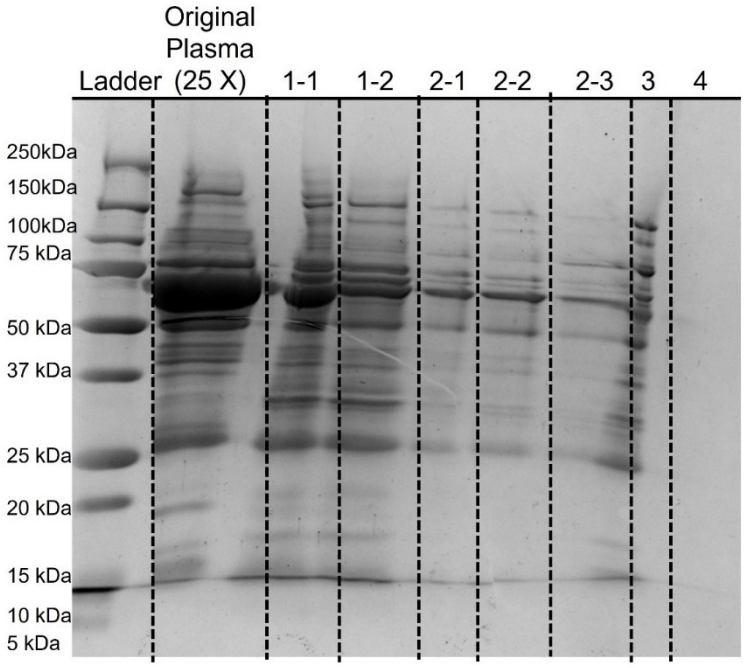

Figure 2.2- SDS-PAGE of human plasma depletion using Proteominer^{TM} (1-1: First fraction of the first elution, 1-2: Second fraction of the second elution, 2-1: First fraction of the second elution, 2-2: Second fraction of the second elution, 2-3: Third fraction of the second elution, 3: Combined fractions of the third elution, 4: Combined fractions of the fourth elution)

Table 2.1 - BCA Assay result of human plasma depletion using Proteominer^{TM}

	Absorbance	Concentration (µg/µL)	Original concentration (µg/µL)
2X diluted 1-1	0.35	0.3	0.6
1-2	0.58	0.73	0.73
2-1	0.27	0.16	0.16
2-2	0.32	0.25	0.25
2-3	0.24	0.1	0.1
3	0.25	0.13	0.13
4	0.10	-0.15	-0.15

2.3 Organic precipitation

2.3.1 Materials

Sodium dodecyl-sulfate polyacrylamide gel electrophoresis (SDS-PAGE) kit, acrylamide (AA)/Bis solution, and ammonium persulfate (APS), tetramethyl ethylenediamine (TEMED) were purchased from BioRad (Hercules, CA). LC/MS CHRAMASOLV® grade HPLC Water, Isopropanol (IPA), acetonitrile (ACN), methanol (MeOH), and ACS reagent acetic acid (HAc) were purchased from Sigma-Aldrich (St. Louis, MO). Phosphate buffered saline (PBS), Tris-HCl, SDS, and Stains-all powder were also purchased from Sigma-Aldrich (St. Louis, MO). Pierce™ Bicinchoninic acid (BCA) protein assay kit, Pierce™ trifluoro-acetic acid (TFA), human plasma, and Coomassie protein assay reagent were purchased from Thermo Scientific (Hanover Park, IL).

2.3.2 Organic Precipitation

For the sample preparation, plasma (50 μg/μL) was centrifuged at 13,000 rpm (4°C) for 60 minutes, and the supernatant was collected and diluted 2 times using 1X PBS (pH 7.4). The diluted solution was heated using an MJ Research PTC-200 thermocycler from Marshall Scientific (Hampton, NH) at 37°C for 10 minutes. The samples were cooled to room temperature for 3 minutes and then placed on ice. Samples were then centrifuged at 10,000 rpm (4°C) using an F-45-58-PCR rotor from Eppendorf (Enfield, CT) for 60 minutes and the resulting supernatant was collected. The supernatants were centrifuged once more at 13,000 rpm (4°C) with S-4-72 rotor for 30 minutes and the final supernatant was collected. Bradford Assay *(2. Bradford assay)* and SDS-PAGE were used to analyze the protein concentration and pattern.

Next, organic precipitation was performed. IPA was mixed with plasma at a 2:1 volume ratio to start the precipitation. The solution was thoroughly vortexed (Vortex Genie 2® from Daigger; Buffalo Grove, IL) for 5 seconds and incubated at room temperature for 30 minutes. Then, the solution was centrifuged at 13,000 rpm for 5 minutes (4°C) and the supernatant was transferred to fresh tubes. The sample was further centrifuged at 13,000 rpm for 5 minutes (4°C) to remove the remaining precipitate and the supernatant was transferred to a fresh Eppendorf tube. The supernatants were concentrated down to approximately 10 µL using a Speedvac® concentrator from Savant (Hyannis, AS). The dried samples were reconstituted to 100 µL in 1X PBS (pH 7.4).

Depleted samples were analyzed by Bradford Assay and SDS-PAGE to observe the protein patterns after the organic precipitation. Then samples were analyzed using top-down RPLC-MS/MS. **Figure 2.3** shows the workflow for organic precipitation (figure was created with Biorender).

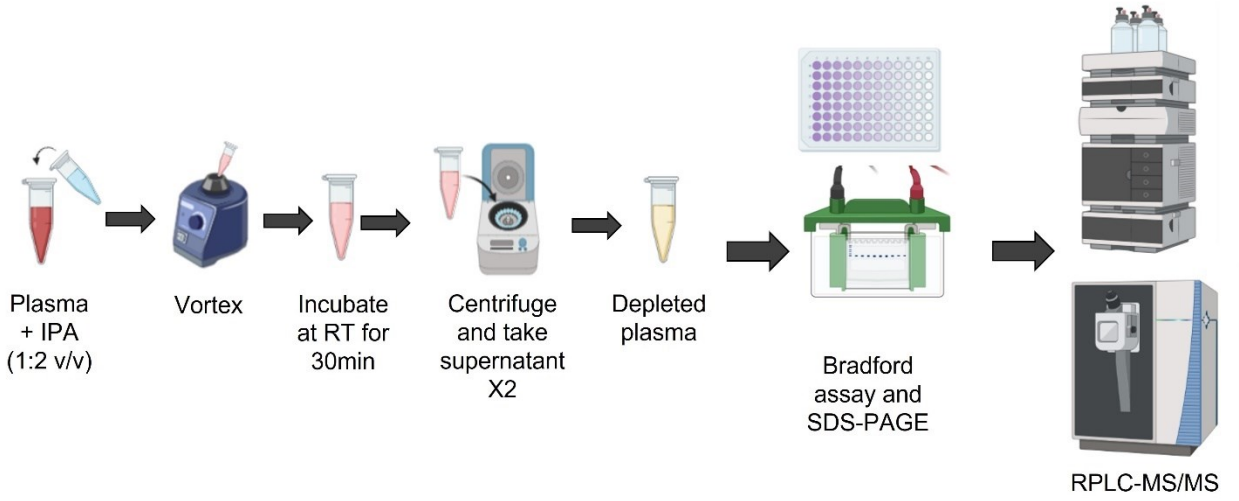

Figure 2.3 - Organic precipitation workflow

2.3.3 Top-down Liquid Chromatography – Mass Spectrometry (LC-MS)

Top-down RPLC-MS/MS was performed with modified Accela LC system from Thermo Scientific (Waltham, MA) and Orbitrap Exploris 240 mass spectrometer with positive mode from Thermo Fisher Scientific (Hanover Park, IL, Bremen, Germany). C2 capillary from CoAnn Technologies (100 µm i.d., 30 cm length, 3 µm diameter, 300 Å pore size) was used for all RPLC separation. The mobile phase A (MPA) was 0.01% TFA, 0.585% Hac, 2.5% IPA and 5% I in HPLC water, and mobile phase B (MPB) was 0.01% TFA, 0.585% HAc, 45% IPA, 45% ACN in HPLC water. 10 µL of sample was loaded onto a solid phase extraction (SPE) column (trapping column, 150 µm i.d., 5 cm length, Jupiter particles, 5 µm diameter, 300 Å pore size), respectively. A 100-minute gradient from 15 % to 85 % MPB was performed with 0.4 µL/minute LC flow rate. The column was flushed using 90% MPB over 10 minutes and equilibrated to 3% of MPA for 30 minutes. The eluent was analyzed using an Orbitrap Exploris 240 mass spectrometer (Thermo Fisher Scientific, Bremen, Germany) with following parameters: inlet capillary temperature was 275 °C; spray voltage was 3.0 kV; resolution for MS1 and MS2 was set to 120, 000 and 60, 000, respectively; AGC target was 1×E6 with 2 microscans for both MS1 and MS2 scans. Maximum injection time was 500 ms for MS1 and 300 ms for MS2 scans; the isolation window was set to 2 m/z. Dynamic exclusion was 90 s; top 6 most abundant precursor ion peaks with charge 4-50 in MS1 scans were selected for MS2 fragmentation with a normalized collision energy of 32%. Xcalibur 3.0 software (Thermo Fisher Scientific) was used for LC-MS/MS data collection.

2.3.4 Data Analysis

Mass features were deconvoluted using Biopharma finder (Thermo Fisher Scientific) and protein identification was performed using TopPIC suite and searched against human protein

database (Uniprot 2020-07-11, 20368 species)[81,82]. MSConvert (Proteowizard, Framingham, MA) was used to convert MS raw files to mzML format[83]. Parameters for TopFD deconvolution were: MS1 signal-to-noise ratio = 3.0, MS2 signal-to-noise = 1.0, the precursor window size was 3.0 m/z, maximum mass was 500,000 Dalton, maximum charge was 50, and m/z error was 0.02. TopPIC was performed with decoy database searching, FDR cutoff 0.01 for spectrum, proteoform level, maximum number of mass shifts was 1, mass shift range was ± 500 Dalton. Parameters not given were default.

2.3.5 Organic precipitation results

In human blood plasma, a total of 22 proteins, albumin, IgG, transferrin, fibrinogen, IgA, alpha-2-macroglobulin, IgM, alpha-1-anti-trypsin, C3 complement, haptoglobulin, alpha-1-acid glycoprotein, apolipoprotein-B, apolipoprotein-A1, lipoprotein a, factor H, ceruloplasmin, C4 complement, complement factor B, pre-albumin, C9 complement, C1q complement, and C8 complement, compose 99% of the total human plasma protein content, while hundreds of other proteins contribute to the remaining 1%[71].

Organic precipitation was first introduced in 1961 by S.E. Michael based on the principle that organic solvent precipitates protein which enables separation of blood proteins in high purity and yields[84]. When the proteins are in aqueous solvent, the water molecules tend to form hydrogen bonds with the protein surface and other water molecules which forms a hydration layer preventing protein interaction. However, when organic solvents that are miscible with water are added into the solution, the overall solvent polarity decreases. Accordingly, the solubility of proteins decreases, and the hydration layer is interrupted, resulting in protein aggregation and precipitation.

The organic depletion method has been further developed and modified using various organic solvents in different ratios to deplete high-abundant proteins in plasma[85].

Organic precipitation was performed on plasma in triplicate using the optimized protocol. When the bands are compared before and after depletion using SDS-PAGE, significantly lighter bands were observed around 60 kDa after depletion **(Figure 2.4)**, suggesting high efficiency of depleting high abundance proteins such as HSA. Furthermore, LC-MS analysis was performed on the depleted plasma sample, and high reproducibility was observed with respect to total ion intensity and elution patterns **(Figure 2.5).**

Figure 2.6 shows the proteoform deconvolution after the organic precipitation, and **Figure 2.7** shows the protein identification. Overall, 355 ± 38 proteoforms from 65 ± 7 proteins were identified from these LC-MS analyses. The number of identified proteins and identified proteoforms were plotted in **Figure 2.8 and Figure 2.9**. The majority of identified proteins after the organic precipitation were known plasma proteins, including apolipoprotein A-I, A-II, A-IV, C-I, C-II, C-III, L-I, Hemoglobin beta chain, histone H1.4, and serum amyloid. These results also suggested that organic precipitation can be applied to deplete high-abundance proteins, enabling the detection of relatively low abundance proteins.

We successfully detected and identified an intact proteoform of apolipoprotein A-I (amino acids 27-267) with the removal of the signal peptides[86] **(Figure 2.10)**. The observed monoisotopic mass was 28089.40 Da, and the theoretical monoisotopic mass was 28089.40 Da. The mass difference was 0.02 ppm with an E-value of 2.70E-4. **Figure 2.10 (A)** shows the crystal structure (PDB: 3K2S), extracted ion chromatogram (EIC), and isotope distribution. The intensity of identified Apolipoprotein A-I was 4.48 E8, which ranked as the 9th among all identified proteoforms of 57. **Figure 2.10 (B)** shows the charge state envelope, and charge state +26 was

selected for MS/MS fragmentation, as shown in **Figure 2.10 (C)**. Apolipoprotein A-I was identified with an unknown mass shift of 277 Da, suggesting a potential PTM. Apolipoprotein A-I is known as a major structural protein of high-density lipoprotein (HDL), and is involved in transporting cholesterol to accelerate its metabolism[87]. Additionally, human plasma apolipoprotein A-I is one of the known biomarkers for Parkinson's disease[88].

Another protein identified in the LC-MS/MS analysis is apolipoprotein C-I with cleavage of the signal peptide[86] **(Figure 2.11)**. The observed monoisotopic mass was 6626.50 Da, and the theoretical monoisotopic mass was 6626.51 Da. The mass difference was -1.19ppm with an E-value of 1.87 E-24. **Figure 2.11 (A)** shows crystal structure (PDB: 1IOJ), EIC, and isotope distribution. Apolipoprotein C-I shows 2nd highest intensity among all identified proteins of 57, which is 1.93 E9. **Figure 2.11 (B)** shows the charge state envelope and charge state +9 was selected for MS/MS fragmentation as shown in **Figure 2.11 (C)**. Apolipoprotein C-I is a known inhibitor of lipoprotein, and it binds to the low density lipoprotein (LDL) receptor[89]. Additionally, human plasma apolipoprotein A-I is important to observe as it is one of the known biomarkers for gastric cancer[90].

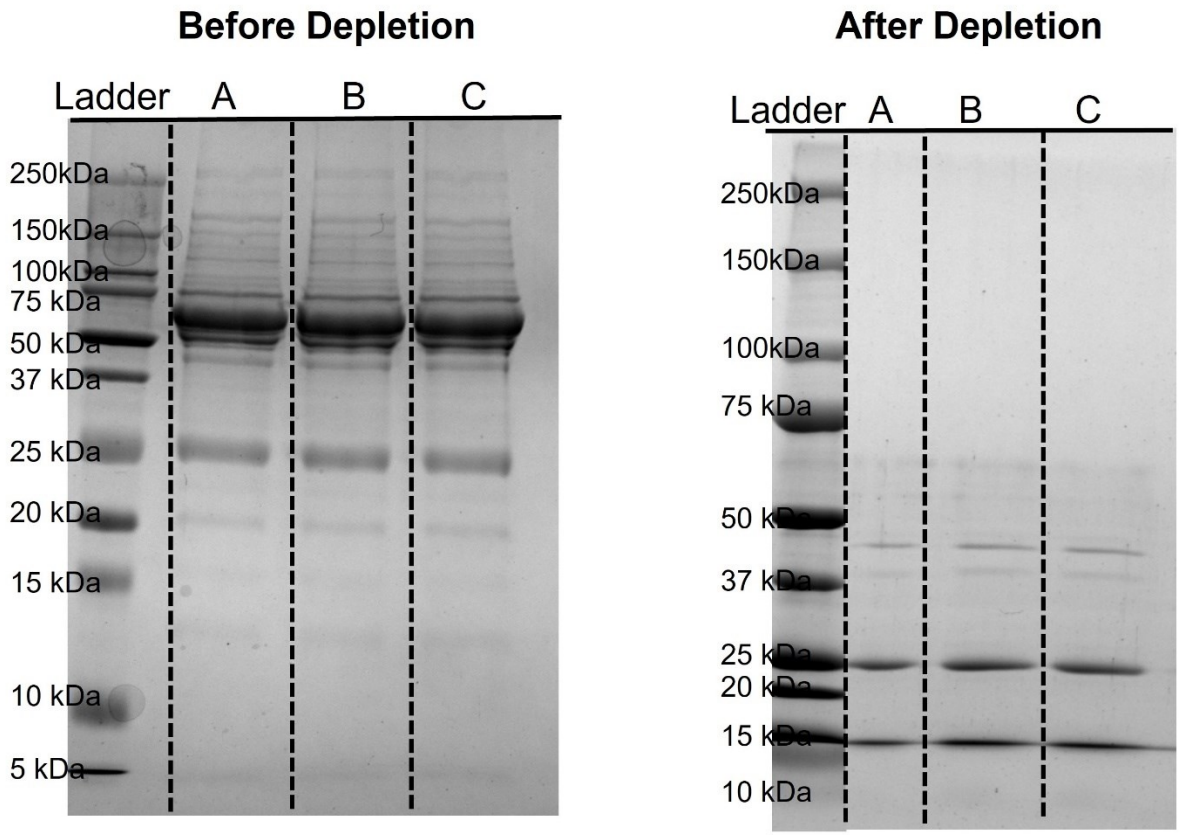

Figure 2.4 - SDS-PAGE of human plasma before and after organic precipitation

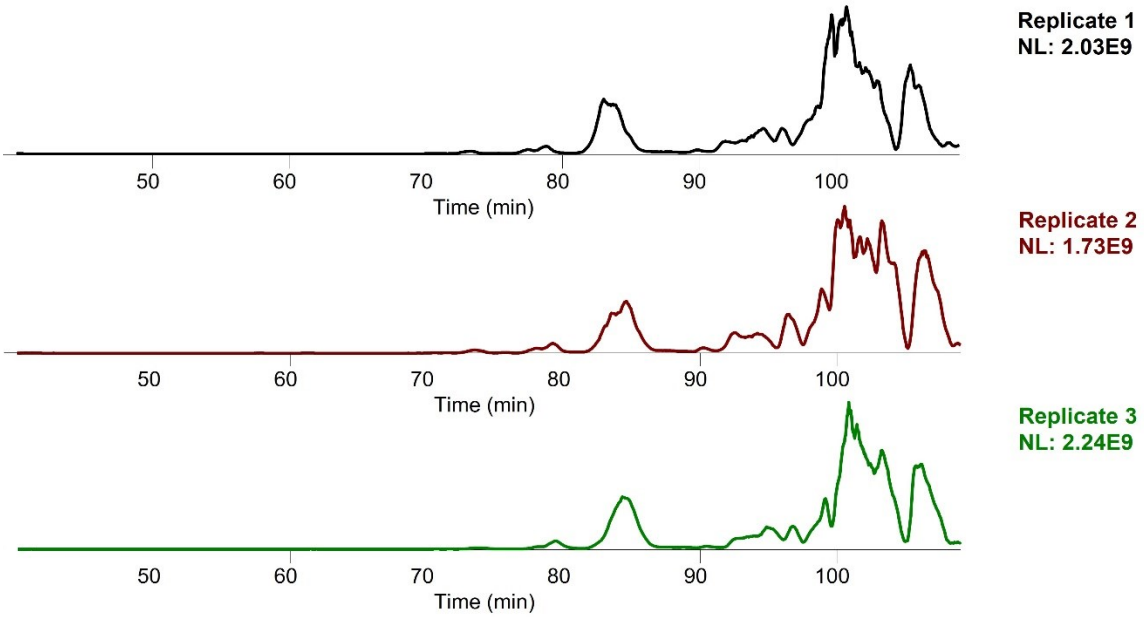

Figure 2.5 - LC chromatogram of organic depleted plasma samples (Total ion chromatogram with retention time range 40.00 – 110.00)

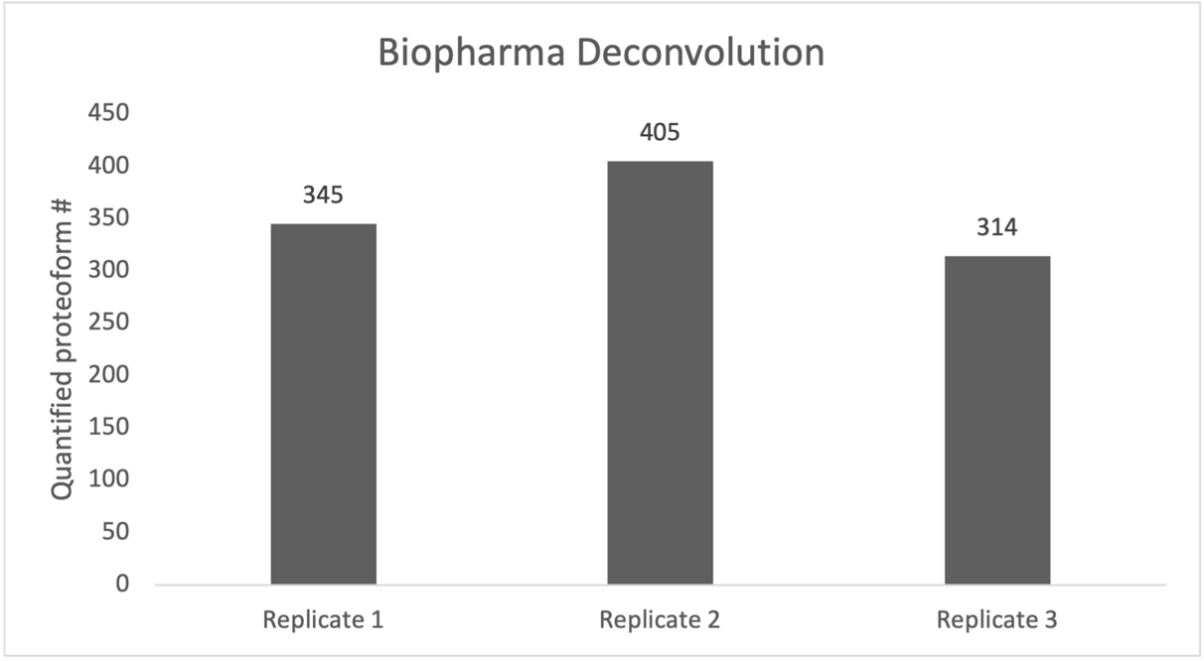

Figure 2.6 - Proteoform quantification after organic precipitation

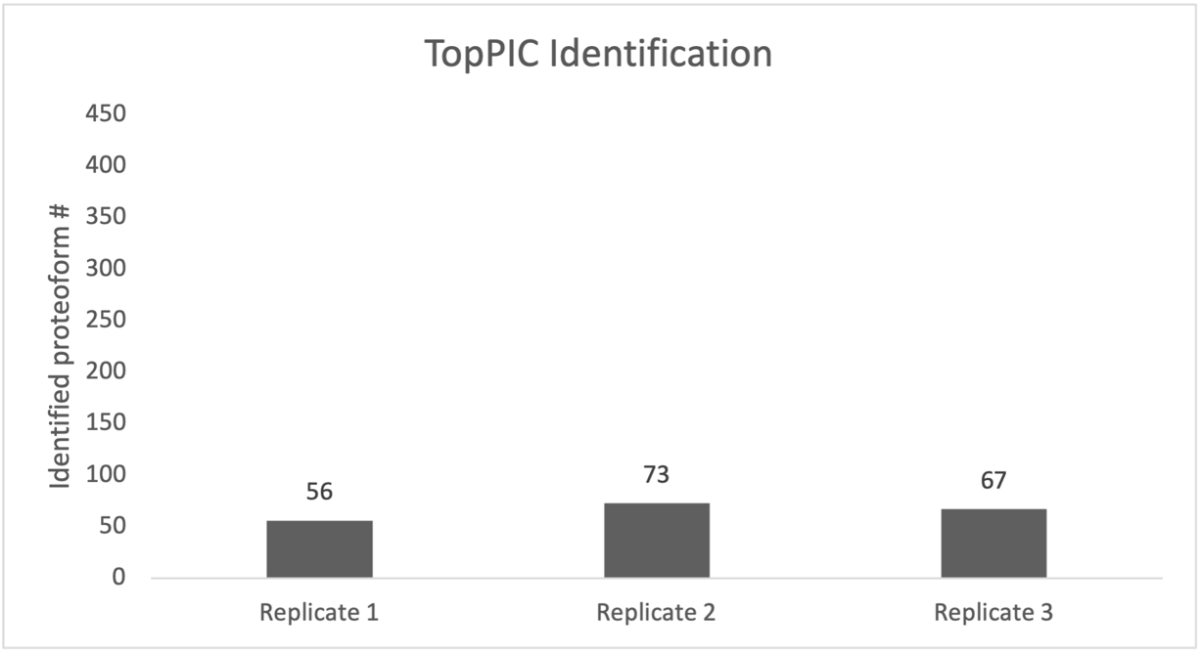

Figure 2.7 - Proteoform identification after organic precipitation

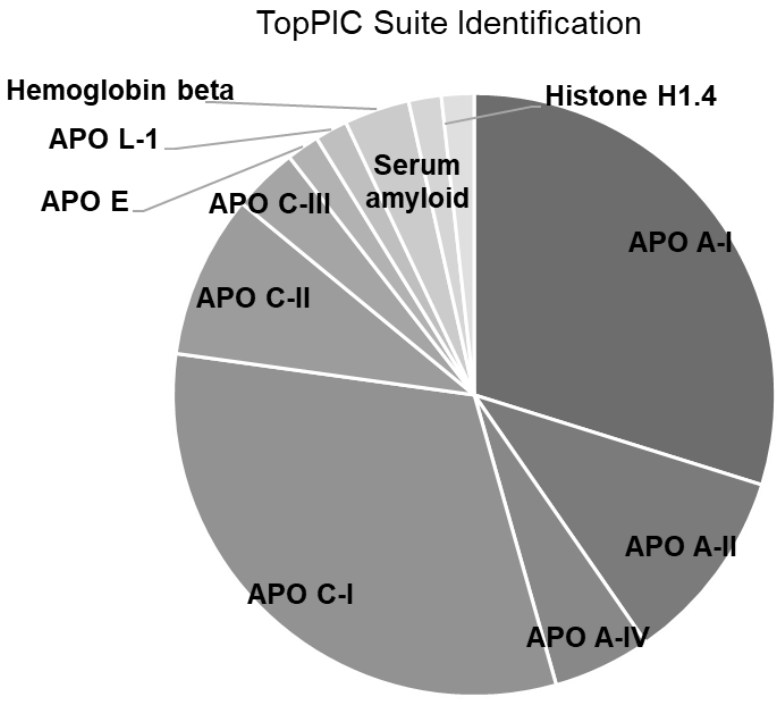

Figure 2.8 - TopPIC Suite proteoform identification result after organic precipitation

Protein	# of proteoform identified
APO A-I	17
APO A-II	6
APO A-IV	3
APO C-I	18
APO C-II	5
APO C-III	2
APO E	1
APO L-1	1
Hemoglobin beta	2
Histone H1.4	1
Serum amyloid	1

Figure 2.9 - TopPic Suite proteoform identification numbers

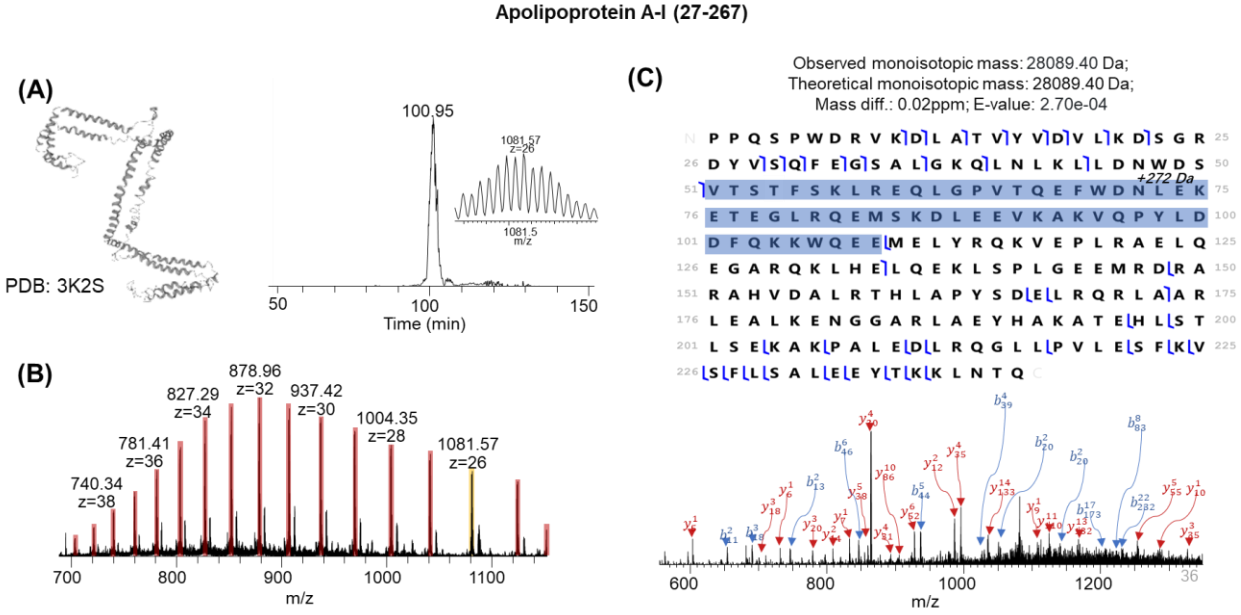

Figure 2.10 – MS detection and MS/MS identification of Apolipoprotein A-I (27-267). (A) Protein structure and extracted ion chromatogram (EIC) with isotopic distribution; (B) charge state envelope with peaks belonging to Apolipoprotein A-I designated in red; yellow highlight represents the precursor ion for selected for MS2 fragmentation (C) Protein sequence and MS/MS spectra with a unknown mass shift of 277 Da.

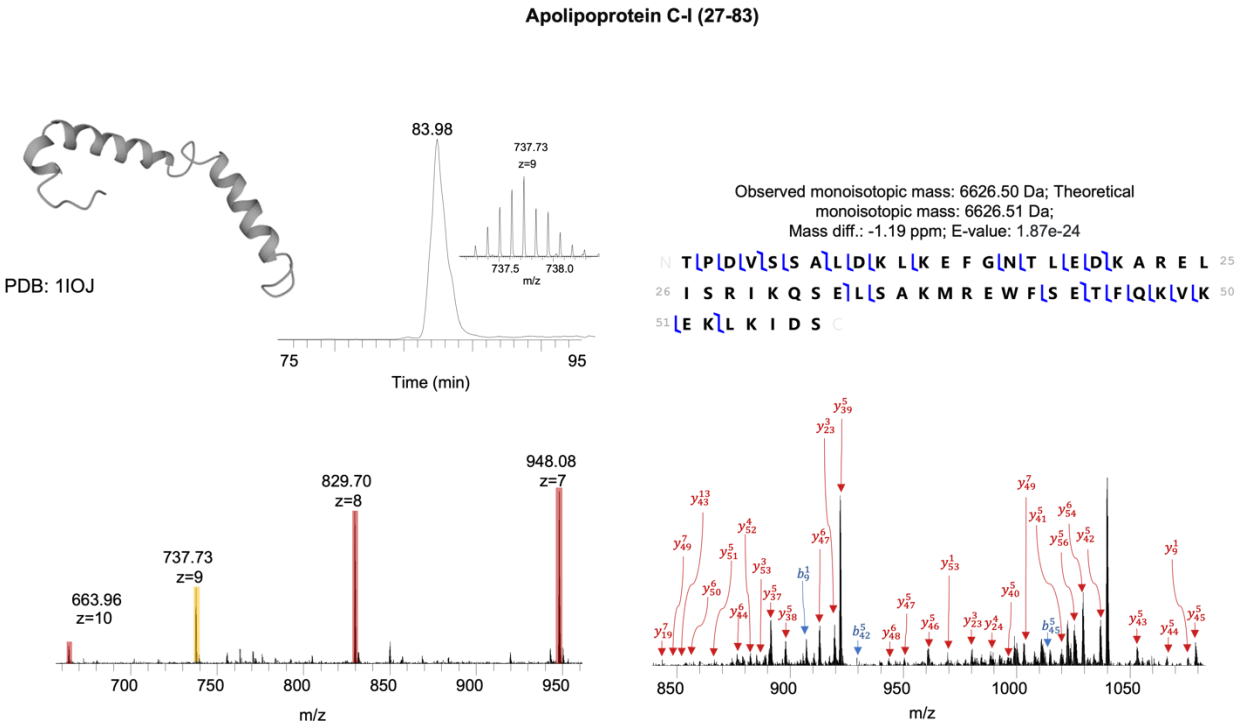

Figure 2.11 - MS detection and MS/MS identification of Apolipoprotein C-I (27-83). (A) Protein structure and EIC with isotopic distribution; (B) charge state envelope; yellow highlight represents precursor ion for MS2 fragmentation, red and yellow highlights represent peaks belonging to Apolipoprotein C-I (C) Protein sequence and MS/MS spectra

2.4 Gel-eluted liquid fraction entrapment electrophoresis (GELFrEE)

2.4.1 Materials

Sodium dodecyl-sulfate polyacrylamide gel electrophoresis (SDS-PAGE) kit, acrylamide (AA)/Bis solution, and ammonium persulfate (APS), tetramethyl ethylenediamine (TEMED) were purchased from BioRad (Hercules, CA). GELFrEE kit was purchased from Expedeon (Cambridge, AS) and 5X Tris-acetate sample buffer was provided by the GELFrEE manufacturer. LC/MS CHRAMASOLV® grade HPLC Water, Isopropanol (IPA), acetonitrile (ACN), methanol (MeOH), and ACS reagent acetic acid (HAc) were purchased from Sigma-Aldrich (St. Louis, MO). Dithiothreitol (DTT), phosphate buffered saline (PBS), Tris-HCl, SDS, and Stains-all powder were also purchased from Sigma-Aldrich (St. Louis, MO). Pierce™ Bicinchoninic acid (BCA) protein assay kit, Pierce™ detergent removal spin column, Pierce™ Trifluoro-acetic acid (TFA), human plasma, and Coomassie protein assay reagent were purchased from Thermo Scientific (Hanover Park, IL).

2.4.2 Gel-eluted liquid fraction entrapment electrophoresis (GELFrEE)

200 µg of plasma was mixed with 8 µL 200 mM DTT and 30 µL of 5X Tris-acetate sample buffer. This sample was then diluted up to 150 µL using 1X PBS (pH 7.4). GELFrEE kit was disassembled, and the glass tubes were filled with the 265 µL resolving gel and 540 µL stacking gel. Resolving gel was made up of 7.2 mL of 30% AA/Bis solution, 2.25 mL of DDI water, 240 µL of 10% SDS solution, 6.5 mL of 40% glycerol solution, 2.25 mL of 3M Tris-HCl solution (pH 8.8) was first mixed, then 200 µL of APS solution and 12 µL TEMED solution were added. Stacking gel was made up of 1.8 mL of 30% AA/Bis Solution, 9.45 mL of DDI water, 240 µL of

10% SDS Solution, 0.75 mL of 1M Tris-HCl solution (pH 6.8) was mixed, then 120 µL APS solution and 12 µL TEMED solution were added. The gels were left undisturbed to solidify for 30 minutes and reassembled.

After reassembling, 6 mL of 1X HEPES buffer was added to cathode chambers and 8mL to anode chambers, plus 150 µL to the sample collection chambers. Then, the prepared samples were added to the sample loading chambers. The cartridge was placed into the GELFrEE instrument from Expedeon (Cambridge, AS), and the electrode arrays was lowered by closing the lid. The optimized method is shown in the Table 2.2.

Table 2.2 - Optimized GELFrEE method

Step	**1**	**2**	**3**	**4**	**5**	**6**
Voltage (V)	50	50	85	85	85	85
Fraction Interval (minute)	16	54.6	21.9	5	5	18
Fraction	1	2	3	4	5	6
Buffer Change	Add 2mL to cathode chambers after step 1	Change buffer for both cathode and anode chambers after step 2	Change buffer for both cathode and anode chambers after step 2			

SDS-PAGE was conducted to observe protein bands from each fraction. Fractions 1 to 3 were combined excluding fraction 4 to 6 which contained high amounts of HSA. Protein concentration of combined fractions was measured by Bradford Assay.

SDS removal was performed using Pierce™ detergent removal spin columns. Briefly, the column was washed by adding 300 µL of 20% EtOH, Milli-Q water, and 1X PBS, respectively, to each tube and centrifuging at 13,000 rpm for 2 minutes (4°C). Each was step was repeated three times. Then, combined fractions were added to the column and centrifuged at 13,000 rpm for 2 minutes (4°C). Sample was filtered through the column twice to completely remove SDS. Final eluent was collected and protein concentration was analyzed using a Bradford assay and SDS-PAGE.

After SDS removal, SDS quantitation was conducted to ensure SDS was removed prior to LC-MS/MS. Stains-all stock solution was prepared by adding 500 µL IPA and 500 µL MilliQ water to 1 mg of Stains-all powder. Stains-all intermediate solution was prepared by adding stains-all stock solution and formamide at an 18:1 ratio to Milli-Q water. 2 µL of samples and 1, 0.5, 0.25, and 0.125% SDS standards were added to 200 µL of stains-all intermediate solution each well on 96 well plate. The plate was analyzed at 438nm using an Infinite M299 spectrophotometer from Tecan (Männedorf, Switzerland). Absorbance was plotted against SDS concentration plot to determine linear range of quantitation. Final SDS concentration for the sample should be lower than the detection limit to prepare the sample for MS analysis.

Samples were analyzed using top-down RPLC-MS/MS. **Figure 2.12** shows the GELFrEE workflow (figure was created with Biorender).

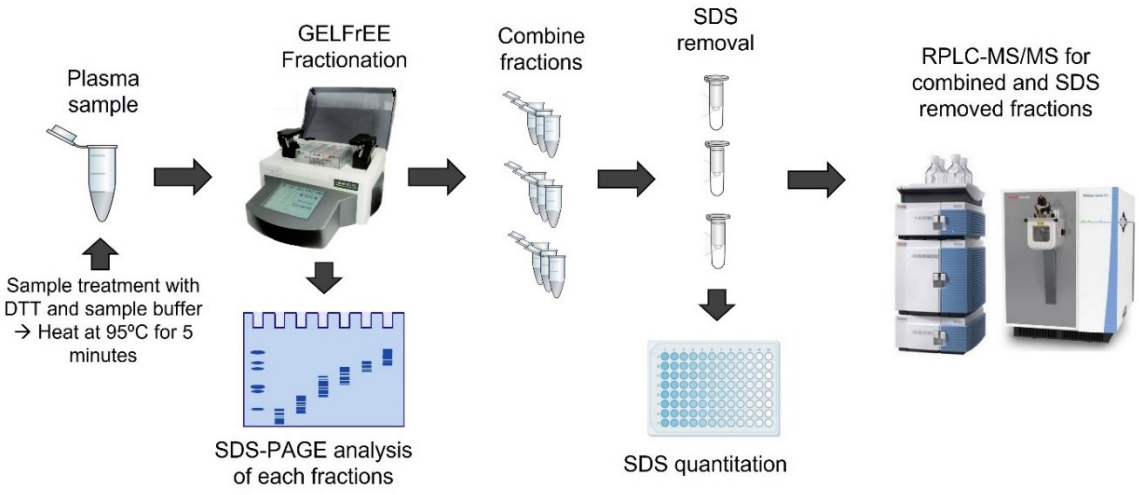

Figure 2.12 – The workflow of plasma depletion using GELFrEE

2.4.3 Top-down Liquid Chromatography – Mass Spectrometry (LC-MS)

The packing materials for packing C5 (Jupiter particles, 5 µm diameter, 300 Å pore size) and C18 (Jupiter particles, 5 µm diameter, 300 Å pore size) columns were purchased from Phenomenex (Torrance, CA).

Top-down RPLC-MS/MS was performed using a modified Accela LC system from Thermo Scientific (Waltham, MA) and Orbitrap Exploris 240 mass spectrometer with positive mode from Thermo Fisher Scientific (Hanover Park, IL, Bremen, Germany). C2 capillary from CoAnn Technologies (100 µm i.d., 30 cm length, 3 µm diameter, 300 Å pore size) was used for all RPLC separation. The mobile phase A (MPA) was 0.01% TFA, 0.585% Hac, 2.5% IPA and 5% I in HPLC water, and mobile phase B (MPB) was 0.01% TFA, 0.585% HAc, 45% IPA, 45% ACN in HPLC water. 50 µL of sample was loaded to solid phase extraction (SPE) column (trapping column, 150 µm i.d., 5 cm length, Jupiter particles, 5 µm diameter, 300 Å pore size), respectively. Total 100 minutes gradient from 15 % to 85 % MPB was performed with 0.4 µL/minute LC flow rate. The column was flushed with 90% MPB over 10 minutes and equilibrated to 3% of MPA for

30 minutes. The eluent was analyzed using an Orbitrap Exploris 240 mass spectrometer (Thermo Fisher Scientific, Bremen, Germany) with following parameters: inlet capillary temperature was 275 °C; spray voltage was 3.0 kV; resolution for MS1 and MS2 was set to 120, 000 and 60, 000, respectively; AGC target was 1×E6 with 2 microscans for both MS1 and MS2 scans. Maximum injection time was 500 ms for MS1 and 300 ms for MS2 scans; the isolation window was set as 2 m/z. Dynamic exclusion was 90 s; top 6 most abundant precursor ion peaks with charge 4-50 in MS1 scans were selected for MS2 fragmentation with a normalized collision energy of 32%. Xcalibur 3.0 software (Thermo Fisher Scientific) was used for LC-MS/MS data collection.

2.4.4 Data Analysis

Mass features were deconvoluted using Biopharma finder (Thermo Fisher Scientific) and protein identification was performed using TopPIC suite and searched against human protein database (Uniprot 2020-07-11, 20368 species)[81,82]. MSConvert (Proteowizard, Framingham, MA) was used to convert MS raw files to mzML format[83]. Parameters for TopFD deconvolution were: MS1 signal-to-noise ratio = 3.0, MS2 signal-to-noise = 1.0, the precursor window size was 3.0 m/z, maximum mass was 500,000 Dalton, maximum charge was 50, and m/z error was 0.02. TopPIC was performed with decoy database searching, FDR cutoff 0.01 for spectrum, proteoform level, maximum number of mass shifts was 1, mass shift range was ± 500 Dalton. Parameters not given were default.

2.4.5 GELFrEE results

GELFrEE is a powerful technique that provides predictable and excellent fractionation[77]. A voltage is applied and the protein samples are separated electrophoretically on an SDS gel column[91]. Proteins are then concentrated in a stacking gel and separated based on their electrophoretic mobilities in a resolving gel[77].

Since GELFrEE fractionates proteins by molecular weight, fractions containing proteins smaller than HSA (67 kDa) were collected and combined. Proteins with larger molecular weight than HSA was not analyzed because these larger proteins are difficult to analyze using currently available high-throughput TD proteomics[92]. Duplicate GELFrEE separation of 200 μg plasma samples was performed using the optimized method.

SDS-PAGE results show that HSA was not eluted in the first 3 fractions, and good reproducibility is demonstrated between runs **(Figure 2.11)**. Fractions 2 and 3 were combined, and SDS was removed for RPLC-MS/MS analysis. The resulting proteins were analyzed using SDS-PAGE. Depletion of HSA was performed with high reproducibility between duplicate 1 and duplicate 2 according to the SDS-PAGE analysis. After SDS removal with a detergent removal column **(Figure 2.12)**, protein patterns between the two replicates were similar, demonstrating good reproducibility. **Figure 2.13** also shows similar patterns in LC chromatograms.

Overall, 908 ± 56 proteoforms from 34 ± 9 proteins were identified from LC-MS analysis of the combined GELFrEE fractions **(Figure 2.16 and Figure 2.17)**. A detailed list of identified proteins and the number of proteoforms is shown **(Figure 2.18 and Figure 2.19)**. The identified plasma proteins include apolipoprotein A-I, A-II, A-IV, C-I, Alpha-2-HS-glycoprotein, 10kDa heat shock protein, Cystatin-A, Dermcidin, Histone H1.4, H2A type 1, H2A type 1-B, H2A type 2-A, H2A type 1-O, H3.1, H3.2, and H3.3. Fibrinogen alpha chain. Immunoglobulin kappa

constant, a highly abundant protein, was also identified, but with low intensities of 1.30E6 compared to the highest intensity observed in apolipoprotein A-1 with 1.64E9. Overall, by removing higher MW proteins, the GELFrEE approach allows a higher number of identified proteins and proteoforms in the enriched low MW protein fractions.

We also identified an intact proteoform of apolipoprotein A-I (25-267) with the cleavage of the signal peptides[86] **(Figure 2.20)** in the LC-MS/MS analysis**.** The observed monoisotopic mass was 28061.66 Da, and the theoretical monoisotopic mass was 28061.47 Da. The mass difference was 6.66 ppm with an E-value of 7.46 E-4. Figure 2.20 (A) shows the structure from Uniprot (PDB: 3K2S), extracted ion chromatogram (EIC), and isotope distribution. Apolipoprotein A-I shows 1st highest intensity among all identified proteins of 41, which is 1.64 E9. Figure 2.20 (B) shows a charge envelope, 878 m/z was selected for MS/MS fragmentation as shown in Figure 2.20 (C). Figure 2.20 (C) shows the Apolipoprotein A-I sequence and MS/MS spectra.

The second example is an intact proteoform of histone H1.4 (2-219) with the removal of initiator methionine **(Figure 2.21)**. The observed monoisotopic mass was 21762.10 Da, and the theoretical monoisotopic mass was 21762.97 Da. The mass difference was -40.11 ppm with an E-value of 2.51 E-3. Figure 2.18 (A) shows the structure from Uniprot (PDB: 7K5Y), extracted ion chromatogram (EIC) and isotope distribution. Histone H1.4 shows 3rd highest intensity among all 41 of identified proteins, which is 1.72 E8. Figure 2.18 (B) shows a charge envelope, 641 m/z was selected for MS/MS fragmentation as shown in Figure 2.18 (C). Figure 2.18 (C) shows the histone H1.4 sequence and MS/MS spectra with the known post-translational modification (acetylation) at the 2nd serine residue[93]. Histone H1 protein involves in binding with linker DNA ultimately

forms the macromolecular structure[94]. Histone H1.4 is considered as a potential biomarker and driver in metastatic prostate cancers[95].

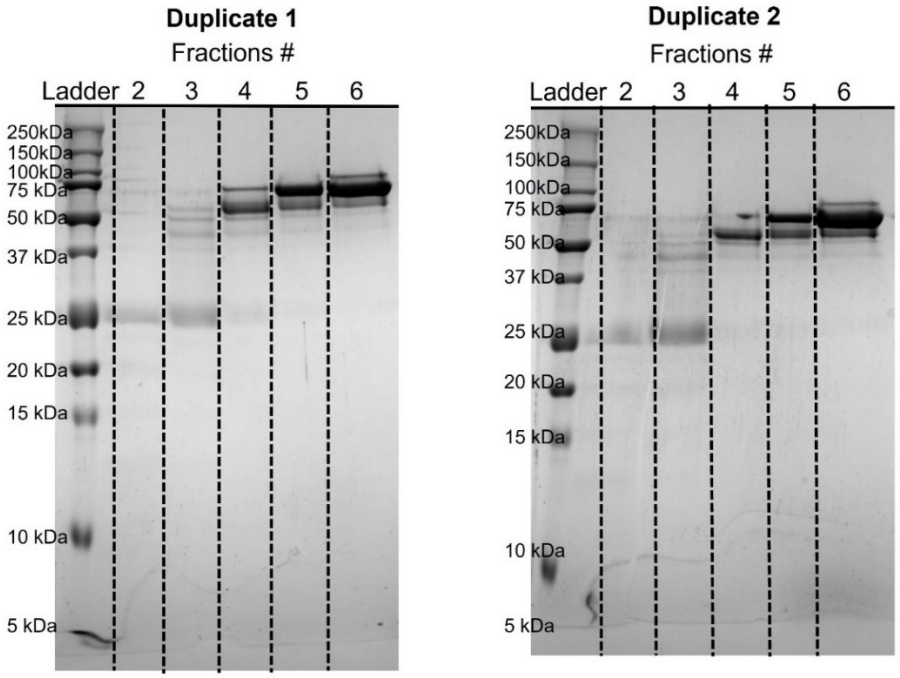

Figure 2.13 - SDS-PAGE result of GELFrEE separated duplicated plasma samples.

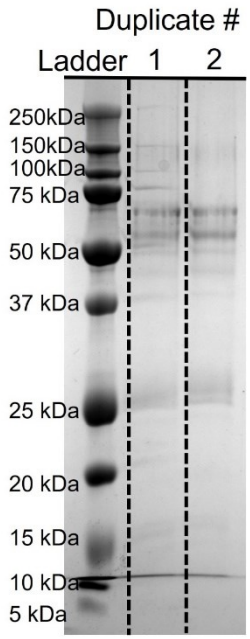

Figure 2.14 - SDS-PAGE of duplicate GELFrEE fractionated plasma samples after SDS removal and combination of GELFrEE fractions 1-3

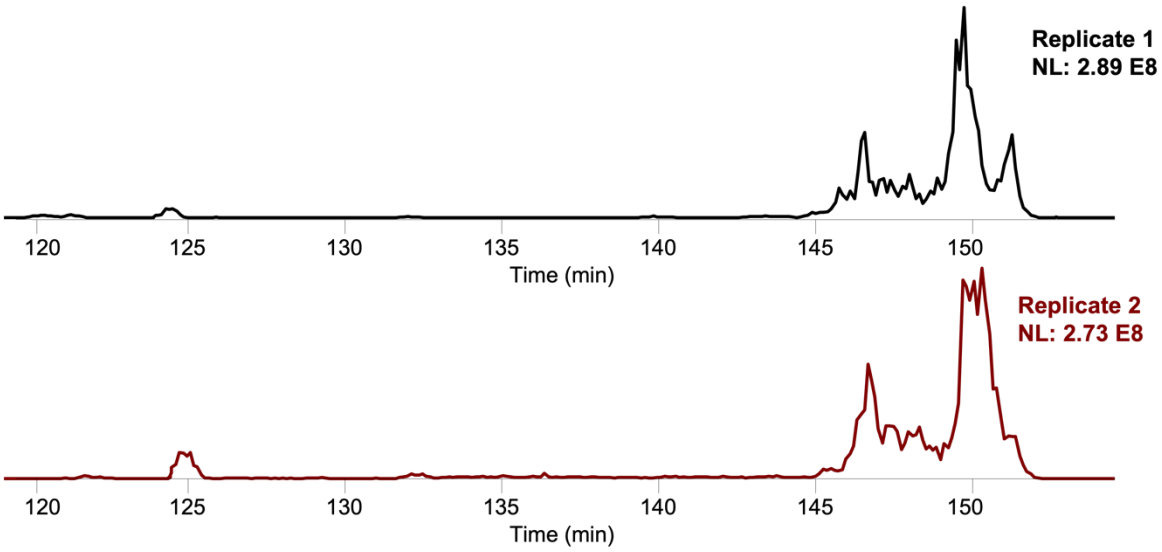

Figure 2.15 - LC chromatogram of duplicate GELFrEE depleted plasma samples (Base peak chromatogram with m/z range 800.00-1600.00)

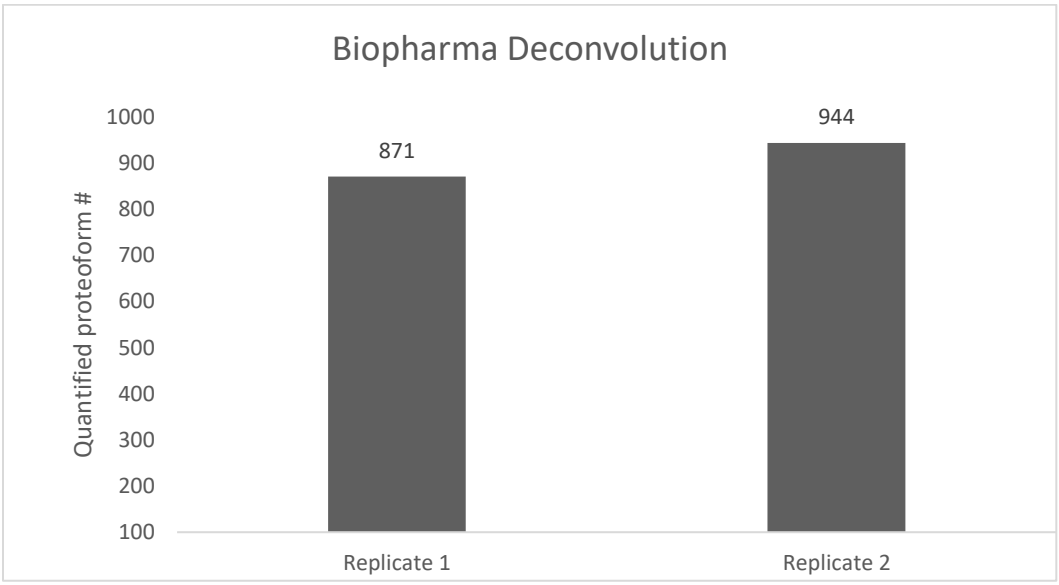

Figure 2.16 - Proteofrom quantification after GELFrEE depletion

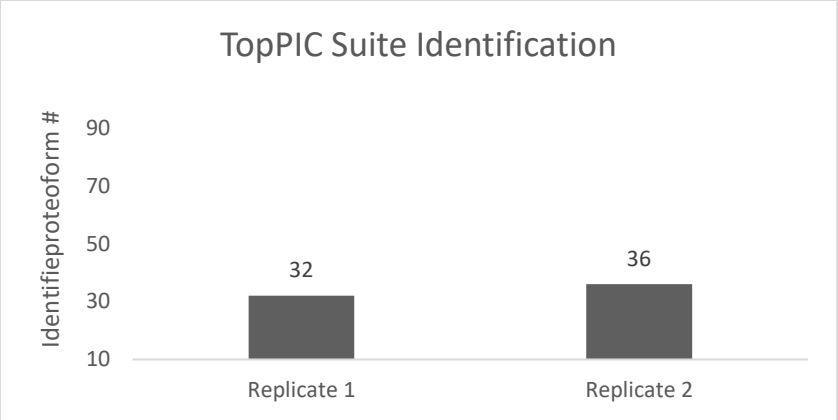

Figure 2.17 - Proteoform identification after GELFrEE depletion

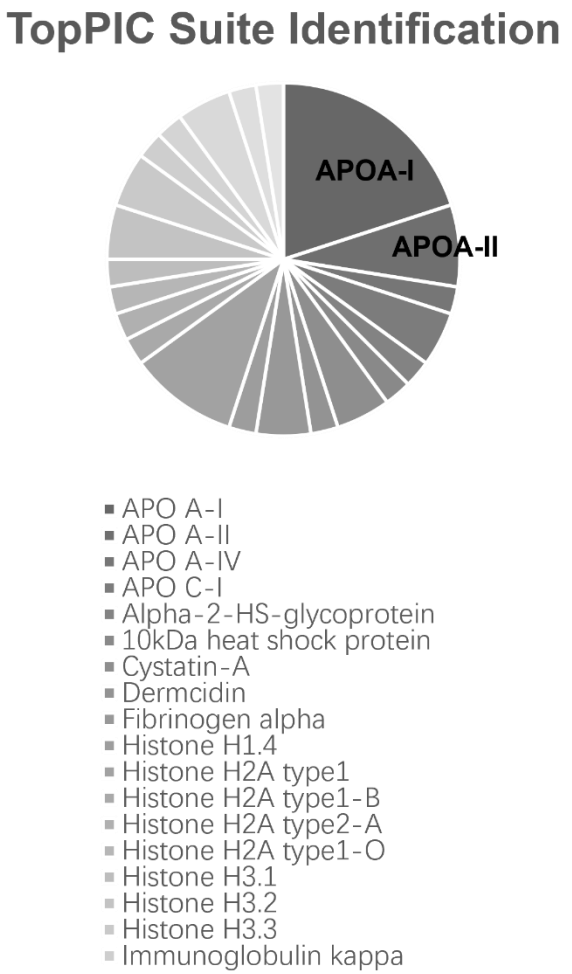

Figure 2.18 - TopPIC Suite identification result after GELFrEE depletion

Protein	# of proteoform identified
APO A-I	8
APO A-II	3
APO A-IV	1
APO C-I	2
Alpha-2-HS-glycoprotein	1
10kDa heat shock protein	1
Cystatin-A	2
Dermcidin	1
Fibrinogen alpha	2
Histone H1.4	1
Histone H2A type1	4
Histone H2A type1-B	1
Histone H2A type2-A	1
Histone H2A type1-O	1
Histone H3.1	1
Histone H3.2	2
Histone H3.3	2
Immunoglobulin kappa	1
plasma protease C1	1
Polyubiquitin-B	2
Polyubiquitin-C	1
Submaxillary gland androgen-regulated protein 3B	1

Figure 2.19 - TopPIC Suite Identification numbers after GELFrEE depletion

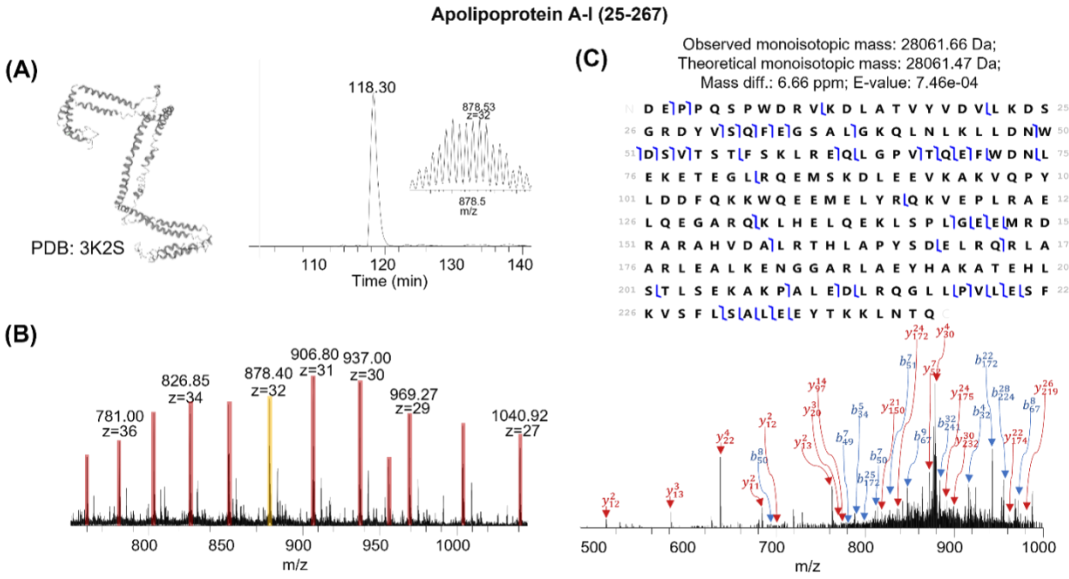

Figure 2.20 - MS detection and MS/MS identification of Apolipoprotein A-I (25-267). (A) Protein structure and extracted ion chromatogram (EIC) with isotopic distribution; (B) charge envelope; yellow highlight represents precursor ion for MS2 fragmentation, red and yellow highlights represent charge envelope (C) Protein sequence and MS/MS spectrum

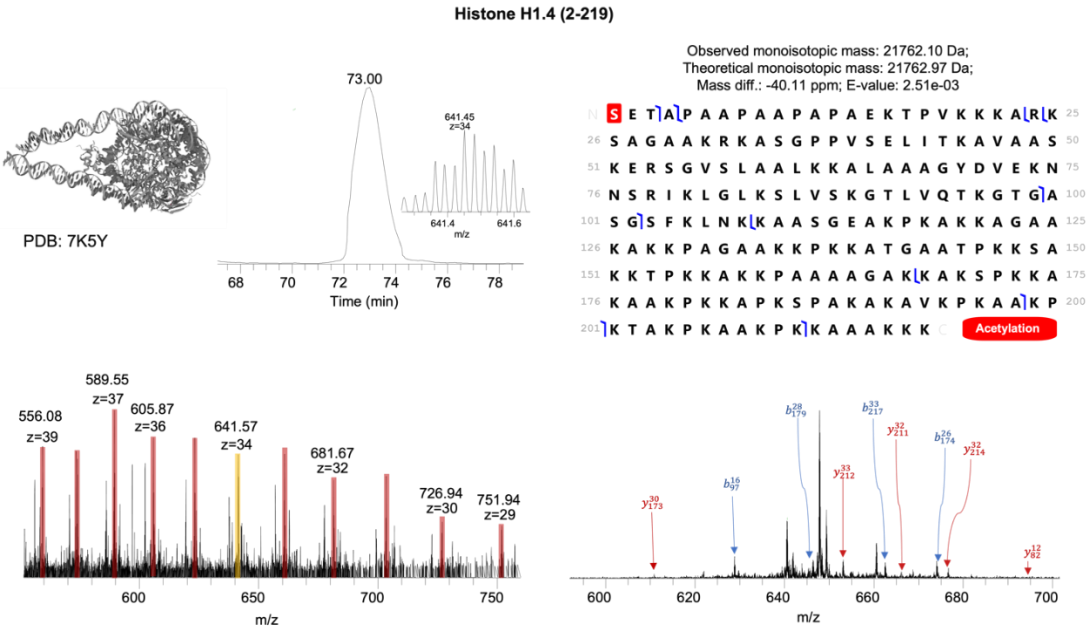

Figure 2.21 - MS detection and MS/MS identification of Histone H1.4 (2-219). Full MS spectrum of proteoform and the extracted ion chromatogram (EIC) are shown. (A) Protein structure and extracted ion chromatogram (EIC) with isotopic distribution; (B) charge envelope; yellow highlight represents precursor ion for MS2 fragmentation, red and yellow highlights represent charge envelope (C) Protein sequence and MS/MS spectra with the known post-translational modification (acetylation) at the 2nd serine residue

2.4 Conclusion

Proteominer™ is a highly reproducible and efficient fractionation method which enables analysis of low abundance proteins in plasma with a highly diverse library of combinatorial hexapeptide ligands[80]. In our studies, Proteominer successfully and reproducibly depleted HSA and other high-abuandance proteins and efficiently compressed the dynamic range of plasma proteins, allowing simultaneous characterization of an extensive range of proteins. We will further evaluate the enrichment efficiency of Proteominer using mass spec-based top-down proteomics.

Organic precipitation was also demonstrated to be an effective, reproducible, and cost-friendly method based on the principle that organic solvents will denature and aggregate large and highly abundant proteins[96]. However, low specificity and yield were observed, which may result in the loss of relevant proteoforms. Further optimization of organic precipitation for low concentration is needed.

GELFrEE has shown high efficiency and good reproducibility in removing high MW proteins from human plasma. Furthermore, many proteoforms of low abundance proteins were identified and quantified using GELFrEE fractionation techniques, making it a good method for further studies of the intact plasma proteome.

Our results suggest that all three depleting/enrichment approaches can be applied to study low abundance proteins in plasma samples using top-down proteomics approaches. In future studies, we will perform a more detailed comparison of the three approaches using both bottom-up and top-down proteomics. Moreover, we will evaluate the possibility of integrating these approaches for deeper proteome sequence coverage.

Chapter 3: Application of Top-down Human Plasma Thermal Proteome Profiling (TPP)

3.1 Introduction

Thermal Proteome Profiling (TPP) is a stability proteomics method that utilizes thermal stability to characterize proteins. TPP was first introduced by Savitski et al in 2014[19] and is based on the principle that when a protein is exposed a temperature gradient, it will denature and subsequently aggregate[19]. This method has been applied to analyze the thermal stability of proteins various systems such as cell lysate, whole blood, and tissue[24]. Here, we have adapted and applied TPP to human plasma to discover the thermal stability features and melting behaviors of plasma proteins at a global scale.

Generally, quantitative bottom-up (BU) proteomics methods are utilized to determine the melting temperature of each protein[23]. However, BU may result in the loss of information that can be obtained from intact proteoform such as post-translational modification (PTM). Top-down (TD) proteomics, however, analyzes the intact proteoforms and can identify and localize PTMs. Here, we applied top-down proteomics methods to thermal proteome profiling (TD-TPP) to elucidate stability of the intact plasma proteoforms. TD TPP analysis is expected to enable the functional characterization of low-abundance clinically relevant proteins. However, it is challenging to elucidate low-abundance proteins in human plasma because high-abundant proteins often mask the detection of low-abundant proteins. In Chapter 2, I systematically evaluated and optimized a depletion protocol to efficiently remove high-abundant proteins in human plasma samples using GELFrEE prior to proteomics analysis.

In this chapter, I have developed and optimized a TD-TPP platform that integrates GELFrEE protein enrichment for intact analysis of functional plasma proteoforms.

3.2 Methods

3.2.1 Materials

Sodium dodecyl-sulfate polyacrylamide gel electrophoresis (SDS-PAGE) kit, acrylamide (AA)/Bis solution, and ammonium persulfate (APS), tetramethyl ethylenediamine (TEMED) were purchased from BioRad (Hercules, CA). GELFrEE kit has been primarily purchased from Expedeon (Cambridge, AS) and 5X Tris-acetate sample buffer was provided by the GELFrEE manufacturer. LC/MS CHRAMASOLV® grade HPLC Water, Isopropanol (IPA), acetonitrile (ACN), methanol (MeOH) and ACS reagent acetic acid (HAc) were purchased from Sigma-Aldrich (St. Louis, MO). Dithiothreitol (DTT), Phosphate buffered saline (PBS), 2-(4-(2-hydroxyethyl)-1-piperazinyl)-ethanesulfonic acid (HEPES), SDS, and Stains-all powder were also purchased from Sigma-Aldrich (St. Louis, MO). Pierce™ Bicinchoninic acid (BCA) protein assay kit, Pierce™ detergent removal spin column, Pierce™ Trifluoro-acetic acid (TFA), human plasma, and Coomassie protein assay reagent were purchased from Thermo Scientific (Hanover Park, IL).

3.2.2 Top-down Human Plasma TPP

The workflow is shown in the **Figure 3.1** (Created with Biorender). Plasma (50 μg/μL) was centrifuged at 13,000 rpm (4°C) for 60 minutes using a 5804 R centrifuge from Eppendorf (Enfield, CT). The supernatant was collected and diluted 2 times using 1X PBS (pH 7.4). The diluted solution was aliquoted to six PCR tubes and individually heated using MJ Research PTC-

200 thermocycler from Marshall Scientific (Hampton, NH) at 0, 37, 50, 63, 76, 89°C for 10 minutes. The samples were cooled to room temperature for 3 minutes and then placed on ice. The samples were then centrifuged at 10,000 rpm (4°C) using an Eppendorf F-45-58-PCR rotor for 60 minutes and the resulting supernatant was collected. The supernatant was centrifuged once more at 13,000 rpm (4°C) using an Eppendorf S-4-72 rotor for 30 minutes and the final supernatant was collected. 100X diluted TPP samples with 1X PBS (pH 7.4) were analyzed by Bradford Assay *(2. Bradford assay)* to discover the protein concentration. 25X diluted TPP samples with 1X PBS (pH 7.4) were analyzed by SDS-PAGE *(3. Sodium Dodecyl-Sulfate Polyacrylamide Gel Electrophoresis (SDS-PAGE))* to visualize protein pattern.

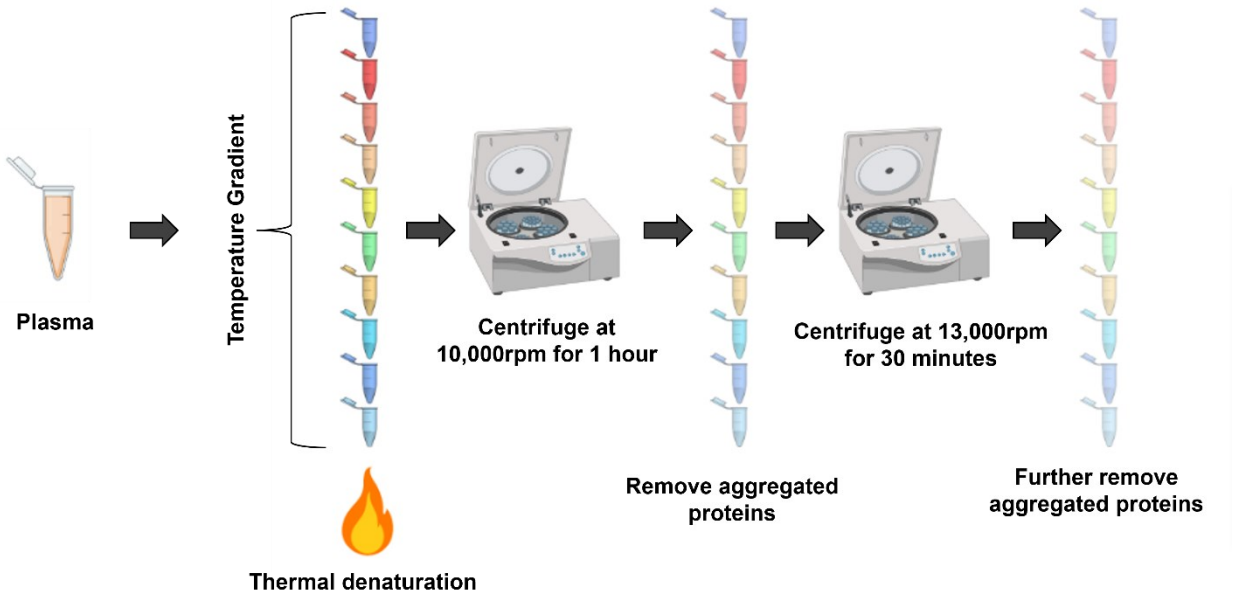

Figure 3.1 - Top-down plasma TPP workflow prior to GELFrEE depletion and LC/MS-MS analysis

3.2.3 GELFrEE Fractionation

The workflow for GELFrEE fractionation of plasma TPP samples is shown in **Figure 3.2** (Created with Biorender). 100 µL of TPP samples were mixed with 8 µL of DTT and 30 µL of 5X Tris-acetate sample buffer. This samples were diluted to 150 µL with 1X PBS (pH 7.4). The GELFrEE kit was disassembled, and the glass tubes were filled with 265 µL of resolving gel and 540 µL stacking gel. Resolving gel was made up of 7.2 mL of 30% AA/Bis solution, 2.25 mL of DDI water, 240 µL of 10% SDS solution, 6.5 mL of 40% glycerol solution, 2.25 mL of 3 M Tris-HCl solution (pH 8.8), 200 µL of APS, and 12 µL TEMED. Stacking gel was made up of 1.8 mL of 30% AA/Bis Solution, 9.45 mL of DDI water, 240 µL of 10% SDS Solution, 0.75 mL of 1M Tris-HCl solution (pH 6.8) was mixed, then 120 µL APS solution and 12 µL TEMED solution were added. The gels were left undisturbed to solidify for 30 minutes and reassembled.

After reassembling, 6 mL of 1X HEPES buffer was added to the cathode chambers, 8 mL was added to the anode chambers, and 150 µL was added to the sample collection chambers. Then, the prepared samples were added to the sample loading chambers. The cartridge was placed into the GELFrEE instrument from Expedeon (Cambridge, AS), and the electrode array was lowered by closing the lid. The optimized method is shown in **Table 2.2**.

SDS-PAGE was conducted to observe protein bands from each fraction. Fractions 1 to 3 were combined for further analysis. Fraction 4 through 6 contained high amounts of has and were not further analyzed. Protein concentration of combined fractions was measured by Bradford Assay.

SDS removal was performed using Pierce^{TM} detergent removal spin columns. Briefly, the column was washed by adding 300 µL of 20% EtOH, Milli-Q water, and 1X PBS, respectively, to each tube and centrifuging at 13,000 rpm for 2 minutes (4°C). Each was step was repeated three

times. Then, combined fractions were added to the column and centrifuged at 13,000 rpm for 2 minutes (4°C). Sample was filtered through the column twice to completely remove SDS. Final eluent was collected and protein concentration was analyzed using a Bradford assay and SDS-PAGE.

After SDS removal, SDS quantitation was conducted to ensure SDS was removed prior to LC-MS/MS. Stains-all stock solution was prepared by adding 500 µL IPA and 500 µL MilliQ water to 1 mg of Stains-all powder. Stains-all intermediate solution was prepared by adding stains-all stock solution and formamide at an 18:1 ratio to Milli-Q water. 2 µL of samples and 1, 0.5, 0.25, and 0.125% SDS standards were added to 200 µL of stains-all intermediate solution each well on 96 well plate. The plate was analyzed at 438nm using an Infinite M299 spectrophotometer from Tecan (Männedorf, Switzerland). Absorbance was plotted against SDS concentration plot to determine linear range of quantitation. Final SDS concentration for the sample should be lower than the detection limit to prepare the sample for MS analysis. Confirming remained SDS in the samples are under detection limit, data acquisition was perform using top-down RPLC-MS/MS.

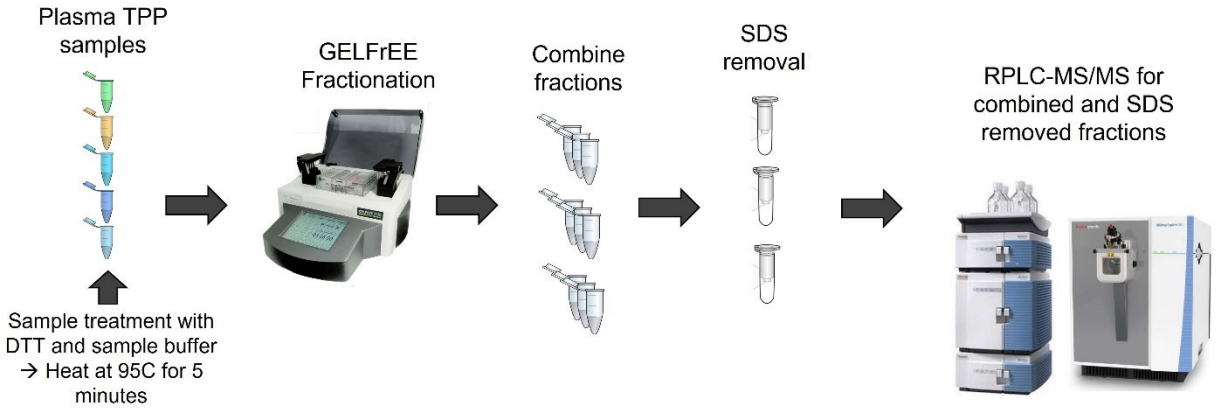

Figure 3.2 - GELFrEE depletion on plasma TPP samples workflow

3.2.4 Top-down Liquid Chromatography – Mass Spectrometry (LC-MS)

The packing materials for packing C5 (Jupiter particles, 5 μm diameter, 300 Å pore size) and C18 (Jupiter particles, 5 μm diameter, 300 Å pore size) columns were purchased from Phenomenex (Torrance, CA).

Top-down RPLC-MS/MS was performed using a modified Accela LC system from Thermo Scientific (Waltham, MA) and Orbitrap Exploris 240 mass spectrometer with positive mode from Thermo Fisher Scientific (Hanover Park, IL, Bremen, Germany). C2 capillary from CoAnn Technologies (100 μm i.d., 30 cm length, 3 μm diameter, 300 Å pore size) was used for all RPLC separation. The mobile phase A (MPA) was 0.01% TFA, 0.585% Hac, 2.5% IPA and 5% I in HPLC water, and mobile phase B (MPB) was 0.01% TFA, 0.585% HAc, 45% IPA, 45% ACN in HPLC water. 50 μL of sample was loaded to solid phase extraction (SPE) column (trapping column, 150 μm i.d., 5 cm length, Jupiter particles, 5 μm diameter, 300 Å pore size), respectively. Total 100 minutes gradient from 15 % to 85 % MPB was performed with 0.4 μL/minute LC flow rate. The column was flushed with 90% MPB over 10 minutes and equilibrated to 3% of MPA for 30 minutes. The eluent was analyzed using an Orbitrap Exploris 240 mass spectrometer (Thermo Fisher Scientific, Bremen, Germany) with following parameters: inlet capillary temperature was 275 °C; spray voltage was 3.0 kV; resolution for MS1 and MS2 was set to 120, 000 and 60, 000, respectively; AGC target was 1×E6 with 2 microscans for both MS1 and MS2 scans. Maximum injection time was 500 ms for MS1 and 300 ms for MS2 scans; the isolation window was set as 2 m/z. Dynamic exclusion was 90 s; top 6 most abundant precursor ion peaks with charge 4-50 in MS1 scans were selected for MS2 fragmentation with a normalized collision energy of 32%. Xcalibur 3.0 software (Thermo Fisher Scientific) was used for LC-MS/MS data collection.

3.3.5 Data Analysis

Data sets were deconvoluted with Biopharma finder (Thermo Fisher Scientific) for quantifying the mass feature, then searched against human protein database (Uniprot 2020-07-11, 20368 species) with TopPIC Suite for proteoform identification[81,82]. MSConvert (Proteowizard, Framingham, MA) was used to convert MS raw files to mzML format[83]. TopFD deconvolution was set with MS1 signal-to-noise ratio of 3.0, MS2 signal-to-noise of 1.0, the precursor window size as 3.0 m/z, maximum mass as 500,000 Dalton, maximum charge 50, and m/z error 0.02. TopPIC were performed with decoy database searching, FDR cutoff 0.01 for spectrum, proteoform level, maximum number of mass shifts of 1, mass shift range is ± 500 Dalton. Parameters not given were default.

3.4 Results

3.4.1 Top-down Human Plasma TPP Results

Human plasma proteins were heated, and soluble fractions were collected through centrifugation. Bradford assay results showed that the protein concentrations decreased from 38.51 μg/μL to below the limit of quantitation as the temperature increased from 0 °C to 89°C **(Table 3.1 and Figure 3.3).** 40 μL of sample from each temperature was loaded onto SDS-PAGE for analysis and SDS-PAGE results showed that the bands became lighter as the temperature increased, indicating that aggregate proteins were removed from the fractions at high temperatures **(Figure 3.4).**

3.4.2 Removal of High-abundance Proteins using GELFrEE

TPP treated plasma proteins at each temperature point (0, 37, 50, 63, 76, 89ºC) were fractionated individually using GELFrEE with the optimized method discussed in Chapter 2.4.2. SDS-PAGE results showed that HSA was not eluted in the first 2 fractions for all the temperatures and only a small amount of HSA was observed in fraction 3 **(Figure 3.5).** Therefore, fractions 1-3 were combined for each temperature for further analysis. SDS was removed using Pierce detergent removal columns and samples were analyzed using SDS-PAGE **(Figure 3.6).** The trend in protein concentration observed after heating was preserved. Protein concentration was measured using a Bradford assay (**3.2)** and the concentrations for each temperature after SDS removal was plotted **(Figure 3.7)**. The plasma protein concentration proteins across the temperature gradient indicating that the trend observed in the original TPP platform was preserved throughout sample preparation.

3.4.3 LC-MS/MS Results

Overall, 903 ± 304 proteoforms from 64 ± 39 proteins were identified from LC-MS/MS analysis of the GELFrEE fractionated TPP serum samples **(Figure 3.8 and Figure 3.9).** I found that a higher number of proteoforms were deconvoluted at higher temperature (76 and 89 ºC) compared with lower temperatures. This was unexpected as the total protein concentration decreased and the number of protein bands observed in SDS-PAGE decreased which would typically demonstrate fewer proteoforms. I performed an analysis of the breakdown of mass features deconvoluted in each temperature by mass. **Figure 3.10** shows the number of quantified proteoforms deconvoluted at different TPP temperatures separated by monoisotopic mass. At higher temperature 76 and 89 ºC, a higher number of small molecular weight <5 kDa proteoforms were deconvoluted. The

unique feature of top-down proteomics discovered that <5 kDa proteoforms are fragmented to smaller pieces due to heating, which caused the higher number of deconvolution and identification.

Detailed compositions of identified proteins for each temperature are shown in **Figure 3.11 and Figure 3.12.** Most of the proteins that were identified after the organic precipitation were low abundant plasma proteins including Alpha-1-antichymotrypsin, APOA-II, APOC-I, APOC-II, APOC-III, Complement C4-A, Dermcidin, Inter-alpha-trypsin inhibitor heavy chain H4, Kininogen-1, Plasma protease C1 inhibitor, Plasma serine protease inhibitor, Polyubiquitin-B, Polyubiquitin-C, Thymosin beta-4, Transthyretin, Ubiquitin-40S ribosomal protein S27. Fibrinogen alpha chain, Fibrinogen beta chain, Immunoglobulin kappa constant, Immunoglobulin lambda constant 7, which are high abundant proteins, were also identified after the depletion, but with the low intensity. These results show that GELFrEE successfully depleted high abundance protein and enabled the detection of the low abundant proteins.

An intact proteoform identified using the TD-TPP platform was apolipoprotein C-I (10-83) without part of signal peptides[97] **(Figure 3.13). Figure 3.12 (A)** shows the EICs at each temperature point (0, 37, 50, 63, 76, 89 ºC) with fixed scale of 1.33 E6. **Figure 3.12 (B)** shows the isotopic distribution at each temperature point (0, 37, 50, 63, 76, 89 ºC). Figure 3.13 (C) shows the Full MS intensity trends as the temperature increases. Figure 3.13 (D) shows the crystal structure (PDB: 1IOJ). **Figure 3.13 (E)** shows the Apolipoprotein C-I sequence and MS/MS spectra. The EIC decreased as the temperature increased, and showed even lower intensity when it comes to 76 and 89ºC. The intensity increased at 63ºC, and further experiment is needed to determine if this phenomenon is repeating.

Apolipoprotein C-I works as an inhibitor of lipoprotein which binds to the low density lipoprotein (LDL) receptor[98]. Human plasma apolipoprotein C-I was discovered as a novel diagnostic and prognostic biomarker for gastric cancer[90].

One low abundance protein identified in the LC-MS/MS apolipoprotein C-II (20-101) with the cleavage of the signal peptides[99]**(Figure 3.14). Figure 3.13 (A)** shows the EIC at each temperature point (0, 37, 50, 63, 76, 89 ºC) with fixed scale of 1.28 E6. **Figure 3.13 (B)** shows the isotopic distribution at each temperature points (0, 37, 50, 63, 76, 89 ºC). **Figure 3.13 (C)** shows the Full MS intensity trends as the temperature increases. **Figure 3.13 (D)** shows the crystal structure (PDB: 1I5J). **Figure 3.13 (E)** shows the Apolipoprotein C-II sequence and MS/MS spectra with unknown mass shift of 248.4673 Da. Similar to the first example, the EIC decreased as the temperature increased, and showed even lower intensity when it comes to 76 and 89ºC.

Apolipoprotein C-II is a component of chylomicrons, very low-density lipoproteins (VLDL), low-density lipoproteins (LDL), and high-density lipoproteins (HDL) in plasma[100]. The protein plays an important role in lipoprotein metabolism as an activator of lipoprotein lipase. Both apolipoprotein C-I and apolipoprotein C-II can activate lipoprotein lipase[100]. The protein is predicted to serve as a prognostic biomarker in cancer[101].

Figure 3.15 shows the identified proteoform immunoglobulin kappa constant fragment (52-107), one of the highly abundant proteins in human plasma[102]. It may be from endogenous proteolysis process or heat-induced degradation, which cannot be observed using the bottom-up TPP approaches. Further experiments should be done to assess it further. Figure 3.15 (A) shows the extracted ion chromatogram (EIC) at each temperature points (0, 37, 50, 63, 76, 89 ºC) with fixed scale of 1.61 E6. Figure 3.15 (B) shows the isotopic distribution at each temperature points (0, 37, 50, 63, 76, 89 ºC). Figure 3.15 (C) shows the Full MS intensity trends as the temperature

increases. Figure 3.15 (D) shows the structure from Uniprot (PDB: 1CLJ). Figure 3.15 (E) shows the Immunoglobulin kappa constant sequence and MS/MS spectra with a mass shift of 2 Da, which is caused by the formation of a disulfide bond between two cysteine residues. Immunoglobulin kappa constant is a constant region of immunoglobulin light chain, which is a membrane-bound antibodies produced by B lymphocytes[103].

Table 3.1 - Bradford assay result of plasma TPP

Temperature (°C)	Absorbance (Abs.) 1 (nm)	Concentrati-on (Conc.) 1 (µg/ µL)	Abs. 2 (nm)	Conc.2 (µg/ µL)	Average Conc. (µg/ µL)	Original Conc. (µg/ µL)
0	0.66	0.39	0.65	0.37	0.38	38.51
37	0.61	0.31	0.65	0.39	0.35	35.25
50	0.63	0.35	0.64	0.36	0.35	35.65
63	0.66	0.39	0.65	0.37	0.38	38.89
76	0.56	0.20	0.55	0.19	0.20	20.15
89	0.42	-0.03	0.40	-0.07	-0.05	-5.82

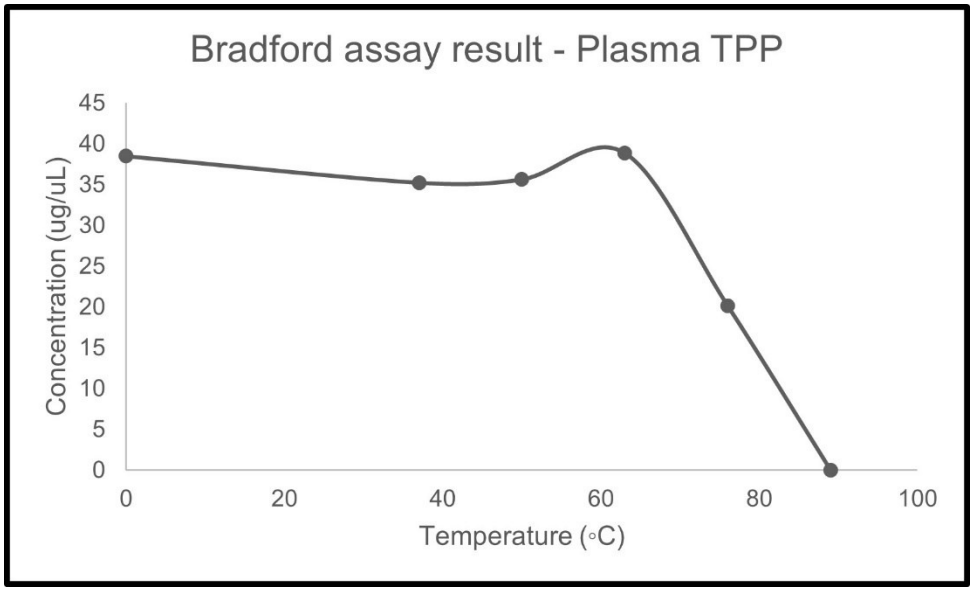

Figure 3.3 - Bradford assay result of plasma TPP

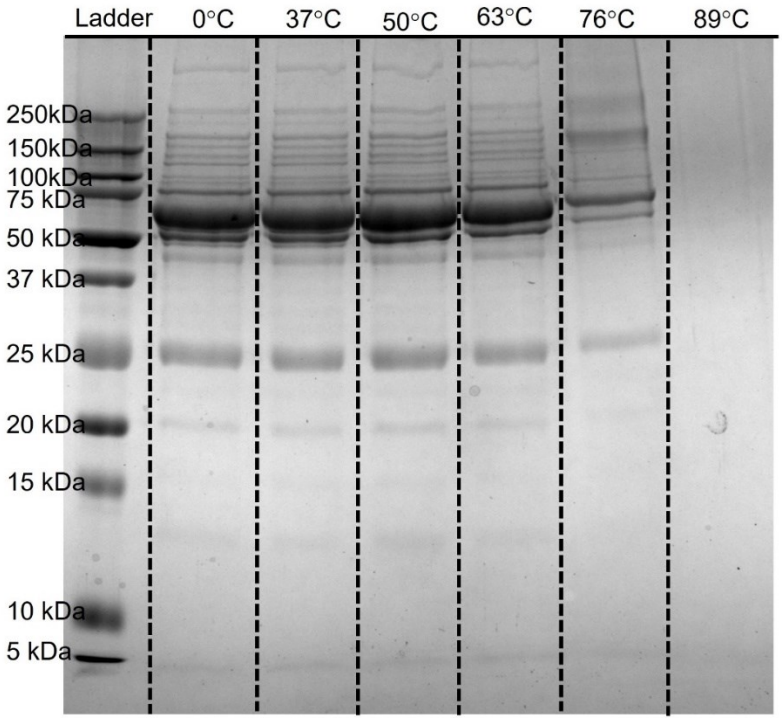

Figure 3.4 - SDS-PAGE of TPP plasma samples

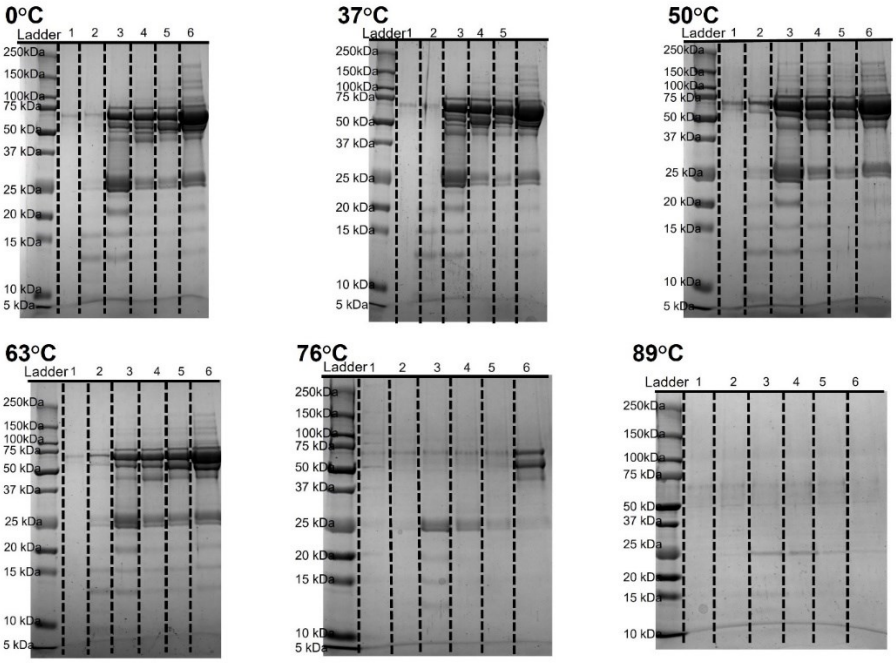

Figure 3.5 - SDS-PAGE results of GELFrEE depleted TPP samples

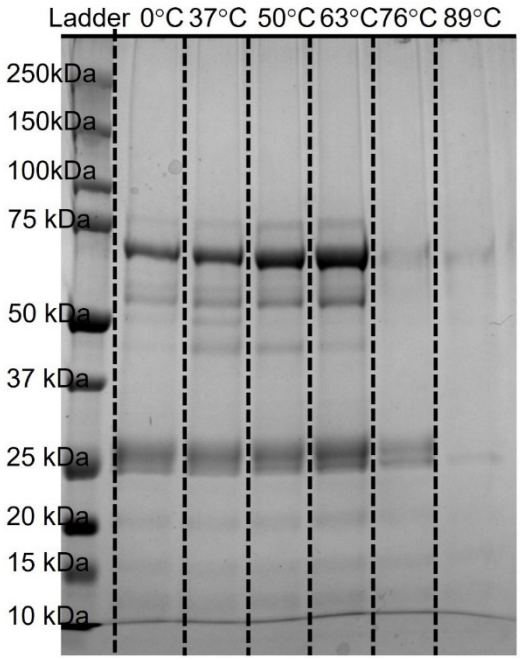

Figure 3.6 - SDS-PAGE result of combined and SDS removed GELFrEE fractions for each temperature

Table 3.2 - Bradford assay result of combined fractions after GELFrEE depletion and SDS removal

Temperature (°C)	Combined fractions concentration (µg/µL)	After SDS removal concentration (ug/uL)
0	0.50	0.27
37	0.51	0.26
50	0.59	0.32
63	0.65	0.32
76	0.42	0.05
89	0.11	0

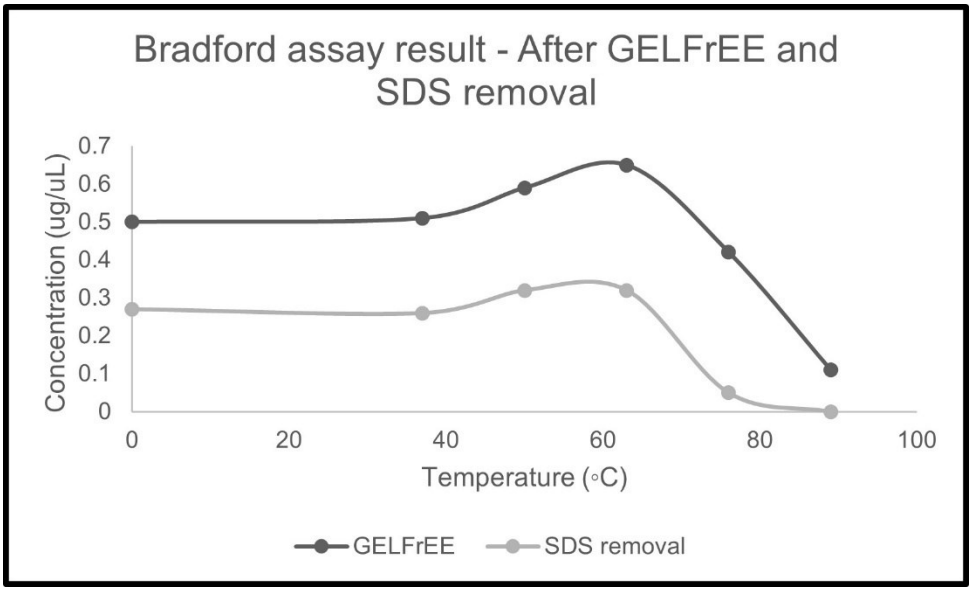

Figure 3.7 - Bradford assay result after GELFrEE depletion and SDS removal

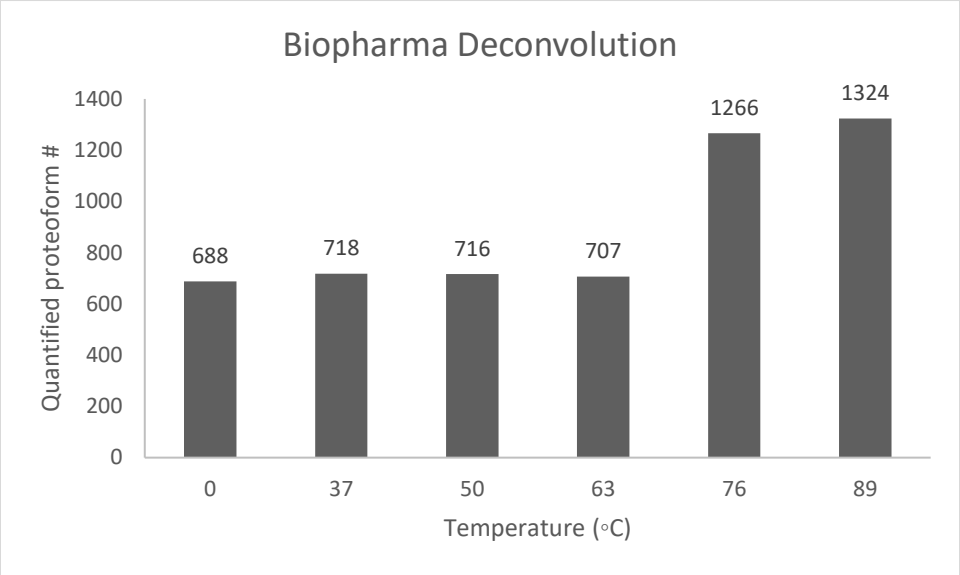

Figure 3.8 - Proteofrom quantification after TPP and GELFrEE depletion

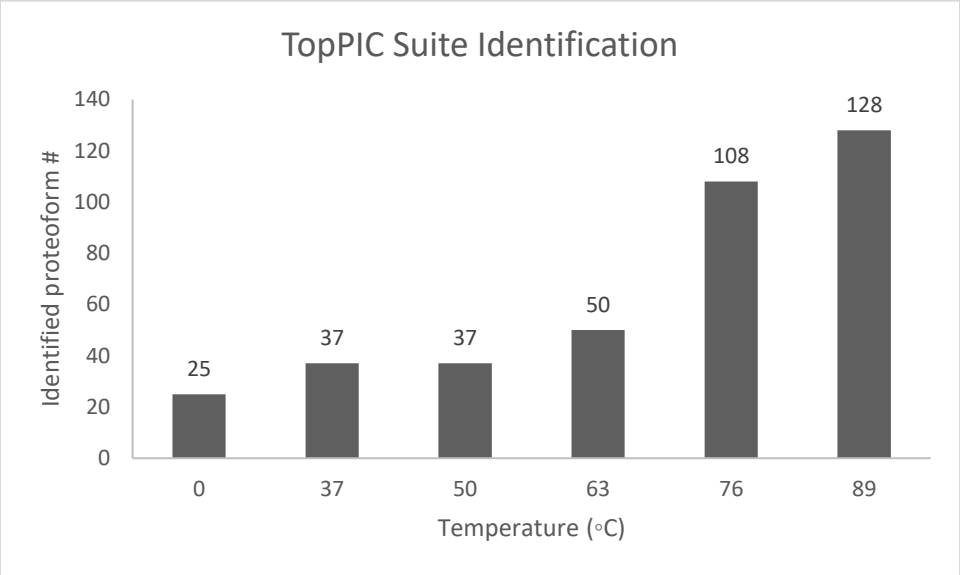

Figure 3.9 -Proteofrom identification after TPP and GELFrEE depletion

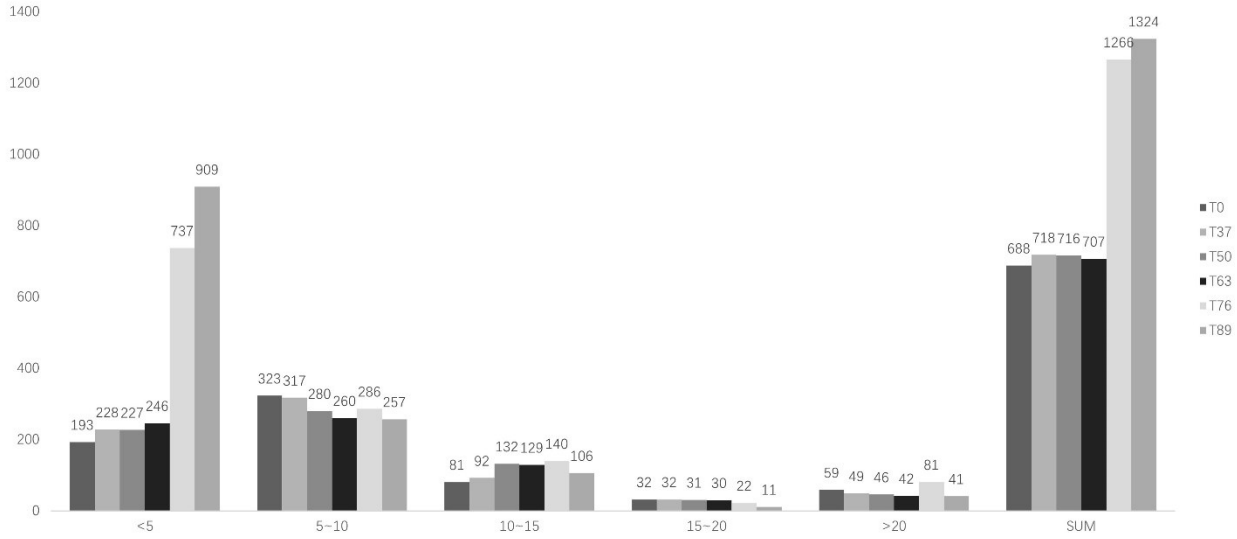

Figure 3.10 - Biopharma deconvolution results for GELFrEE depleted plasma TPP samples

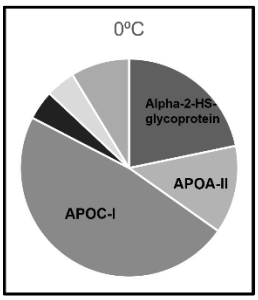

Protein	# of proteoform identified
Alpha-2-HS-glycoprotein	5
APOA-II	3
APOC-I	11
APOC-II	1
Immunoglobulin kappa constant	1
Inter-alpha-trypsin inhibitor heavy chain H4	2

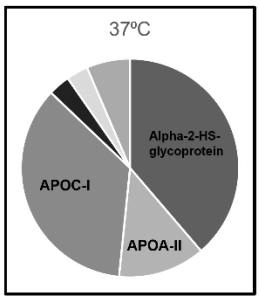

Protein	# of proteoform identified
Alpha-2-HS-glycoprotein	12
APOA-II	4
APOC-I	11
APOC-II	1
Immunoglobulin kappa constant	1
Inter-alpha-trypsin inhibitor heavy chain H4	2

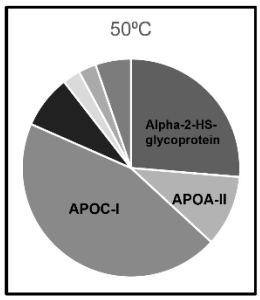

Protein	# of proteoform identified
Alpha-2-HS-glycoprotein	10
APOA-II	4
APOC-I	17
APOC-II	3
Immunoglobulin kappa constant	1
Inter-alpha-trypsin inhibitor heavy chain H4	1

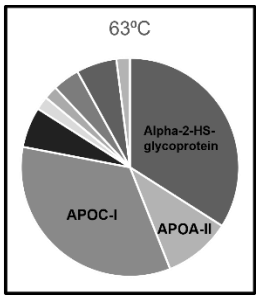

Protein	# of proteoform identified
Alpha-2-HS-glycoprotein	17
APOA-II	5
APOC-I	17
APOC-II	3
Fibrinogen alpha	1
Fibrinogen beta	1
Immunoglobulin	2
Inter-alpha-trypsin	3
Ubiquitin-60S	1

Figure 3.11 - TopPIC Suite Identification for TPP and GELFrEE treated plasma samples at 0, 37, 50, 63 ºC

Protein	# of proteoform identified
Alpha-2-HS-glycoprotein	28
Alpha-1-antichymotrypsin	4
Alpha-1-antitrypsin	2
APOA-II	6
APOC-I	29
APOC-II	5
APOC-III	3
Fibrinogen alpha chain	9
Fibrinogen beta chain	1
Haptoglobin	2
Inter-alpha-trypsin inhibitor heavy chain H4	7
Kininogen-1	1
Plasma protease C1 inhibitor	2
Polyubiquitin-B	7
Transthyretin	2

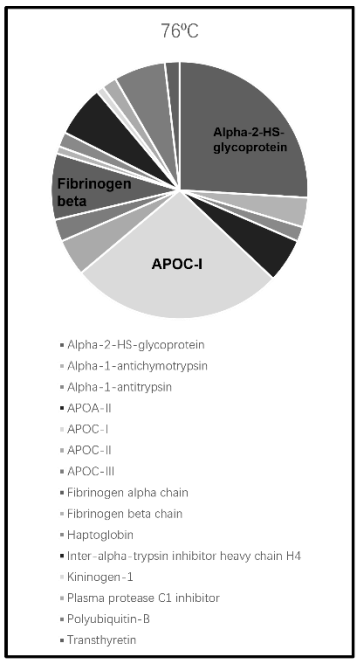

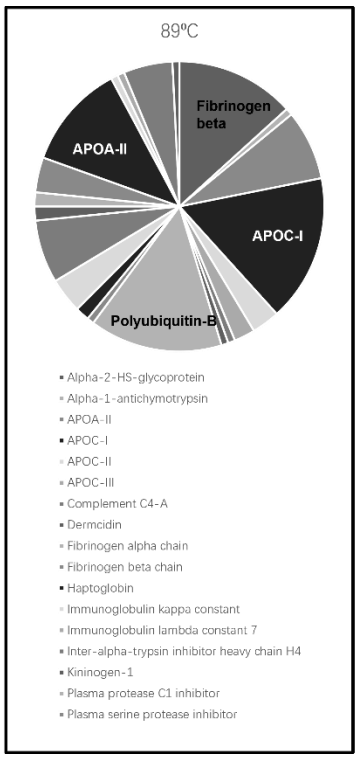

Protein	# of proteoform identified
Alpha-1-antichymotrypsin	1
APOA-II	10
APOC-I	21
APOC-II	4
APOC-III	3
Complement C4-A	1
Dermcidin	1
Fibrinogen alpha chain	19
Fibrinogen beta chain	1
Haptoglobin	2
Immunoglobulin kappa constant	5
Immunoglobulin lambda constant	7
Inter-alpha-trypsin	9
Kininogen-1	2
Plasma protease C1 inhibitor	2
Plasma serine protease inhibitor	5
Polyubiquitin-B	15
Polyubiquitin-C	1
Thymosin beta-4	1
Transthyretin	7
Ubiquitin-40S ribosomal protein S27a	1

Figure 3.12 - TopPIC Suite Identification for TPP and GELFrEE treated plasma samples at 76 and 89 ºC

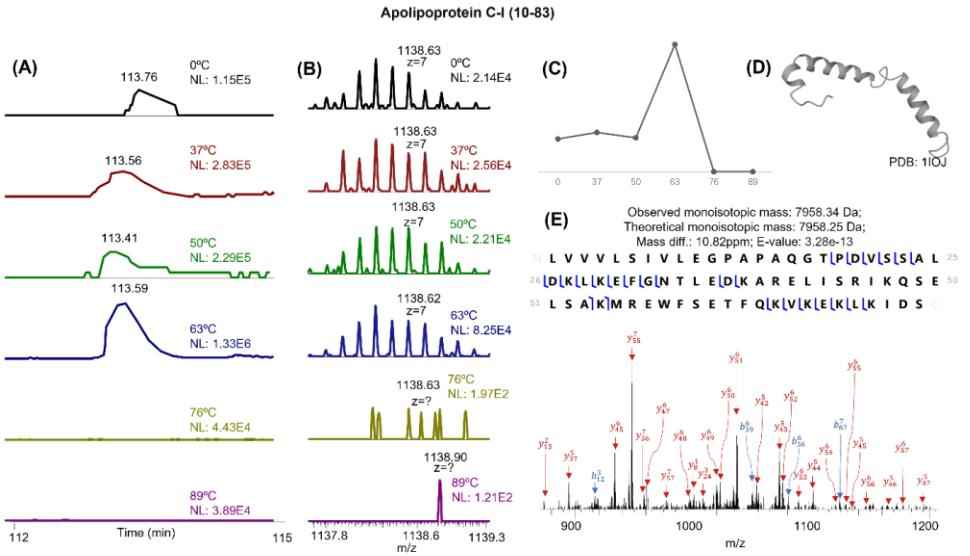

Figure 3.13 - MS detection and MS/MS identification of Apolipoprotein C-I (10-83). (A) Extracted ion chromatogram at each temperature point (0, 37, 50, 63, 76, 89 ºC) with fixed scale of 1.33 E6 (B) Isotopic distribution at each temperature points (0, 37, 50, 63, 76, 89 ºC) (C) EIC intensities at different temperatures (D)Protein structure; (E) Protein sequence and MS/MS spectra

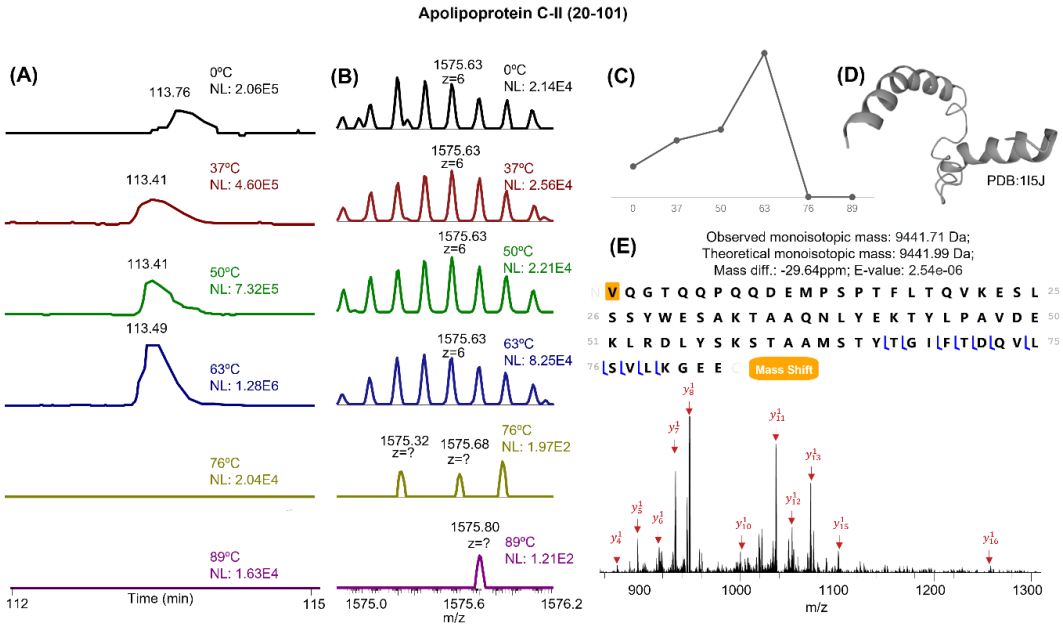

Figure 3.14 - MS detection and MS/MS identification of Apolipoprotein C-II (20-101). (A) Extracted ion chromatogram at each temperature points (0, 37, 50, 63, 76, 89 ºC) with fixed scale of 1.33 E6 (B) Isotopic distribution at each temperature points (0, 37, 50, 63, 76, 89 ºC) (C) EIC intensities at different temperatures (D)Protein structure; (E) Protein sequence and MS/MS spectra with unknown mass shift of 248.4673 Da

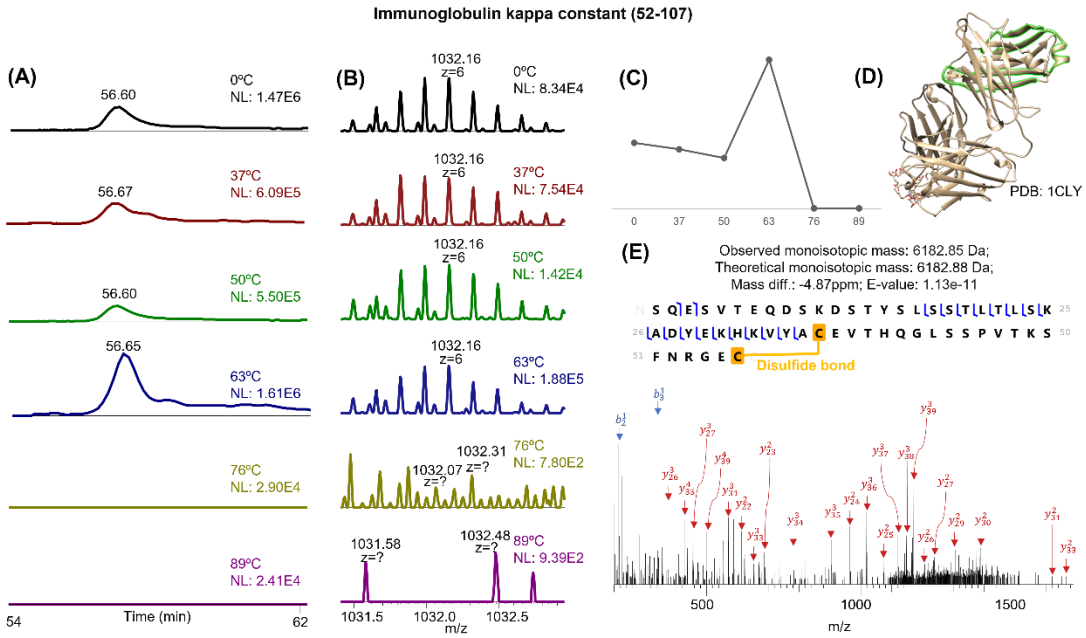

Figure 3.15 - MS detection and MS/MS identification of Immunoglobulin kappa constant (52-107). (A) Extracted ion chromatogram at each temperature points (0, 37, 50, 63, 76, 89 ºC) with fixed scale of 1.61 E6 (B) Isotopic distribution at each temperature points (0, 37, 50, 63, 76, 89 ºC) (C) Full MS spectra intensity trend (D)Protein structure; (E) Protein sequence and MS/MS spectra with unknown mass shift of -2.0303 Da

3.5 Conclusion and Discussion

I have adapted a TD-TPP platform for the analysis of the thermal stability of intact Proteoforms in human plasma samples. Plasma proteins show the typical TPP melting behavior. As the temperature increased, the proteins are denatured and aggregated; therefore, fewer proteins are observed in the soluble fractions. Additionally, GELFrEE fractionation enhanced the detection of intact low-abundance plasma proteins. Moreover, we noticed that a much higher number of small molecular weight proteoforms (<5 kDa) were detected at higher temperatures, suggesting the potential endogenous proteolysis process or heat-induced degradation, which cannot be directly observed using the classical bottom-up TPP approaches. With further optimization, this novel TD-TPP platform can elucidate the thermal stability of intact proteoforms in human plasma which may lead to a better understanding of plasma proteoform functionality and may apply to biomarker discovery.

References

(1) Schaffer, L. V.; Millikin, R. J.; Miller, R. M.; Anderson, L. C.; Fellers, R. T.; Ge, Y.; Kelleher, N. L.; LeDuc, R. D.; Liu, X.; Payne, S. H.; Sun, L.; Thomas, P. M.; Tucholski, T.; Wang, Z.; Wu, S.; Wu, Z.; Yu, D.; Shortreed, M. R.; Smith, L. M. Identification and Quantification of Proteoforms by Mass Spectrometry. *Proteomics* **2019**, *19* (10), 1800361. https://doi.org/10.1002/pmic.201800361.

(2) Aebersold, R.; Mann, M. Mass Spectrometry-Based Proteomics. **2003**, *422*, 10.

(3) Yee, A.; Chang, X.; Pineda-Lucena, A.; Wu, B.; Semesi, A.; Le, B.; Ramelot, T.; Lee, G. M.; Bhattacharyya, S.; Gutierrez, P.; Denisov, A.; Lee, C.-H.; Cort, J. R.; Kozlov, G.; Liao, J.; Finak, G.; Chen, L.; Wishart, D.; Lee, W.; McIntosh, L. P.; Gehring, K.; Kennedy, M. A.; Edwards, A. M.; Arrowsmith, C. H. An NMR Approach to Structural Proteomics. *Proceedings of the National Academy of Sciences* **2002**, *99* (4), 1825–1830. https://doi.org/10.1073/pnas.042684599.

(4) Smyth, M. S.; Martin, J. H. J. X Ray Crystallography. *Mol Pathol* **2000**, *53* (1), 8–14.

(5) *A visual approach to proteomics | Nature Reviews Molecular Cell Biology*. https://www.nature.com/articles/nrm1861 (accessed 2022-09-07).

(6) Vénien-Bryan, C.; Li, Z.; Vuillard, L.; Boutin, J. A. Cryo-Electron Microscopy and X-Ray Crystallography: Complementary Approaches to Structural Biology and Drug Discovery. *Acta Crystallogr F Struct Biol Commun* **2017**, *73* (4), 174–183. https://doi.org/10.1107/S2053230X17003740.

(7) Aebersold, R.; Mann, M. Mass-Spectrometric Exploration of Proteome Structure and Function. *Nature* **2016**, *537* (7620), 347–355. https://doi.org/10.1038/nature19949.

(8) Konermann, L.; Pan, J.; Liu, Y.-H. Hydrogen Exchange Mass Spectrometry for Studying Protein Structure and Dynamics. *Chem Soc Rev* **2011**, *40* (3), 1224–1234. https://doi.org/10.1039/c0cs00113a.

(9) Johnson, D. T.; Di Stefano, L. H.; Jones, L. M. Fast Photochemical Oxidation of Proteins (FPOP): A Powerful Mass Spectrometry-Based Structural Proteomics Tool. *J Biol Chem* **2019**, *294* (32), 11969–11979. https://doi.org/10.1074/jbc.REV119.006218.

(10) Xu, G.; Takamoto, K.; Chance, M. R. Radiolytic Modification of Basic Amino Acid Residues in Peptides: Probes for Examining Protein-Protein Interactions. *Anal Chem* **2003**, *75* (24), 6995–7007. https://doi.org/10.1021/ac035104h.

(11) Liu, X. R.; Zhang, M. M.; Gross, M. L. Mass Spectrometry-Based Protein Footprinting for Higher-Order Structure Analysis: Fundamentals and Applications. *Chem. Rev.* **2020**, *120* (10), 4355–4454. https://doi.org/10.1021/acs.chemrev.9b00815.

(12) Takamoto, K.; Chance, M. R. RADIOLYTIC PROTEIN FOOTPRINTING WITH MASS SPECTROMETRY TO PROBE THE STRUCTURE OF MACROMOLECULAR COMPLEXES. *Annu. Rev. Biophys. Biomol. Struct.* **2006**, *35* (1), 251–276. https://doi.org/10.1146/annurev.biophys.35.040405.102050.

(13) Bischof, J. C. Thermal Stability of Proteins. *Annals of the New York Academy of Sciences* **2005**, *1066* (1), 12–33. https://doi.org/10.1196/annals.1363.003.

(14) Lomenick, B.; Hao, R.; Jonai, N.; Chin, R. M.; Aghajan, M.; Warburton, S.; Wang, J.; Wu, R. P.; Gomez, F.; Loo, J. A.; Wohlschlegel, J. A.; Vondriska, T. M.; Pelletier, J.; Herschman, H. R.; Clardy, J.; Clarke, C. F.; Huang, J. Target Identification Using Drug Affinity Responsive Target Stability (DARTS). *Proceedings of the National Academy of Sciences* **2009**, *106* (51), 21984–21989. https://doi.org/10.1073/pnas.0910040106.

(15) Feng, Y.; De Franceschi, G.; Kahraman, A.; Soste, M.; Melnik, A.; Boersema, P. J.; de Laureto, P. P.; Nikolaev, Y.; Oliveira, A. P.; Picotti, P. Global Analysis of Protein Structural Changes in Complex Proteomes. *Nat Biotechnol* **2014**, *32* (10), 1036–1044. https://doi.org/10.1038/nbt.2999.

(16) *Pulse proteolysis: A simple method for quantitative determination of protein stability and ligand binding | Nature Methods*. https://www.nature.com/articles/nmeth740 (accessed 2022-09-02).

(17) Ma, R.; Meng, H.; Wiebelhaus, N.; Fitzgerald, M. C. Chemo-Selection Strategy for Limited Proteolysis Experiments on the Proteomic Scale. *Anal. Chem.* **2018**, *90* (23), 14039–14047. https://doi.org/10.1021/acs.analchem.8b04122.

(18) West, G. M.; Tang, L.; Fitzgerald, M. C. Thermodynamic Analysis of Protein Stability and Ligand Binding Using a Chemical Modification- and Mass Spectrometry-Based Strategy. *Anal Chem* **2008**, *80* (11), 4175–4185. https://doi.org/10.1021/ac702610a.

(19) Savitski, M. M.; Reinhard, F. B. M.; Franken, H.; Werner, T.; Savitski, M. F.; Eberhard, D.; Molina, D. M.; Jafari, R.; Dovega, R. B.; Klaeger, S.; Kuster, B.; Nordlund, P.; Bantscheff, M.; Drewes, G. Tracking Cancer Drugs in Living Cells by Thermal Profiling of the Proteome. *Science* **2014**, *346* (6205), 1255784. https://doi.org/10.1126/science.1255784.

(20) Meng, H.; Ma, R.; Fitzgerald, M. C. Chemical Denaturation and Protein Precipitation Approach for Discovery and Quantitation of Protein–Drug Interactions. *Anal. Chem.* **2018**, *90* (15), 9249–9255. https://doi.org/10.1021/acs.analchem.8b01772.

(21) Beusch, C. M.; Sabatier, P.; Zubarev, R. A. Ion-Based Proteome-Integrated Solubility Alteration Assays for Systemwide Profiling of Protein–Molecule Interactions. *Anal. Chem.* **2022**, *94* (19), 7066–7074. https://doi.org/10.1021/acs.analchem.2c00391.

(22) Kaur, U.; Meng, H.; Lui, F.; Ma, R.; Ogburn, R. N.; Johnson, J. H. R.; Fitzgerald, M. C.; Jones, L. M. Proteome-Wide Structural Biology: An Emerging Field for the Structural Analysis of Proteins on the Proteomic Scale. *J. Proteome Res.* **2018**, *17* (11), 3614–3627. https://doi.org/10.1021/acs.jproteome.8b00341.

(23) Reinhard, F. B. M.; Eberhard, D.; Werner, T.; Franken, H.; Childs, D.; Doce, C.; Savitski, M. F.; Huber, W.; Bantscheff, M.; Savitski, M. M.; Drewes, G. Thermal Proteome Profiling Monitors Ligand Interactions with Cellular Membrane Proteins. *Nat Methods* **2015**, *12* (12), 1129–1131. https://doi.org/10.1038/nmeth.3652.

(24) Mateus, A.; Kurzawa, N.; Becher, I.; Sridharan, S.; Helm, D.; Stein, F.; Typas, A.; Savitski, M. M. Thermal Proteome Profiling for Interrogating Protein Interactions. *Mol Syst Biol* **2020**, *16* (3). https://doi.org/10.15252/msb.20199232.

(25) Saxena, C. Identification of Protein Binding Partners of Small Molecules Using Label-Free Methods. *Expert Opinion on Drug Discovery* **2016**, *11* (10), 1017–1025. https://doi.org/10.1080/17460441.2016.1227316.

(26) Chang, J.; Kim, Y.; Kwon, H. J. Advances in Identification and Validation of Protein Targets of Natural Products without Chemical Modification. *Nat. Prod. Rep.* **2016**, *33* (5), 719–730. https://doi.org/10.1039/C5NP00107B.

(27) Mateus, A.; Määttä, T. A.; Savitski, M. M. Thermal Proteome Profiling: Unbiased Assessment of Protein State through Heat-Induced Stability Changes. *Proteome Sci* **2016**, *15* (1), 13. https://doi.org/10.1186/s12953-017-0122-4.

(28) Rolland, T.; Taşan, M.; Charloteaux, B.; Pevzner, S. J.; Zhong, Q.; Sahni, N.; Yi, S.; Lemmens, I.; Fontanillo, C.; Mosca, R.; Kamburov, A.; Ghiassian, S. D.; Yang, X.; Ghamsari, L.; Balcha, D.; Begg, B. E.; Braun, P.; Brehme, M.; Broly, M. P.; Carvunis, A.-R.; Convery-Zupan, D.; Corominas, R.; Coulombe-Huntington, J.; Dann, E.; Dreze, M.; Dricot, A.; Fan, C.; Franzosa, E.; Gebreab, F.; Gutierrez, B. J.; Hardy, M. F.; Jin, M.; Kang, S.; Kiros, R.; Lin, G. N.; Luck, K.; MacWilliams, A.; Menche, J.; Murray, R. R.; Palagi, A.; Poulin, M. M.; Rambout, X.; Rasla, J.; Reichert, P.; Romero, V.; Ruyssinck, E.; Sahalie, J. M.; Scholz, A.; Shah, A. A.; Sharma, A.; Shen, Y.; Spirohn, K.; Tam, S.; Tejeda, A. O.; Trigg, S. A.; Twizere, J.-C.; Vega, K.; Walsh, J.; Cusick, M. E.; Xia, Y.; Barabási, A.-L.; Iakoucheva, L. M.; Aloy, P.; De Las Rivas, J.; Tavernier, J.; Calderwood, M. A.; Hill, D. E.; Hao, T.; Roth, F. P.; Vidal, M. A Proteome-Scale Map of the Human Interactome Network. *Cell* **2014**, *159* (5), 1212–1226. https://doi.org/10.1016/j.cell.2014.10.050.

(29) Sahni, N.; Yi, S.; Taipale, M.; Fuxman Bass, J. I.; Coulombe-Huntington, J.; Yang, F.; Peng, J.; Weile, J.; Karras, G. I.; Wang, Y.; Kovács, I. A.; Kamburov, A.; Krykbaeva, I.; Lam, M. H.; Tucker, G.; Khurana, V.; Sharma, A.; Liu, Y.-Y.; Yachie, N.; Zhong, Q.; Shen, Y.; Palagi, A.; San-Miguel, A.; Fan, C.; Balcha, D.; Dricot, A.; Jordan, D. M.; Walsh, J. M.; Shah, A. A.; Yang, X.; Stoyanova, A. K.; Leighton, A.; Calderwood, M. A.; Jacob, Y.; Cusick, M. E.; Salehi-Ashtiani, K.; Whitesell, L. J.; Sunyaev, S.; Berger, B.; Barabási, A.-L.; Charloteaux, B.; Hill, D. E.; Hao, T.; Roth, F. P.; Xia, Y.; Walhout, A. J. M.; Lindquist, S.; Vidal, M. Widespread Macromolecular Interaction Perturbations in Human Genetic Disorders. *Cell* **2015**, *161* (3), 647–660. https://doi.org/10.1016/j.cell.2015.04.013.

(30) Beltrao, P.; Bork, P.; Krogan, N. J.; van Noort, V. Evolution and Functional Cross-Talk of Protein Post-Translational Modifications. *Molecular Systems Biology* **2013**, *9* (1), 714. https://doi.org/10.1002/msb.201304521.

(31) Duan, G.; Walther, D. The Roles of Post-Translational Modifications in the Context of Protein Interaction Networks. *PLOS Computational Biology* **2015**, *11* (2), e1004049. https://doi.org/10.1371/journal.pcbi.1004049.

(32) Tan, C. S. H.; Go, K. D.; Bisteau, X.; Dai, L.; Yong, C. H.; Prabhu, N.; Ozturk, M. B.; Lim, Y. T.; Sreekumar, L.; Lengqvist, J.; Tergaonkar, V.; Kaldis, P.; Sobota, R. M.; Nordlund, P. Thermal Proximity Coaggregation for System-Wide Profiling of Protein Complex Dynamics in Cells. *Science* **2018**, *359* (6380), 1170–1177. https://doi.org/10.1126/science.aan0346.

(33) Hashimoto, Y.; Sheng, X.; Murray-Nerger, L. A.; Cristea, I. M. Temporal Dynamics of Protein Complex Formation and Dissociation during Human Cytomegalovirus Infection. *Nat Commun* **2020**, *11* (1), 806. https://doi.org/10.1038/s41467-020-14586-5.

(34) Mateus, A.; Hevler, J.; Bobonis, J.; Kurzawa, N.; Shah, M.; Mitosch, K.; Goemans, C. V.; Helm, D.; Stein, F.; Typas, A.; Savitski, M. M. The Functional Proteome Landscape of Escherichia Coli. *Nature* **2020**, *588* (7838), 473–478. https://doi.org/10.1038/s41586-020-3002-5.

(35) Justice, J. L.; Kennedy, M. A.; Hutton, J. E.; Liu, D.; Song, B.; Phelan, B.; Cristea, I. M. Systematic Profiling of Protein Complex Dynamics Reveals DNA-PK Phosphorylation of IFI16 En Route to Herpesvirus Immunity. *Sci Adv* **2021**, *7* (25), eabg6680. https://doi.org/10.1126/sciadv.abg6680.

(36) Bagwan, N.; El Ali, H. H.; Lundby, A. Proteome-Wide Profiling and Mapping of Post Translational Modifications in Human Hearts. *Sci Rep* **2021**, *11* (1), 2184. https://doi.org/10.1038/s41598-021-81986-y.

(37) Seet, B. T.; Dikic, I.; Zhou, M.-M.; Pawson, T. Reading Protein Modifications with Interaction Domains. *Nat Rev Mol Cell Biol* **2006**, *7* (7), 473–483. https://doi.org/10.1038/nrm1960.

(38) Ardito, F.; Giuliani, M.; Perrone, D.; Troiano, G.; Lo Muzio, L. The Crucial Role of Protein Phosphorylation in Cell Signaling and Its Use as Targeted Therapy (Review). *International Journal of Molecular Medicine* **2017**, *40* (2), 271–280. https://doi.org/10.3892/ijmm.2017.3036.

(39) Reily, C.; Stewart, T. J.; Renfrow, M. B.; Novak, J. Glycosylation in Health and Disease. *Nat Rev Nephrol* **2019**, *15* (6), 346–366. https://doi.org/10.1038/s41581-019-0129-4.

(40) Huang, J. X.; Lee, G.; Cavanaugh, K. E.; Chang, J. W.; Gardel, M. L.; Moellering, R. E. High Throughput Discovery of Functional Protein Modifications by Hotspot Thermal Profiling. *Nat Methods* **2019**, *16* (9), 894–901. https://doi.org/10.1038/s41592-019-0499-3.

(41) Nishi, H.; Shaytan, A.; Panchenko, A. R. Physicochemical Mechanisms of Protein Regulation by Phosphorylation. *Front. Genet.* **2014**, *5*. https://doi.org/10.3389/fgene.2014.00270.

(42) Johnson, L. N. The Regulation of Protein Phosphorylation. *Biochemical Society Transactions* **2009**, *37* (4), 627–641. https://doi.org/10.1042/BST0370627.

(43) Azimi, A.; Caramuta, S.; Seashore-Ludlow, B.; Boström, J.; Robinson, J. L.; Edfors, F.; Tuominen, R.; Kemper, K.; Krijgsman, O.; Peeper, D. S.; Nielsen, J.; Hansson, J.; Egyhazi

Brage, S.; Altun, M.; Uhlen, M.; Maddalo, G. Targeting CDK 2 Overcomes Melanoma Resistance against BRAF and Hsp90 Inhibitors. *Mol Syst Biol* **2018**, *14* (3). https://doi.org/10.15252/msb.20177858.

(44) Smith, I. R.; Hess, K. N.; Bakhtina, A. A.; Valente, A. S.; Rodríguez-Mias, R. A.; Villén, J. Identification of Phosphosites That Alter Protein Thermal Stability. *Nat Methods* **2021**, *18* (7), 760–762. https://doi.org/10.1038/s41592-021-01178-4.

(45) Potel, C. M.; Kurzawa, N.; Becher, I.; Typas, A.; Mateus, A.; Savitski, M. M. Impact of Phosphorylation on Thermal Stability of Proteins. *Nat Methods* **2021**, *18* (7), 757–759. https://doi.org/10.1038/s41592-021-01177-5.

(46) Lenz, T.; Stühler, K. Small Molecule Arranged Thermal Proximity Coaggregation (SmarTPCA)—A Novel Approach to Characterize Protein–Protein Interactions in Living Cells by Similar Isothermal Dose–Responses. *International Journal of Molecular Sciences* **2022**, *23* (10), 5605. https://doi.org/10.3390/ijms23105605.

(47) Stein, B. D.; Huang, J. X.; Wu, D.; Cantley, L. C.; Moellering, R. E. Diverse Hotspot Thermal Profiling Methods Detect Phosphorylation-Dependent Changes in Protein Stability. bioRxiv May 1, 2021, p 2021.05.01.441686. https://doi.org/10.1101/2021.05.01.441686.

(48) King, D. T.; Serrano-Negrón, J. E.; Zhu, Y.; Moore, C. L.; Shoulders, M. D.; Foster, L. J.; Vocadlo, D. J. Thermal Proteome Profiling Reveals the O-GlcNAc-Dependent Meltome. *J. Am. Chem. Soc.* **2022**, *144* (9), 3833–3842. https://doi.org/10.1021/jacs.1c10621.

(49) Yang, X.; Qian, K. Protein O-GlcNAcylation: Emerging Mechanisms and Functions. *Nat Rev Mol Cell Biol* **2017**, *18* (7), 452–465. https://doi.org/10.1038/nrm.2017.22.

(50) Drake, W. R.; Hou, C.-W.; Zachara, N. E.; Grimes, C. L. New Use for CETSA: Monitoring Innate Immune Receptor Stability via Post-Translational Modification by OGT. *J Bioenerg Biomembr* **2018**, *50* (3), 231–240. https://doi.org/10.1007/s10863-018-9754-z.

(51) Issad, T.; Al-Mukh, H.; Bouaboud, A.; Pagesy, P. Protein O-GlcNAcylation and the Regulation of Energy Homeostasis: Lessons from Knock-out Mouse Models. *Journal of Biomedical Science* **2022**, *29* (1), 64. https://doi.org/10.1186/s12929-022-00851-w.

(52) Justice, S. A. P.; Barron, M. P.; Qi, G. D.; Wijeratne, H. R. S.; Victorino, J. F.; Simpson, E. R.; Vilseck, J. Z.; Wijeratne, A. B.; Mosley, A. L. Mutant Thermal Proteome Profiling for Characterization of Missense Protein Variants and Their Associated Phenotypes within the Proteome. *Journal of Biological Chemistry* **2020**, *295* (48), 16219–16238. https://doi.org/10.1074/jbc.RA120.014576.

(53) Mateus, A.; Bobonis, J.; Kurzawa, N.; Stein, F.; Helm, D.; Hevler, J.; Typas, A.; Savitski, M. M. Thermal Proteome Profiling in Bacteria: Probing Protein State in Vivo. *Molecular Systems Biology* **2018**, *14* (7), e8242. https://doi.org/10.15252/msb.20188242.

(54) Viéitez, C.; Busby, B. P.; Ochoa, D.; Mateus, A.; Galardini, M.; Jawed, A.; Memon, D.; Potel, C. M.; Vonesch, S. C.; Tu, C. S.; Shahraz, M.; Stein, F.; Steinmetz, L. M.; Savitski, M. M.; Typas, A.; Beltrao, P. *Towards a Systematic Map of the Functional Role of Protein Phosphorylation*; preprint; Systems Biology, 2019. http://biorxiv.org/lookup/doi/10.1101/872770 (accessed 2022-08-31).

(55) Peck Justice, S. A.; McCracken, N. A.; Victorino, J. F.; Qi, G. D.; Wijeratne, A. B.; Mosley, A. L. Boosting Detection of Low-Abundance Proteins in Thermal Proteome Profiling Experiments by Addition of an Isobaric Trigger Channel to TMT Multiplexes. *Anal. Chem.* **2021**, *93* (18), 7000–7010. https://doi.org/10.1021/acs.analchem.1c00012.

(56) Banzhaf, M.; Yau, H. C.; Verheul, J.; Lodge, A.; Kritikos, G.; Mateus, A.; Cordier, B.; Hov, A. K.; Stein, F.; Wartel, M.; Pazos, M.; Solovyova, A. S.; Breukink, E.; van Teeffelen, S.; Savitski, M. M.; den Blaauwen, T.; Typas, A.; Vollmer, W. Outer Membrane Lipoprotein NlpI Scaffolds Peptidoglycan Hydrolases within Multi-Enzyme Complexes in Escherichia Coli. *The EMBO Journal* **2020**, *39* (5), e102246. https://doi.org/10.15252/embj.2019102246.

(57) Wu, S.; Lourette, N. M.; Tolić, N.; Zhao, R.; Robinson, E. W.; Tolmachev, A. V.; Smith, R. D.; Paša-Tolić, L. An Integrated Top-Down and Bottom-Up Strategy for Broadly Characterizing Protein Isoforms and Modifications. *J. Proteome Res.* **2009**, *8* (3), 1347–1357. https://doi.org/10.1021/pr800720d.

(58) Gregorich, Z. R.; Ge, Y. Top-down Proteomics in Health and Disease: Challenges and Opportunities. **2015**, 28.

(59) Cupp-Sutton, K. A.; Wu, S. High-Throughput Quantitative Top-down Proteomics. *Mol. Omics* **2020**, 10.1039.C9MO00154A. https://doi.org/10.1039/C9MO00154A.

(60) Guo, Y.; Yu, D.; Cupp-Sutton, K. A.; Liu, X.; Wu, S. A Benchmarking Protocol for Intact Protein-Level Tandem Mass Tag (TMT) Labeling for Quantitative Top-down Proteomics. *MethodsX* **2022**, *9*, 101873. https://doi.org/10.1016/j.mex.2022.101873.

(61) Guo, Y.; Yu, D.; Cupp-Sutton, K. A.; Liu, X.; Wu, S. Optimization of Protein-Level Tandem Mass Tag (TMT) Labeling Conditions in Complex Samples with Top-down Proteomics. *Analytica Chimica Acta* **2022**, *1221*, 340037. https://doi.org/10.1016/j.aca.2022.340037.

(62) Yu, D.; Wang, Z.; Cupp-Sutton, K. A.; Guo, Y.; Kou, Q.; Smith, K.; Liu, X.; Wu, S. Quantitative Top-Down Proteomics in Complex Samples Using Protein-Level Tandem

Mass Tag Labeling. *J. Am. Soc. Mass Spectrom.* **2021**, jasms.0c00464. https://doi.org/10.1021/jasms.0c00464.

(63) Wang, Z.; Yu, D.; Cupp-Sutton, K. A.; Liu, X.; Smith, K.; Wu, S. Development of an Online 2D Ultrahigh-Pressure Nano-LC System for High-PH and Low-PH Reversed Phase Separation in Top-Down Proteomics. *Anal. Chem.* **2020**, acs.analchem.0c03395. https://doi.org/10.1021/acs.analchem.0c03395.

(64) Geyer, P. E.; Holdt, L. M.; Teupser, D.; Mann, M. Revisiting Biomarker Discovery by Plasma Proteomics. *Molecular Systems Biology* **2017**, 15.

(65) Perrin, J.; Werner, T.; Kurzawa, N.; Rutkowska, A.; Childs, D. D.; Kalxdorf, M.; Poeckel, D.; Stonehouse, E.; Strohmer, K.; Heller, B.; Thomson, D. W.; Krause, J.; Becher, I.; Eberl, H. C.; Vappiani, J.; Sevin, D. C.; Rau, C. E.; Franken, H.; Huber, W.; Faelth-Savitski, M.; Savitski, M. M.; Bantscheff, M.; Bergamini, G. Identifying Drug Targets in Tissues and Whole Blood with Thermal-Shift Profiling. *Nat Biotechnol* **2020**, *38* (3), 303–308. https://doi.org/10.1038/s41587-019-0388-4.

(66) Das, N. K.; Ghosh, N.; Kale, A. P.; Mondal, R.; Anand, U.; Ghosh, S.; Tiwari, V. K.; Kapur, M.; Mukherjee, S. Temperature Induced Morphological Transitions from Native to Unfolded Aggregated States of Human Serum Albumin. *J. Phys. Chem. B* **2014**, *118* (26), 7267–7276. https://doi.org/10.1021/jp5030944.

(67) Wu, J.; Wang, X.; Wang, Q.; Lou, Z.; Li, S.; Zhu, Y.; Qin, L.; Wei, H. Nanomaterials with Enzyme-like Characteristics (Nanozymes): Next-Generation Artificial Enzymes (II). *Chem. Soc. Rev.* **2019**, *48* (4), 1004–1076. https://doi.org/10.1039/C8CS00457A.

(68) Roth, M. J.; Plymire, D. A.; Chang, A. N.; Kim, J.; Maresh, E. M.; Larson, S. E.; Patrie, S. M. Sensitive and Reproducible Intact Mass Analysis of Complex Protein Mixtures with

Superficially Porous Capillary Reversed-Phase Liquid Chromatography Mass Spectrometry. *Anal. Chem.* **2011**, *83* (24), 9586–9592. https://doi.org/10.1021/ac202339x.

(69) Lee, J. E.; Kellie, J. F.; Tran, J. C.; Tipton, J. D.; Catherman, A. D.; Thomas, H. M.; Ahlf, D. R.; Durbin, K. R.; Vellaichamy, A.; Ntai, I.; Marshall, A. G.; Kelleher, N. L. A Robust Two-Dimensional Separation for Top-Down Tandem Mass Spectrometry of the Low-Mass Proteome. *J Am Soc Mass Spectrom* **2009**, *20* (12), 2183–2191. https://doi.org/10.1016/j.jasms.2009.08.001.

(70) Cao, Z.; Tang, H.-Y.; Wang, H.; Liu, Q.; Speicher, D. W. Systematic Comparison of Fractionation Methods for In-Depth Analysis of Plasma Proteomes. *J. Proteome Res.* **2012**, *11* (6), 3090–3100. https://doi.org/10.1021/pr201068b.

(71) Adkins, J. N.; Varnum, S. M.; Auberry, K. J.; Moore, R. J.; Angell, N. H.; Smith, R. D.; Springer, D. L.; Pounds, J. G. Toward a Human Blood Serum Proteome. *Molecular & Cellular Proteomics* **2002**, *1* (12), 947–955. https://doi.org/10.1074/mcp.M200066-MCP200.

(72) Ignjatovic, V.; Geyer, P. E.; Palaniappan, K. K.; Chaaban, J. E.; Omenn, G. S.; Baker, M. S.; Deutsch, E. W.; Schwenk, J. M. Mass Spectrometry-Based Plasma Proteomics: Considerations from Sample Collection to Achieving Translational Data. **2020**, 26.

(73) Liumbruno, G.; D'Alessandro, A.; Grazzini, G.; Zolla, L. Blood-Related Proteomics. *Journal of Proteomics* **2010**, *73* (3), 483–507. https://doi.org/10.1016/j.jprot.2009.06.010.

(74) Lee, P. Y.; Osman, J.; Low, T. Y.; Jamal, R. Plasma/Serum Proteomics: Depletion Strategies for Reducing High-Abundance Proteins for Biomarker Discovery. *Bioanalysis* **2019**, *11* (19), 1799–1812. https://doi.org/10.4155/bio-2019-0145.

(75) Millioni, R.; Tolin, S.; Puricelli, L.; Sbrignadello, S.; Fadini, G. P.; Tessari, P.; Arrigoni, G. High Abundance Proteins Depletion vs Low Abundance Proteins Enrichment: Comparison of Methods to Reduce the Plasma Proteome Complexity. *PLOS ONE* **2011**, *6* (5), e19603. https://doi.org/10.1371/journal.pone.0019603.

(76) Boschetti, E.; Righetti, P. G. The ProteoMiner in the Proteomic Arena: A Non-Depleting Tool for Discovering Low-Abundance Species. *J Proteomics* **2008**, *71* (3), 255–264. https://doi.org/10.1016/j.jprot.2008.05.002.

(77) Tran, J. C.; Doucette, A. A. Gel-Eluted Liquid Fraction Entrapment Electrophoresis: An Electrophoretic Method for Broad Molecular Weight Range Proteome Separation. *Anal Chem* **2008**, *80* (5), 1568–1573. https://doi.org/10.1021/ac702197w.

(78) Altomare, A.; Fasoli, E.; Colzani, M.; Paredes Parra, X. M.; Ferrari, M.; Cilurzo, F.; Rumio, C.; Cannizzaro, L.; Carini, M.; Righetti, P. G.; Aldini, G. An in Depth Proteomic Analysis Based on ProteoMiner, Affinity Chromatography and Nano-HPLC–MS/MS to Explain the Potential Health Benefits of Bovine Colostrum. *Journal of Pharmaceutical and Biomedical Analysis* **2016**, *121*, 297–306. https://doi.org/10.1016/j.jpba.2016.01.013.

(79) Hartwig, S.; Czibere, A.; Kotzka, J.; Paßlack, W.; Haas, R.; Eckel, J.; Lehr, S. Combinatorial Hexapeptide Ligand Libraries (ProteoMiner™): An Innovative Fractionation Tool for Differential Quantitative Clinical Proteomics. *Archives of Physiology and Biochemistry* **2009**, *115* (3), 155–160. https://doi.org/10.1080/13813450903154224.

(80) Li, L. Dynamic Range Compression with ProteoMiner™: Principles and Examples. In *Proteomic Profiling: Methods and Protocols*; Posch, A., Ed.; Methods in Molecular

Biology; Springer: New York, NY, 2015; pp 99–107. https://doi.org/10.1007/978-1-4939-2550-6_9.

(81) Kou, Q.; Xun, L.; Liu, X. TopPIC: A Software Tool for Top-down Mass Spectrometry-Based Proteoform Identification and Characterization. *Bioinformatics* **2016**, btw398. https://doi.org/10.1093/bioinformatics/btw398.

(82) Liu, Z.; Wang, R.; Liu, J.; Sun, R.; Wang, F. Global Quantification of Intact Proteins via Chemical Isotope Labeling and Mass Spectrometry. *J. Proteome Res.* **2019**, *18* (5), 2185–2194. https://doi.org/10.1021/acs.jproteome.9b00071.

(83) Chambers, M. C.; Maclean, B.; Burke, R.; Amodei, D.; Ruderman, D. L.; Neumann, S.; Gatto, L.; Fischer, B.; Pratt, B.; Egertson, J.; Hoff, K.; Kessner, D.; Tasman, N.; Shulman, N.; Frewen, B.; Baker, T. A.; Brusniak, M.-Y.; Paulse, C.; Creasy, D.; Flashner, L.; Kani, K.; Moulding, C.; Seymour, S. L.; Nuwaysir, L. M.; Lefebvre, B.; Kuhlmann, F.; Roark, J.; Rainer, P.; Detlev, S.; Hemenway, T.; Huhmer, A.; Langridge, J.; Connolly, B.; Chadick, T.; Holly, K.; Eckels, J.; Deutsch, E. W.; Moritz, R. L.; Katz, J. E.; Agus, D. B.; MacCoss, M.; Tabb, D. L.; Mallick, P. A Cross-Platform Toolkit for Mass Spectrometry and Proteomics. *Nat Biotechnol* **2012**, *30* (10), 918–920. https://doi.org/10.1038/nbt.2377.

(84) MICHAEL, S. The Isolation of Albumin from Blood Serum or Plasma by Means of Organic Solvents. *Biochemical Journal* **1962**, *82* (1), 212–218. https://doi.org/10.1042/bj0820212.

(85) Polson, C.; Sarkar, P.; Incledon, B.; Raguvaran, V.; Grant, R. Optimization of Protein Precipitation Based upon Effectiveness of Protein Removal and Ionization Effect in Liquid Chromatography-Tandem Mass Spectrometry. *J Chromatogr B Analyt Technol Biomed Life Sci* **2003**, *785* (2), 263–275. https://doi.org/10.1016/s1570-0232(02)00914-5.

(86) Sharpe, C. R.; Sidoli, A.; Shelley, C. S.; Lucero, M. A.; Shoulders, C. C.; Baralle, F. E. Human Apolipoproteins AI, AII, CII and CIII. CDNA Sequences and MRNA Abundance. *Nucleic Acids Res* **1984**, *12* (9), 3917–3932.

(87) Akerlöf, E.; Jörnvall, H.; Slotte, H.; Pousette, A. Identification of Apolipoprotein A1 and Immunoglobulin as Components of a Serum Complex That Mediates Activation of Human Sperm Motility. *Biochemistry* **1991**, *30* (37), 8986–8990. https://doi.org/10.1021/bi00101a011.

(88) Qiang, J. K.; Wong, Y. C.; Siderowf, A.; Hurtig, H. I.; Xie, S. X.; Lee, V. M.-Y.; Trojanowski, J. Q.; Yearout, D.; Leverenz, J.; Montine, T. J.; Stern, M.; Mendick, S.; Jennings, D.; Zabetian, C.; Marek, K.; Chen-Plotkin, A. S. Plasma Apolipoprotein A1 as a Biomarker for Parkinson's Disease. *Ann Neurol* **2013**, *74* (1), 119–127. https://doi.org/10.1002/ana.23872.

(89) Fuior, E. V.; Gafencu, A. V. Apolipoprotein C1: Its Pleiotropic Effects in Lipid Metabolism and Beyond. *IJMS* **2019**, *20* (23), 5939. https://doi.org/10.3390/ijms20235939.

(90) Yi, J.; Ren, L.; Wu, J.; Li, W.; Zheng, X.; Du, G.; Wang, J. Apolipoprotein C1 (APOC1) as a Novel Diagnostic and Prognostic Biomarker for Gastric Cancer. *Ann Transl Med* **2019**, *7* (16), 380. https://doi.org/10.21037/atm.2019.07.59.

(91) Witkowski, C.; Harkins, J. Using the GELFREE 8100 Fractionation System for Molecular Weight-Based Fractionation with Liquid Phase Recovery. *J Vis Exp* **2009**, No. 34, 1842. https://doi.org/10.3791/1842.

(92) *Top-down proteomics: Turning protein mass spec upside-down*. https://www.science.org/content/article/top-down-proteomics-turning-protein-mass-spec-upside-down (accessed 2022-11-07).

(93) Gauci, S.; Helbig, A. O.; Slijper, M.; Krijgsveld, J.; Heck, A. J. R.; Mohammed, S. Lys-N and Trypsin Cover Complementary Parts of the Phosphoproteome in a Refined SCX-Based Approach. *Anal Chem* **2009**, *81* (11), 4493–4501. https://doi.org/10.1021/ac9004309.

(94) Gomes, A. V.; Zong, C.; Edmondson, R. D.; Li, X.; Stefani, E.; Zhang, J.; Jones, R. C.; Thyparambil, S.; Wang, G.-W.; Qiao, X.; Bardag-Gorce, F.; Ping, P. Mapping the Murine Cardiac 26S Proteasome Complexes. *Circ Res* **2006**, *99* (4), 362–371. https://doi.org/10.1161/01.RES.0000237386.98506.f7.

(95) Scaffidi, P. Histone H1 Alterations in Cancer. *Biochimica et Biophysica Acta (BBA) - Gene Regulatory Mechanisms* **2016**, *1859* (3), 533–539. https://doi.org/10.1016/j.bbagrm.2015.09.008.

(96) Luque-Garcia, J. L.; Neubert, T. A. Sample Preparation for Serum/Plasma Profiling and Biomarker Identification by Mass Spectrometry. *Journal of Chromatography A* **2007**, *1153* (1–2), 259–276. https://doi.org/10.1016/j.chroma.2006.11.054.

(97) Shulman, R. S.; Herbert, P. N.; Wehrly, K.; Fredrickson, D. S. Thf Complete Amino Acid Sequence of C-I (ApoLp-Ser), an Apolipoprotein from Human Very Low Density Lipoproteins. *J Biol Chem* **1975**, *250* (1), 182–190.

(98) Puppione, D. L. Higher Primates, but Not New World Monkeys, Have a Duplicate Set of Enhancers Flanking Their ApoC-I Genes. *Comp Biochem Physiol Part D Genomics Proteomics* **2014**, *11*, 45–48. https://doi.org/10.1016/j.cbd.2014.08.001.

(99) Jackson, R. L.; Baker, H. N.; Gilliam, E. B.; Gotto, A. M. Primary Structure of Very Low Density Apolipoprotein C-II of Human Plasma. *Proc Natl Acad Sci U S A* **1977**, *74* (5), 1942–1945. https://doi.org/10.1073/pnas.74.5.1942.

(100) Bengtsson-Olivecrona, G.; Sletten, K. Primary Structure of the Bovine Analogues to Human Apolipoproteins CII and CIII. Studies on Isoforms and Evidence for Proteolytic Processing. *Eur J Biochem* **1990**, *192* (2), 515–521. https://doi.org/10.1111/j.1432-1033.1990.tb19255.x.

(101) Liu, Y.; Meng, Y.; Zhang, T.; Alachkar, H. Deregulation of Apolipoprotein C2 Gene in Cancer: A Potential Metabolic Vulnerability. *Clin Transl Med* **2021**, *11* (6), e406. https://doi.org/10.1002/ctm2.406.

(102) Teng, G.; Papavasiliou, F. N. Immunoglobulin Somatic Hypermutation. *Annu Rev Genet* **2007**, *41*, 107–120. https://doi.org/10.1146/annurev.genet.41.110306.130340.

(103) McHeyzer-Williams, M.; Okitsu, S.; Wang, N.; McHeyzer-Williams, L. Molecular Programming of B Cell Memory. *Nat Rev Immunol* **2011**, *12* (1), 24–34. https://doi.org/10.1038/nri3128.

Appendix

A. Standard Operating Procedures

1. BCA assay

Pierce™ BCA protein assay kit from Thermo Scientific (Hanover Park, IL) was used with bovine serum albumin (BSA) standard that is provided from manufacturer. 10uL of protein standards (1, 0.75, 0.5, 0.25, 0.125, 0.025ug/uL) and 10uL of samples are added to 200uL of kit working reagent in 96 well plate. The plate is shaken for 30 seconds at 300rpm with Thermomixer C from Eppendorf (Enfield, CT) then incubated at 37°C for 30 minutes. Plate is scanned at absorbance of 562 nm in Infinite M200 spectrometer from Tecan (Männedorf, Switzerland). Absorbance against concentration plot is generated to calculate protein mass concentration.

2. Bradford assay

Pierce™ BCA protein assay kit from Thermo Scientific (Hanover Park, IL) was used with bovine serum albumin (BSA) standard that is provided from manufacturer. 5uL of protein standards (1, 0.75, 0.5, 0.25, 0.125, 0.025ug/uL) and 5uL of samples are added to 200uL of Coomassie protein assay reagent in 96 well plate. The plate is shaken for 30 seconds at 300rpm with Thermomixer C from Eppendorf then incubated at room temperature for 20 minutes. Plate is scanned at absorbance of 562nm in Infinite M200 spectrometer. Absorbance against concentration plot is generated to calculate protein mass concentration.

3. Sodium Dodecyl-Sulfate Polyacrylamide Gel Electrophoresis (SDS-PAGE)

Gels for SDS-PAGE are in-hose stacked with a mixture of 30% AA/Bis solution, double-distilled (DDI) water, 10% SDS solution, 40% glycerol solution, 1M (pH 8.8) /3M (pH 6.8) Tris-HCl solution, APS, and TEMED.

12% running gels are made by mixing 7.2 mL of 30% AA/Bis solution, 2.25mL of DDI water, 240 µL of 10% SDS solution, 6.25 mL of 40% glycerol in water, 2.25mL of 3M Tris-HCl (pH 8.8), 120µL of 10% APS solution, and 12 µL of TEMED. The mixtures are then loaded into a mold. Then, 4% stacking gels are made by mixing 1.8mL of 30% AA/Bis, 9.45mL of DDI water, 240 µL of 10% SDS solution, 750µL of 1M Tris-HCl (pH 6.8), 200µL of APS solution, and 12 µL of TEMED. The stacking gels are then added to the top of the running gel solidified for 30 minutes.

For the sample preparation, protein samples are mixed with Laemmi sample buffer containing β-mercaptoethanol. Prepared samples are then heated at 95°C for 5 minutes with ThermoMixer C.

To run the gel, in-house stacked SDS-PAGE gels are loaded into a Mini PROTEAN Tetra Cell from Biorad. The cell is then filled with Tris/SDS/Glycine buffer. Precision Plus Protein Dual Xtra Standards protein ladder is used to indicate the known protein molecular weight. Gels are placed in Bio-Rad Power Pac and run for 1 hour and 30 minutes at 120 Volts. After running, the gels are then incubated in fixing buffer (50% MeOH, 10% HAc, 40% distilled water) for 30minutes. The gels are stained in staining buffer (60mg Coomassie blue powder in fixing buffer) for another 30 mintues. Once the gels are stained, gels are incubated in destaining buffer (5% MeOH, 7.5% HAc, 87.5% distilled water) for 2 hours. Finally, the stained gels are scanned in a ChemiDoc MP Imaging System from Biorad.

B. Supplementary Table

1. TopPIC Suite Searching Results for Depleted Plasma using Organic Precipitation

Sample	Precursor mass	Adjusted precursor mass	Feature intensity	Protein accession	Proteoform	E-value
rep1	6626.498	6626.506	4.02E+09	sp|P02654|APOC1_HUMAN	G.TPDVSSALDKLKEFGNTLEDKARELISRIKQSELSAKMREWFSETFQKVKEKLKIDS.	1.87E-24
rep1	6642.493	6642.493	1.93E+09	sp|P02654|APOC1_HUMAN	G.TPDVSSALDKLKEFGNTLED(KARELISRIKQSELSAKMREWFSE)[15.9873]TFQKVKEKLKIDS.	3.17E-15
rep1	6428.382	6428.405	1.28E+09	sp|P02654|APOC1_HUMAN	P.DVSSALDKLKEFGNTLEDKARELISRIKQSELSAKMREWFSETFQKVKEKLKIDS.	1.26E-19
rep1	8804.425	8804.415	1.01E+09	sp|P02652|APOA2_HUMAN	R.(RQAKEPCV)[-54.1245]ESLVSQYFQTVTDYGKDLMEKVKSPELQAEAKSYFEKSKEQLTPLIKKAGTELVNFLSYFVELGTQPATQ.	8.70E-18
rep1	6444.389	6444.389	8.68E+08	sp|P02654|APOC1_HUMAN	P.DVSSALDKLKEFGNTLEDKARELISRIKQSE(LSAKMREWFSE)[15.9832]TFQKVKEKLKIDS.	3.71E-14
rep1	8820.387	8820.397	7.20E+08	sp|P02652|APOA2_HUMAN	R.RQAKEPCVESLVSQYFQTVTDYGKD(LMEKV)[-38.1428]KSPELQAEAKSYFEKSKEQLTPLIKKAGTELVNFLSYFVELGTQPATQ.	7.65E-09
rep1	9414.426	9414.706	6.01E+08	sp|P02654|APOC1_HUMAN	.((M)[Acetyl]RLFLSLPVLVVVLSIVLEGPAPAQGTP)[489.8464]DVSSALDKLKEFGNTLE	0.000455

					DKARELISRIKQSELSAKMREWFSETFQKVKEKL.K	
rep1	8676.351	8676.351	5.30E+08	sp|P02652|APOA2_HUMAN	V.(RRQAKEPCV)[-210.2311]ESLVSQYFQTVTDYGKDLMEKVKSPELQAEAKSYFEKSKEQLTPLIKKAGTELVNFLSYFVELGTQPAT.Q	4.79E-09
rep1	28089.4	28089.41	4.48E+08	sp|P02647|APOA1_HUMAN	E.PPQSPWDRVKDLATVYVDVLKDSGRDYVSQFEGSALGKQLNLKLLDNWDS(VTSTFSKLREQLGPVTQEFWDNLEKETEGLRQE)[272.0040]MSKDLEEVKAKVQPYLDDFQKKWQEEMELYRQKVEPLRAELQEGARQKLHELQEKLSPLGEEMRDRARAHVDALRTHLAPYSDELRQRLAARLEALKENGGARLAEYHAKATEHLSTLSEKAKPALEDLRQGLLPVLESFKVSFLSALEEYTKKLNTQ.	0.00027
rep1	8820.395	8820.655	2.89E+08	sp|P02654|APOC1_HUMAN	F.(LSLPVLVVVLSIVLEGPAPAQG)[41.8621]TPDVSSALDKLKEFGNTLEDKARELISRIKQSELSAKMREWFSETFQKVKEKLKIDS.	6.21E-06
rep1	6888.754	6888.724	2.34E+08	sp|P02654|APOC1_HUMAN	G.TPDVSSALDKLKEFGNTLED(KARELISRIKQSELSAKMREWFSE)[262.2179]TFQKVKEKLKIDS.	1.72E-14
rep1	8941.376	8941.641	2.19E+08	sp|P02655|APOC2_HUMAN	G.TQQPQQDE(MPSPTFLTQVKESLSSYWESAKTAAQNLYEKTYLPAVDEKLRDLYSKSTAAMST)[32.2630]YTGIFTDQVLSVLKGEE.	9.30E-11
rep1	6864.72	6864.74	2.07E+08	sp|P02654|APOC1_HUMAN	G.TPDVSSALDKLKEFGNTLED(KARELISRIKQSELSAKMREWFSE)[238.2339]TFQKVKEKLKIDS.	2.81E-14
rep1	7611.02	7611.044	1.71E+08	sp|O14791|APOL1_HUMAN	R.GVKLTDVAPVSFFLVLDVVYLVYESKHLHEGAKSETAEELKKVAQELEEKLNILNNNYKILQADQEL.	8.16E-09
rep1	6938.67	6938.875	1.54E+08	sp|P02654|APOC1_HUMAN	A.(PAQG)[-40.8008]TPDVSSALDKLKEFGNTLEDKARELISRIKQSELSAKMREWFSETFQKVKEKLKIDS.	2.94E-12

rep1	12887.31	12887.33	1.35E+08	sp|P35542|SAA4_HUMAN	G.VTSESWRSFFKEALQGVG(DMGRAYWDIMISNHQNSNRYLYA)[-195.1020]RGNYDAAQRGPGGVWAAKLISRSRVYLQGLIDCYLFGNSSTVLEDSKSNEKAEEWGRSGKDPDRFRPDGLPKKY.	0.009837
rep1	8925.394	8925.659	1.25E+08	sp|P02655|APOC2_HUMAN	G.TQQ(PQQDEMPSPTFLTQVKESLSSYWESAKTAAQNLYEKTYLPAVDEKLRDLYSKSTAAMSTYT)[16.2809]GIFTDQVLSVLKGEE.	4.33E-09
rep1	6669.509	6669.479	8.27E+07	sp|P02654|APOC1_HUMAN	G.TPDVSSALDKLKEF(GNTLEDKAR)[42.9731]ELISRIKQSELSAKMREWFSETFQKVKEKLKIDS.	6.78E-05
rep1	6912.766	6912.721	8.08E+07	sp|P02654|APOC1_HUMAN	G.TPDVSSALDKLKEFGNTLEDKARELISRIKQSEL(SAKMREWFSE)[286.2156]TFQKVKEKLKIDS.	2.21E-15
rep1	9300.988	9300.969	7.71E+07	sp|P02647|APOA1_HUMAN	R.THLAPYSDELRQRLAARLEALKENGGARLAEYHAKATEHLSTLSEKAKPALEDLRQGLLPVLESFKVSFLSALEEYTKKLNTQ.	3.64E-05
rep1	6690.65	6690.63	7.65E+07	sp|P02654|APOC1_HUMAN	P.DVSSALDKLKEFGNTLED(KARELISRIKQSELSAKMREWFSE)[262.2245]TFQKVKEKLKIDS.	1.40E-12
rep1	6434.359	6434.339	7.37E+07	sp|P06727|APOA4_HUMAN	R.SLAPYAQDTQEKLNHQL(EGLTFQMKKNAEE)[15.9934]LKARISASAEELRQRLAPLAEDVRGNL.R	0.006832
rep1	6666.678	6666.628	6.56E+07	sp|P02654|APOC1_HUMAN	P.DVSSALDKLKEFGNTLED(KARELISRIKQSELSAKMREWFSE)[238.2230]TFQKVKEKLKIDS.	5.57E-11
rep1	8839.437	8839.702	6.19E+07	sp|P02654|APOC1_HUMAN	.(MRLFLSLPVLVVVLSIVLEGPAPAQGTPDVSS)[-486.3851]ALDKLKEFGNTLEDKARELISRIKQSELSAKMREWFSETFQKVKEKLKIDS.	8.71E-05
rep1	6739.568	6739.583	5.41E+07	sp|P02654|APOC1_HUMAN	Q.(G)[56.0553]TPDVSSALDKLKEFGNTLEDKARELISRIKQSELSAKMREWFSETFQKVKEKLKIDS.	3.66E-08
rep1	14157.9	14158.1	4.35E+07	sp|P02647|APOA1_HUMAN	P.LRAELQEGARQKLHELQEKLSPLGEEMRDRARAHVDALRTHLAPYSDE(LRQRLAAR	0.002791

					LEALKENGGAR)[326.7172]LAEYHAKATE HLSTLSEKAKPALEDLRQGLLPVLESFKVS FLSALEEYTKKLNTQ.	
rep1	4064.992	4065.112	3.91E+07	sp|P02649|APOE_HUMAN	K.SW(FEPLVEDMQRQWAGLVEKVQAAV) [16.1382]GTSAAPVPSDNH.	0.002913
rep1	7060.642	7060.852	3.80E+07	sp|P02647|APOA1_HUMAN	E.(ALKENGGARLAE)[- 19.9410]YHAKATEHLSTLSEKAKPALEDLR QGLLPVLESFKVSFLSALEEYTKKLNTQ.	0.008246
rep1	8791.203	8791.463	3.58E+07	sp|P02656|APOC3_HUMAN	A.SEAEDASLL(SFMQGYMKHATKTAKDA LSSVQESQVAQQARGWVTDGFSSLKDYW STVKDKFSEFW)[32.2451]DLDPEVRPTSAV AA.	0.000152
rep1	10064.38	10063.38	3.55E+07	sp|P02647|APOA1_HUMAN	R.AHVDALRTHLAPYSDELRQRLAARLEA LKENGGARLAEYHAKATEHLSTLSEKAKP ALEDLRQGLLPVLESFKVSFLSALEEYTKK LNTQ.	1.82E-07
rep1	10063.41	10063.29	3.55E+07	sp|P06727|APOA4_HUMAN	K.(IDQNVEELKGRLTPYADEFKVKIDQTVE ELRRSL)[- 168.0625]APYAQDTQEKLNHQLEGLTFQM KKNAEELKARISASAEELRQRLAPLAEDV RGNL.R	0.000238
rep1	8759.181	8759.218	3.54E+07	sp|P02656|APOC3_HUMAN	A.SEAEDASLLSFMQGYMKHATKTAKDAL SSVQESQVAQQARGWVTDGFSSLKDYWS TVKDKFSEFWDLDPEVRPTSAVAA.	5.27E-09
rep1	15871.2	15871.25	3.18E+07	sp|P68871|HBB_HUMAN	M.VHLTPEEKSAVTALWGKVNVDEVGGE ALGRLLVVYPWTQRFFESFGDLST(PDAV M)[14.0040]GNPKVKAHGKKVLGAFSDGL AHLDNLKGTFATLSELHCDKLHVDPENFR LLGNVLVCVLAHHFGKEFTPPVQAAYQK VVAGVANALAHKYH.	1.04E-05
rep1	8685.431	8685.406	2.88E+07	sp|P02652|APOA2_HUMAN	R.(QAKE)[- 17.0324]PCVESLVSQYFQTVTDYGKDLME KVKSPELQAEAKSYFEKSKEQLTPLIKKAG TELVNFLSYFVELGTQPATQ.	8.75E-11

rep1	8861.419	8861.439	2.80E+07	sp|P02652|APOA2_HUMAN	Q.(AKEPCV)[287.0589]ESLVSQYFQTVTDYGKDLMEKVKSPELQAEAKSYFEKSKEQLTPLIKKAGTELVNFLSYFVELGTQPATQ.	2.48E-05
rep1	6715.647	6715.637	2.72E+07	sp|P02654|APOC1_HUMAN	P.DVSSALDKLKEFGNTLEDKARELISRIKQSE(LSAKMREWFS)[287.2318]ETFQKVKEKLKIDS.	1.70E-09
rep1	8231.035	8231.28	2.66E+07	sp|P02655|APOC2_HUMAN	Q.DEMPSPTFLTQVKE(SLSSYWESAKTAAQNLYEKTYLPAVDEKLRDLYSKSTAAMSTY)[32.2364]TGIFTDQVLSVLKGEE.	4.12E-07
rep1	8215.053	8215.298	1.55E+07	sp|P02655|APOC2_HUMAN	Q.(DEMPSPTFLTQVKESLSSYWESAKTAAQNLYEKTYLPAVDEKLRDLYSKSTAAMSTY)[16.2547]TGIFTDQVLSVLKGEE.	1.12E-07
rep1	8557.406	8557.351	1.45E+07	sp|P02652|APOA2_HUMAN	A.(K)[182.0665]EPCVESLVSQYFQTVTDYGKDLMEKVKSPELQAEAKSYFEKSKEQLTPLIKKAGTELVNFLSYFVELGTQPAT.Q	2.07E-05
rep1	6936.74	6936.72	1.38E+07	sp|P02654|APOC1_HUMAN	G.TPDVSSALDKLKEFG(NTLEDKARELISRIKQSELSAKMREWFSETFQKVK)[310.2144]EKLKIDS.	1.36E-05
rep1	5985.164	5985.167	1.36E+07	sp|P02654|APOC1_HUMAN	P.DVSSALDKLKEFGNTLEDKARELISRIKQSELSAKMREWFSETFQKVKEKL.K	0.000509
rep1	27412.66	27412.71	9.65E+06	sp|P02647|APOA1_HUMAN	E.PPQSPWDRVKDLATVYVDVLKDSGRDYVSQ(FEGSAL)[-404.6922]GKQLNLKLLDNWDSVTSTFSKLREQLGPVTQEFWDNLEKETEGLRQEMSKDLEEVKAKVQPYLDDFQKKWQEEMELYRQKVEPLRAELQEGARQKLHELQEKLSPLGEEMRDRARAHVDALRTHLAPYSDELRQRLAARLEALKENGGARLAEYHAKATEHLSTLSEKAKPALEDLRQGLLPVLESFKVSFLSALEEYTKKLNTQ.	0.006615
rep1	6061.195	6061.176	8.11E+06	sp|P06727|APOA4_HUMAN	R.VLRENADSLQASLRPHADELKAKIDQNVEELKGRLTPYADEFKVKIDQTVEEL.R	0.006928
rep1	8910.383	8909.378	7.74E+06	sp|P02655|APOC2_HUMAN	G.TQQPQQDEMPSPTFLTQVKESLSSYWESAKTAAQNLYEKTYLPAVDEKLRDLYSKSTAAMSTYTGIFTDQVLSVLKGEE.	4.72E-06

rep1	5871.135	5871.146	7.42E+06	sp|P02647|APOA1_HUMAN	E.YHAKATEHLSTLSEKAKPALEDLRQGLLPVLESFKVSFLSALEEYTKKLNTQ.	7.29E-08
rep1	3181.736	3181.727	6.15E+06	sp|P02647|APOA1_HUMAN	R.QGLLPVLESFKVSFLSALEEYTKKLNTQ.	5.98E-06
rep1	9738.891	9739.016	5.10E+06	sp|P02647|APOA1_HUMAN	V.DALRTHLAPYSDELRQRLAAR(LEALKENGGARLAEYHAKATEHL)[-17.2024]STLSEKAKPALEDLRQGLLPVLESFKVSFLSALEEYTKKLNTQ.	0.001484
rep1	9765.992	9766.222	3.15E+06	sp|P02647|APOA1_HUMAN	V.DALRTHLAPYSDELRQRLAARLEALKENGGARLAEYHAKATEHLST(LSEKAK)[10.0032]PALEDLRQGLLPVLESFKVSFLSALEEYTKKLNTQ.	0.009862
rep1	7193.042	7193.257	2.79E+06	sp|P02647|APOA1_HUMAN	E.PPQSPWDRVKDLATVYVDVLKDSGRDYVSQFEGSALGKQLNLKLLDNWD(SVTSTFSKLREQLGP)[-12.4535].V	0.001019
rep1	5371.896	5371.892	2.71E+06	sp|P02647|APOA1_HUMAN	K.ATEHLSTLSEKAKPALEDLRQGLLPVLESFKVSFLSALEEYTKKLNTQ.	0.001854
rep1	3557.965	3558.07	1.21E+06	sp|P02647|APOA1_HUMAN	K.PALEDLRQGLL(PVLESFKVSF)[-418.0859]LSALEEYTKKLNTQ.	0.003607
rep1	4580.038	4580.173	1.07E+06	sp|P02647|APOA1_HUMAN	T.(LSEKAK)[-52.3691]PALEDLRQGLLPVLESFKVSFLSALEEYTKKLNTQ.	0.002443
rep1	5031.157	5031.127	1.06E+06	sp|P10412|H14_HUMAN	K.PAAAAGAKKAKSPKKAKAAKPKKAPKSPAKAKAVKPKAAKPKTAKPKAA(KP)[-4.0328].K	0.000356
rep1	6353.677	6353.867	6.09E+05	sp|P02647|APOA1_HUMAN	A.(RLAEYHAKATEHLSTLSEKAK)[13.4555]PALEDLRQGLLPVLESFKVSFLSALEEYTKKLNTQ.	0.009888
rep1	9807.387	9807.677	4.93E+05	sp|P02647|APOA1_HUMAN	H.VDALRTHLAPYSDELRQR(LAARLEALKENGGARLAEYHAKATEHLSTLSEKAK)[-47.6102]PALEDLRQGLLPVLESFKVSFLSALEEYTKKLNTQ.	0.004082
rep1	3733.556	3733.666	2.53E+05	sp|P68871|HBB_HUMAN	M.VHLTPEEKSAVTALWGKVNVDEVGGEALGRLLVV(Y)[-14.3541].P	7.49E-05
rep1	5510.233	5510.398	1.82E+05	sp|P02647|APOA1_HUMAN	A.KATEHLSTLSEKA(K)[10.4112]PALEDLRQGLLPVLESFKVSFLSALEEYTKKLNTQ.	1.40E-05

rep2	10064.37	10063.38	5.02E+07	sp|P02647|APOA1_HUMAN	R.AHVDALRTHLAPYSDELRQRLAARLEALKENGGARLAEYHAKATEHLSTLSEKAKPALEDLRQGLLPVLESFKVSFLSALEEYTKKLNTQ.	3.62E-08
rep2	9299.937	9300.969	9.13E+07	sp|P02647|APOA1_HUMAN	R.THLAPYSDELRQRLAARLEALKENGGARLAEYHAKATEHLSTLSEKAKPALEDLRQGLLPVLESFKVSFLSALEEYTKKLNTQ.	2.61E-07
rep2	8759.223	8759.218	6.39E+07	sp|P02656|APOC3_HUMAN	A.SEAEDASLLSFMQGYMKHATKTAKDALSSVQESQVAQQARGWVTDGFSSLKDYWSTVKDKFSEFWDLDPEVRPTSAVAA.	3.72E-07
rep2	4064.994	4065.114	5.18E+07	sp|P02649|APOE_HUMAN	K.SWF(EPLVEDMQRQWAGLVEKVQAAV)[16.1395]GTSAAPVPSDNH.	0.000465
rep2	8210.138	8210.121	3.09E+07	sp|Q9NZT1|CALL5_HUMAN	M.(A)[Acetyl]GELTPEEEAQYKKAFSAVDTDGNGTINAQELGAALKATGKNLSEAQLRKLISEVDSDGDGEISFQEFLTAAKKARAG.L	1.21E-11
rep2	8792.189	8792.449	3.19E+07	sp|P02656|APOC3_HUMAN	A.SEAED(ASLLSFMQGYMKHATKTAKDALSSVQESQVAQQARGWVTDGFSSLKDYWSTVKDKFSEFW)[33.2315]DLDPEVRPTSAVAA.	0.00028
rep2	13886.88	13886.9	1.58E+08	sp|P02766|TTHY_HUMAN	E.AGPTGTGESKCPLMVKVLDAVRGSP(AINVAVHVFRKA)[62.9770]ADDTWEPFASGKTSESGELHGLTTEEEFVEGIYKVEIDTKSYWKALGISPFHEHAEVVFTANDSGPRRYTIAALLSPYSYSTTAVVTNPKE.	0.000125
rep2	7611.061	7611.044	4.94E+08	sp|O14791|APOL1_HUMAN	R.GVKLTDVAPVSFFLVLDVVYLVYESKHLHEGAKSETAEELKKVAQELEEKLNILNNNYKILQADQEL.	1.73E-12
rep2	8776.19	8776.37	1.87E+07	sp|P02656|APOC3_HUMAN	A.SEA(EDASLLSFMQGYMKHATKTAKDALSSVQESQVAQQARGWVTDGFSSLKDYWSTVKDKFSEF)[17.1526]WDLDPEVRPTSAVAA.	1.15E-06
rep2	6626.498	6626.506	5.66E+09	sp|P02654|APOC1_HUMAN	G.TPDVSSALDKLKEFGNTLEDKARELISRIKQSELSAKMREWFSETFQKVKEKLKIDS.	2.65E-24
rep2	6427.394	6428.405	1.99E+09	sp|P02654|APOC1_HUMAN	P.DVSSALDKLKEFGNTLEDKARELISRIKQSELSAKMREWFSETFQKVKEKLKIDS.	4.35E-20

rep2	10065.38	10065.33	5.02E+07	sp|P06727|APOA4_HUMAN	I.(DQNVEELKGRLTPYADEFKVKIDQTVEELRRSL)[-52.9416]APYAQDTQEKLNHQLEGLTFQMKKNAEELKARISASAEELRQRLAPLAEDVRGNL.R	0.000547
rep2	6418.331	6418.346	1.59E+07	sp|P06727|APOA4_HUMAN	R.SLAPYAQDTQEKLNHQLEGLTFQMKKNAEELKARISASAEELRQRLAPLAEDVRGNL.R	8.69E-07
rep2	6061.174	6061.176	6.59E+06	sp|P06727|APOA4_HUMAN	R.VLRENADSLQASLRPHADELKAKIDQNVEELKGRLTPYADEFKVKIDQTVEEL.R	0.001464
rep2	6444.372	6444.402	2.11E+08	sp|P02654|APOC1_HUMAN	P.DVSSALDKLKEFGNTLEDKARELISRIKQSEL(SAKMR)[15.9961]EWFSETFQKVKEKLKIDS.	3.78E-14
rep2	5029.681	5029.831	2.12E+06	sp|P02647|APOA1_HUMAN	A.(TEHLSTLSEKAKPALEDLRQGLL)[-271.0239]PVLESFKVSFLSALEEYTKKLNTQ.	0.002097
rep2	5985.145	5985.167	2.32E+07	sp|P02654|APOC1_HUMAN	P.DVSSALDKLKEFGNTLEDKARELISRIKQSELSAKMREWFSETFQKVKEKL.K	1.03E-05
rep2	12872.32	12872.34	7.27E+07	sp|P35542|SAA4_HUMAN	E.SWRSFFKEALQGVGDMGRAYWDIMISNHQNSNRYLYARGNYDAAQRGPGG(VWAAKLISRSRVYLQGLIDC)[206.1047]YLFGNSSTVLEDSKSNEKAEEWGRSGKDPDRFRPDGLPKKY.	0.002669
rep2	6443.399	6443.589	2.11E+08	sp|P35542|SAA4_HUMAN	A.(KLISRSRVYLQGLIDCY)[-103.7458]LFGNSSTVLEDSKSNEKAEEWGRSGKDPDRFRPDGLPKKY.	0.000113
rep2	15871.3	15871.25	5.33E+07	sp|P68871|HBB_HUMAN	M.VHLTPEEKSAVTALWGKVNVDEVGGEALGRLLVVYPWTQRFFESFGDLSTPDAVMGNPKV(KAHGKKVLGAFSDGLAHLDNLKGTFATLSELHCDKLHVDPENF)[13.9973]RLLGNVLVCVLAHHFGKEFTPPVQAAYQKVVAGVANALAHKYH.	2.37E-06
rep2	1695.883	1695.933	1.31E+05	sp|P69905|HBA_HUMAN	D.(KFLA)[-3.0339]SVSTVLTSKYR.	0.002976
rep2	6612.494	6612.484	3.75E+07	sp|P02654|APOC1_HUMAN	G.TPDVSSALDKLKEFGNTLEDKARELISRIKQSEL(SAKMREWFSETFQKV)[-14.0218]KEKLKIDS.	6.66E-08

rep2	6414.413	6414.378	8.82E+06	sp|P02654|APOC1_HUMAN	P.DVSSALDKLKEFGNTLEDKARELISRIKQSELSAKMREWFSE(TFQ)[-14.0276]KVKEKLKIDS.	4.37E-08
rep2	5871.163	5871.146	8.52E+06	sp|P02647|APOA1_HUMAN	E.YHAKATEHLSTLSEKAKPALEDLRQGLLPVLESFKVSFLSALEEYTKKLNTQ.	2.28E-12
rep2	5372.887	5371.892	5.42E+06	sp|P02647|APOA1_HUMAN	K.ATEHLSTLSEKAKPALEDLRQGLLPVLESFKVSFLSALEEYTKKLNTQ.	1.11E-10
rep2	4814.621	4815.623	5.03E+06	sp|P81605|DCD_HUMAN	R.SSLLEKGLDGAKKAVGGLGKLGKDAVEDLESVGKGAVHDVKDVLDSVL.	6.43E-17
rep2	9414.452	9414.732	7.16E+08	sp|P02654|APOC1_HUMAN	.(M)[Acetyl]RLFLSLPVLVVVLSIVLEGPAPAQG(TP)[489.8727]DVSSALDKLKEFGNTLEDKARELISRIKQSELSAKMREWFSETFQKVKEKL.K	2.20E-08
rep2	3814.005	3814.979	1.12E+08	sp|P02768|ALBU_HUMAN	R.DAHKSEVAHRFKDLGEENFKALVLIAFAQYLQQ.C	8.71E-08
rep2	3164.691	3164.781	4.03E+07	sp|P02647|APOA1_HUMAN	L.PVLESF(KV)[394.3021]SFLSALEEYTKKLNTQ.	1.10E-08
rep2	8228.013	8228.258	8.67E+06	sp|P02655|APOC2_HUMAN	Q.QDEMPSPTFLTQVKESL(SSYWESAKTAAQNLYEKTYLPAVDEKLRDLYSKSTAAMSTY)[-98.8446]TGIFTDQVLSVLKGEE.	1.30E-07
rep2	6788.531	6788.586	4.09E+08	sp|P02654|APOC1_HUMAN	G.TPDVSSALD(KL)[162.0801]KEFGNTLEDKARELISRIKQSELSAKMREWFSETFQKVKEKLKIDS.	2.47E-05
rep2	6588.445	6588.53	1.51E+08	sp|P02654|APOC1_HUMAN	G.(TP)[-37.9762]DVSSALDKLKEFGNTLEDKARELISRIKQSELSAKMREWFSETFQKVKEKLKIDS.	8.84E-05
rep2	3181.723	3181.727	5.78E+06	sp|P02647|APOA1_HUMAN	R.QGLLPVLESFKVSFLSALEEYTKKLNTQ.	2.49E-06
rep2	6642.481	6642.501	1.12E+09	sp|P02654|APOC1_HUMAN	G.TPDVSSALDKLKEFGNTLED(KARELISRIKQSELSAKMREWFSE)[15.9947]TFQKVKEKLKIDS.	1.97E-14
rep2	6446.399	6446.374	3.27E+08	sp|P02654|APOC1_HUMAN	P.DVSSALDKLKEF(GNTLEDKARELISRIKQSELSAKMREWFSETFQKV)[17.9684]KEKLKIDS.	0.005323

rep2	6741.578	6741.693	8.48E+07	sp|P02654|APOC1_HUMAN	Q.(G)[58.1657]TPDVSSALDKLKEFGNTLEDKARELISRIKQSELSAKMREWFSETFQKVKEKLKIDS.	2.74E-12
rep2	6938.667	6938.872	2.32E+08	sp|P02654|APOC1_HUMAN	A.(PAQG)[-40.8041]TPDVSSALDKLKEFGNTLEDKARELISRIKQSELSAKMREWFSETFQKVKEKLKIDS.	5.11E-09
rep2	6654.511	6654.501	7.67E+07	sp|P02654|APOC1_HUMAN	G.TPDVSSALDKLKEFGNTLEDKARELISRIKQSELSAKMREWFSE(TFQKVK)[27.9949]EKLKIDS.	9.12E-07
rep2	6668.514	6668.494	1.60E+08	sp|P02654|APOC1_HUMAN	G.TPDVSSALDKLKEFGNTLED(KARELISRIKQSELSAKMREWFSETFQK)[41.9878]VKEKLKIDS.	1.55E-09
rep2	6471.427	6471.427	7.01E+07	sp|P02654|APOC1_HUMAN	P.DVSSALDKL(KEFGNTLEDKARELISRIKQSELSAKMREWFSETFQK)[43.0215]VKEKLKIDS.	0.000217
rep2	8941.37	8941.635	1.49E+08	sp|P02655|APOC2_HUMAN	G.TQQPQQDE(MPSPTFLTQVKESLSSYWESAKTAAQNLYEKTYLPAVDEKLRDLYSKSTAAMST)[32.2563]YTGIFTDQVLSVLKGEE.	1.40E-10
rep2	9251.606	9251.881	3.49E+06	sp|P02655|APOC2_HUMAN	E.(VQGTQQPQQDEMPSPTFLTQVKESLSSYWESAKTAAQNLYEKTYLPAVDEKLRDLYSKSTAAMSTYT)[58.3537]GIFTDQVLSVLKGEE.	1.17E-05
rep2	8925.361	8925.626	2.54E+08	sp|P02655|APOC2_HUMAN	T.QQP(QQDEMPSPTFLTQVKESLSSYWESAKTAAQNLYEKTYLPAVDEKLRDLYSKSTAAMST)[117.2955]YTGIFTDQVLSVLKGEE.	4.55E-10
rep2	8231.035	8231.28	1.90E+07	sp|P02655|APOC2_HUMAN	Q.DE(MPSPTFLTQVKESLSSYWESAKTAAQNLYEKTYLPAVDEKLRDLYSKSTAAMSTY)[32.2363]TGIFTDQVLSVLKGEE.	1.63E-08
rep2	8215.06	8215.035	3.56E+07	sp|P02655|APOC2_HUMAN	Q.QDE(M)[-112.0669]PSPTFLTQVKESLSSYWESAKTAAQNLYEKTYLPAVDEKLRDLYSKSTAAMSTYTGIFTDQVLSVLKGEE.	4.54E-09

rep2	8877.445	8877.435	3.97E+07	sp|P02652|APOA2_HUMAN	R.RQAKEPCVESL(VSQYFQTV)[18.8954]TDYGKDLMEKVKSPELQAEAKSYFEKSKEQLTPLIKKAGTELVNFLSYFVELGTQPATQ.	1.14E-05
rep2	8820.398	8820.658	1.26E+09	sp|P02654|APOC1_HUMAN	F.(LSLPVLVVVLSIVLEGPAPAQG)[41.8655]TPDVSSALDKLKEFGNTLEDKARELISRIKQSELSAKMREWFSETFQKVKEKLKIDS.	3.46E-08
rep2	8692.365	8692.35	5.51E+08	sp|P02652|APOA2_HUMAN	R.RQAKEPCVESL(VS)[-38.1313]QYFQTVTDYGKDLMEKVKSPELQAEAKSYFEKSKEQLTPLIKKAGTELVNFLSYFVELGTQPAT.Q	0.008718
rep2	8820.395	8820.41	1.26E+09	sp|P02652|APOA2_HUMAN	R.RQAKEPCVESLVSQY(FQTVTDYGKDLMEKVKSPELQAEAK)[-38.1300]SYFEKSKEQLTPLIKKAGTELVNFLSYFVELGTQPATQ.	1.72E-09
rep2	8861.489	8861.434	5.00E+07	sp|P02652|APOA2_HUMAN	R.(RQAKEPC)[2.8943]VESLVSQYFQTVTDYGKDLMEKVKSPELQAEAKSYFEKSKEQLTPLIKKAGTELVNFLSYFVELGTQPATQ.	1.62E-11
rep2	8804.401	8804.406	1.99E+09	sp|P02652|APOA2_HUMAN	R.(RQAKEPCV)[-54.1331]ESLVSQYFQTVTDYGKDLMEKVKSPELQAEAKSYFEKSKEQLTPLIKKAGTELVNFLSYFVELGTQPATQ.	3.76E-18
rep2	2723.383	2723.382	1.35E+07	sp|Q14624|ITIH4_HUMAN	R.PGVLSSRQLGLPGPPDVPDHAAYHPF.R	0.009886
rep2	8676.332	8676.357	9.45E+08	sp|P02652|APOA2_HUMAN	R.(RQAKEPCV)[-54.1240]ESLVSQYFQTVTDYGKDLMEKVKSPELQAEAKSYFEKSKEQLTPLIKKAGTELVNFLSYFVELGTQPAT.Q	2.00E-13
rep2	6936.745	6936.725	1.25E+07	sp|P02654|APOC1_HUMAN	G.TPDVSSALDKLKEFGNTLED(KARELISRIKQSELSAKMREWFSE)[310.2196]TFQKVKEKLKIDS.	1.63E-08
rep2	6888.796	6888.721	2.72E+08	sp|P02654|APOC1_HUMAN	G.TPDVSSALDKLKEFG(NTLED)[262.2152]KARELISRIKQSELSAKMREWFSETFQKVKEKLKIDS.	1.71E-12
rep2	6912.791	6912.721	8.32E+07	sp|P02654|APOC1_HUMAN	G.TPDVSSALDKLKEFGNTLEDKARELISRIKQSEL(SAKMREWFSET)[286.2147]FQKVKEKLKIDS.	1.19E-19

rep2	6690.65	6690.63	8.18E+07	sp|P02654|APOC1_HUMAN	P.DVSSALDKLKEFGNTLED(KARELISRIKQSELSAKMREWFSE)[262.2242]TFQKVKEKLKIDS.	5.29E-12
rep2	6714.636	6714.641	2.40E+07	sp|P02654|APOC1_HUMAN	P.DVSSALDKLKEFGNT(LEDKARELISRIKQSELSAKMREWFSETFQK)[286.2357]VKEKLKIDS.	3.02E-06
rep2	6864.682	6864.752	2.53E+08	sp|P02654|APOC1_HUMAN	G.TPDVSSALDKLKEFGNTLED(KARELISRIKQSELSAKMREWFSE)[238.2458]TFQKVKEKLKIDS.	7.06E-14
rep2	28090.52	28090.57	5.61E+08	sp|P02647|APOA1_HUMAN	E.PPQSPWDRVKDLATVYVDVLKDSGRDYVSQFEGSALGKQLNLKLLDNWDSVTSTFSKL(REQLGPVTQE)[273.1667]FWDNLEKETEGLRQEMSKDLEEVKAKVQPYLDDFQKKWQEEMELYRQKVEPLRAELQEGARQKLHELQEKLSPLGEEMRDRARAHVDALRTHLAPYSDELRQRLAARLEALKENGGARLAEYHAKATEHLSTLSEKAKPALEDLRQGLLPVLESFKVSFLSALEEYTKKLNTQ.	0.002906
rep2	6666.612	6666.642	6.84E+07	sp|P02654|APOC1_HUMAN	P.DVSSALDKLKEFGNTLED(KARELISRIKQSELSAKMREWFSE)[238.2366]TFQKVKEKLKIDS.	7.12E-15
rep2	2807.054	2807.134	1.54E+06	sp|P02647|APOA1_HUMAN	L.(LPV)[-76.4291]LESFKVSFLSALEEYTKKLNTQ.	0.008758
rep2	5615.466	5615.631	4.01E+07	sp|P02647|APOA1_HUMAN	E.PPQSPWDRVKDLATVYVDVL(KDSGRDYVSQFEGSALGKQLNLKLLDNWD)[40.7888].S	0.001557
rep2	5544.073	5544.238	3.67E+06	sp|P02647|APOA1_HUMAN	H.AKATEHLSTLSEKAKPALEDLRQG(LLPV)[-26.7864]LESFKVSFLSALEEYTKKLNTQ.	0.007547
rep2	5647.702	5647.867	3.34E+07	sp|P02647|APOA1_HUMAN	E.PPQSPWDRVKDLATVYVDVLKDSGRDYVSQFEGS(AL)[-14.0077]GKQLNLKLLDNWDS.V	9.66E-07
rep2	7068.19	7068.4	1.78E+06	sp|P02647|APOA1_HUMAN	E.(ALKENGGARLAEYHAKATEHLSTLSEKAKPALED)[-12.3930]LRQGLLPVLESFKVSFLSALEEYTKKLNTQ.	6.48E-06

rep2	4722.268	4722.408	4.16E+06	sp|P02647|APOA1_HUMAN	S.(TLSEKAK)[-11.1819]PALEDLRQGLLPVLESFKVSFLSALEEYTKKLNTQ.	0.00154
rep2	12886.13	12886.29	1.47E+06	sp|P02647|APOA1_HUMAN	Q.KLHELQEKLSPLGEEMRDRARAHVDALRTHLAPYSDELRQRLAAR(LEALKENGGAR)[306.5780]LAEYHAKATEHLSTLSEKAKPALEDLRQGLLPVLESFKVSFLSALEEYTKKLNTQ.	0.002127
rep2	6839.802	6840.007	3.80E+06	sp|P02647|APOA1_HUMAN	L.KENGGARL(AEYHAKATEHL)[-56.6651]STLSEKAKPALEDLRQGLLPVLESFKVSFLSALEEYTKKLNTQ.	5.77E-05
rep2	13636.66	13636.71	1.50E+06	sp|P02647|APOA1_HUMAN	R.AELQEGARQKLHE(LQEKLSPLGEEM)[74.5144]RDRARAHVDALRTHLAPYSDELRQRLAARLEALKENGGARLAEYHAKATEHLSTLSEKAKPALEDLRQGLLPVLESFKVSFLSALEEYTKKLNTQ.	0.00665
rep2	6338.818	6339.008	1.32E+05	sp|P02647|APOA1_HUMAN	G.(GARLAEYHAKATEHLSTL)[-129.4619]SEKAKPALEDLRQGLLPVLESFKVSFLSALEEYTKKLNTQ.	0.006344
rep2	3911.374	3911.489	1.22E+05	sp|P02647|APOA1_HUMAN	K.(PALED)[-64.6675]LRQGLLPVLESFKVSFLSALEEYTKKLNTQ.	7.41E-07
rep2	3745.319	3745.429	1.85E+05	sp|P02647|APOA1_HUMAN	L.(ED)[50.4469]LRQGLLPVLESFKVSFLSALEEYTKKLNTQ.	0.000792
rep2	2758.534	2758.614	2.25E+05	sp|P02647|APOA1_HUMAN	L.(PVL)[-11.8658]ESFKVSFLSALEEYTKKLNTQ.	1.27E-05

2. TopPIC Suite Searching Results for Depleted Plasma using GELFrEE

Sample	Precursor mass	Adjusted precursor mass	Feature intensity	Protein accession	Proteoform	E-value

rep1	28061.66	28061.47	1.64E+09	sp|P02647|APOA1_HUMAN	Q.DEPPQSPWDRVKDLATVYVDVLKDSGR DYVSQFEGSALGKQLNLKLLDNWDSVTST FSKLREQLGPVTQEFWDNLEKETEGLRQE MSKDLEEVKAKVQPYLDDFQKKWQEEME LYRQKVEPLRAELQEGARQKLHELQEKLS PLGEEMRDRARAHVDALRTHLAPYSDELR QRLAARLEALKENGGARLAEYHAKATEH LSTLSEKAKPALEDLRQGLLPVLESFKVSF LSALEEYTKKLNTQ.	0.000746
rep1	14361.33	14361.19	1.98E+08	sp|P02647|APOA1_HUMAN	Q.DEPPQSPWDRVKDLATVYVDVLKDSGR DYVSQFEGSALGKQLNLKLLDNWDSVTST FSKLREQLGPVTQEFWDNLEKETEGLRQE MSKDLEEVKAKVQPYLDDFQKKWQEEME LYRQKVEPL.R	1.19E-11
rep1	21762.1	21762.97	1.72E+08	sp|P10412|H14_HUMAN	M.(S)[Acetyl]ETAPAAPAAPAPAEKTPVKK KARKSAGAAKRKASGPPVSELITKAVAAS KERSGVSLAALKKALAAAGYDVEKNNSRI KLGLKSLVSKGTLVQTKGTGASGSFKLNK KAASGEAKPKAKKAGAAKAKKPAGAAK KPKKATGAATPKKSAKKTPKKAKKPAAA AGAKKAKSPKKAKAAKPKKAPKSPAKAK AVKPKAAKPKTAKPKAAKPKKAAAKKK.	0.002508
rep1	4150.227	4150.166	1.58E+08	sp|P05155|IC1_HUMAN	R.TLLVFEVQQPFLFVLWDQQHKFPVFMG RVYDPRA.	2.52E-08
rep1	8756.512	8756.452	8.67E+07	sp|P02652|APOA2_HUMAN	R.(QAKEPC)[54.0133]VESLVSQYFQTVTDY GKDLMEKVKSPELQAEAKSYFEKSKEQLT PLIKKAGTELVNFLSYFVELGTQPATQ.	2.05E-28
rep1	8559.763	8559.638	6.77E+07	sp|P0CG48|UBC_HUMAN	G.MQIFVKTLTGKTITLEVEPSDTIENVKAK IQDKEGIPPDQQRLIFAGKQLEDGRTLSD(Y)[-99.0466]NIQKESTLHLVLRLRGGV.	5.02E-24
rep1	8559.727	8559.617	6.77E+07	sp|P0CG47|UBB_HUMAN	.MQIFVKTLTGKTITLEVEPSDTIENVKAKI QDKEGIPPDQQRLIFAGKQLEDGRTLSDYN IQKESTLHLVLRLRGG.M	1.11E-24
rep1	8628.502	8628.392	5.14E+07	sp|P02652|APOA2_HUMAN	Q.(AKEPC)[182.0706]VESLVSQYFQTVTDY GKDLMEKVKSPELQAEAKSYFEKSKEQLT PLIKKAGTELVNFLSYFVELGTQPAT.Q	2.51E-24

rep1	4182.19	4182.315	3.46E+07	sp|P06727|APOA4_HUMAN	D.(TQEKLN)[14.1452]HQLEGLTFQMKKNAEELKARISASAEELRQ.R	2.42E-07
rep1	5982.207	5982.152	2.42E+07	sp|P02647|APOA1_HUMAN	R.THLAPYSDELRQRLAARLEALKE(N)[1.0007]GGARLAEYHAKATEHLSTLSEKAKPALEDL.R	8.22E-12
rep1	3376.746	3376.716	2.25E+07	sp|P02647|APOA1_HUMAN	R.AELQEGARQKLHELQEKLSPLGEE(MR)[358.1603].D	0.000172
rep1	6864.79	6864.995	1.69E+07	sp|P02647|APOA1_HUMAN	E.PPQSPWDRVKDLATVYVDVLKDSGRDYVSQFEGSALGKQLNLKLLDNWDSVT(STFSKL)[54.5018]RE.Q	0.000871
rep1	14214.21	14214.07	1.64E+07	sp|P04908|H2A1B_HUMAN	M.(S)[Acetyl]GRGKQGGKARAKAKTRSSRAGLQFPVGRVHRLLRKGNYSERVGAGAPVYLAAVLEYL(TAE)[489.3614]ILELAGNAARDNKKTRIIPRHLQLAIRNDEELNKLLGRVTIAQGGVLPNIQAVLLPKKTESHHKA.K	5.90E-05
rep1	8685.516	8685.416	1.60E+07	sp|P02652|APOA2_HUMAN	R.(QAK)[-17.0223]EPCVESLVSQYFQTVTDYGKDLMEKVKSPELQAEAKSYFEKSKEQLTPLIKKAGTELVNFLSYFVELGTQPATQ.	7.40E-19
rep1	4815.701	4815.636	1.48E+07	sp|P81605|DCD_HUMAN	R.SSLLEKGLDGAKKAVGGLGKL(GK)[0.0130]DAVEDLESVGKGAVHDVKDVLDSVL.	4.65E-23
rep1	14478.38	14478.2	1.15E+07	sp|P0C0S8|H2A1_HUMAN	M.(S)[Acetyl]GRGKQGGKARAKAKTRSSRAGLQFPVGRVHRLLRKGNYAERVGAGAPVYLAAVLEYLTAEILELAGNAARDNKKTRIIPRHLQLAIRNDEELNKLLGKVTIAQGGV(LPNIQAVLLPKKTESHHKAKGK)[484.2817].	0.003653
rep1	4231.27	4231.23	1.13E+07	sp|P02647|APOA1_HUMAN	A.ARLEALKE(N)[0.9899]GGARLAEYHAKATEHLSTLSEKAKPALEDL.R	7.22E-10
rep1	14014.07	14014.05	1.01E+07	sp|P0C0S8|H2A1_HUMAN	M.(S)[Acetyl]GRGKQGGKARAKAKTRSSRAGLQFPVGRVHRLLRKGNYAERVGAGAPVYLAAVLEY(LTA)[333.3466]EILELAGNAARDNKKTRIIPRHLQLAIRNDEELNKLLGKVTIAQGGVLPNIQAVLLPKKTESHHKA.K	0.000708
rep1	14013.05	14012.9	1.01E+07	sp|Q6FI13|H2A2A_HUMAN	.MSGRGKQGGKARAKAKSRSSRAGLQ(FPVGRVHRLLRKGNYAERV)[438.3509]GAGAPVYMAAVLEYLTAEILELAGNAARDNKKT	8.99E-05

					RIIPRHLQLAIRNDEELNKLLGKVTIAQGG VLPNIQAVLLPKKTESHH.K	
rep1	6626.595	6626.506	9.51E+06	sp|P02654|APOC1_HUMAN	G.TPDVSSALDKLKEFGNTLEDKARELISRI KQSELSAKMREWFSETFQKVKEKLKIDS.	3.44E-22
rep1	13947.05	13946.91	8.96E+06	sp|P0C0S8|H2A1_HUMAN	M.(S)[Acetyl]GRGKQGGKARAKAKTRSSRA GLQFPVGRVHRLLRKGNYAERVGAGAPV YLAAVLE(Y)[266.2010]LTAEILELAGNAA RDNKKTRIIPRHLQLAIRNDEELNKLLGKV TIAQGGVLPNIQAVLLPKKTESHHKA.K	2.11E-07
rep1	13747.91	13747.81	7.66E+06	sp|P0C0S8|H2A1_HUMAN	M.(S)[Acetyl]GRGKQGGKARAKAKTRSSRA GLQFPVGRVHRLLRKGNYAERVGAGAPV YLAA(V)[266.2312]LEYLTAEILELAGNAA RDNKKTRIIPRHLQLAIRNDEELNKLLGKV TIAQGGVLPNIQAVLLPKKTESHH.K	3.70E-10
rep1	6892.865	6892.795	7.34E+06	sp|P02654|APOC1_HUMAN	G.TPDVSSALDKLKEFGNTLEDKARELISRI KQSEL(SAKMREWFSETFQKVK)[266.2887] EKLKIDS.	2.12E-11
rep1	13403.52	13403.4	7.14E+06	sp|P23527|H2B1O_HUMAN	.(M)[Acetyl]PDPAKSAPAPKKGSKKAVTKA QKKDGKKRKRSRKESYSIYVYKVLKQVH PDTGIS(S)[358.3092]KAMGIMNSFVNDIFE RIAGEASRLAHYNKRSTITSREIQTAVRLLL PGELAKHAVSEGTKA.V	0.001706
rep1	10867.74	10868.62	6.77E+06	sp|P01040|CYTA_HUMAN	M.IPGGLSEAKPATPEIQEIVDKVKPQLEEK TNETYGKLEAVQYKTQVVAGTNYYIKVR AGDNKYMHLKVFKSLPGQNEDLVLTGYQ VDKNKDDELTGF.	2.33E-05
rep1	10852.99	10852.86	6.77E+06	sp|P61604|CH10_HUMAN	M.(A)[Acetyl]GQAFRKFLPLFDRVLVERSA AE(TVTKGGIML)[17.0220]PEKSQGKVLQA TVVAVGSGSKGKGGEIQPVSVKVGDKVLL PEYGGTKVVLDDKDYFLFRDGDILGKYVD .	2.20E-07
rep1	10884.75	10884.63	6.07E+06	sp|P01040|CYTA_HUMAN	M.IPGGLSEAKPATPEIQEIVDKVKPQLEEK TNETYGKLEAVQYKTQVVAGTNYYIKVR AGD(NKYMHLKVFKSL)[16.0065]PGQNED LVLTGYQVDKNKDDELTGF.	1.78E-10

rep1	15329.75	15329.62	6.06E+06	sp|Q71DI3|H32_HUMAN	.MARTKQTARKSTGGKAPRKQLATKAAR KSAPATGGVKKPHRYRPGTVALREIRRYQ KSTELLIRKL(PFQRLVREI)[-48.8882]AQDFKTDLRFQSSAVMALQEASE AYLVGLFEDTNLCAIHAKRVTIMPKDIQLA RRIRGERA.	2.42E-05
rep1	8445.695	8445.574	5.83E+06	sp|P0CG47|UBB_HUMAN	.MQIFVKTLTGKTITLEVEPSDTIENVKAKI QDKEGIPPDQQRLIFAGKQLEDGRTLSDYN IQKESTLHLVLRLR.G	3.02E-08
rep1	15345.72	15345.6	5.67E+06	sp|Q71DI3|H32_HUMAN	.MARTKQTARKSTGGKAPRKQLATKAAR KSAPATGGVKKPHRYRPGTVA(LREIRRY QKSTELLIRKLPFQRLVREI)[-32.9017]AQDFKTDLRFQSSAVMALQEASE AYLVGLFEDTNLCAIHAKRVTIMPKDIQLA RRIRGERA.	8.80E-06
rep1	15343.79	15343.71	5.67E+06	sp|P84243|H33_HUMAN	M.ARTKQTARKSTGGKAPRKQLATKAAR KSAPSTGGVKKPHRYRPGTVALREIRRY(Q KSTELLIRKLPFQRLVREIAQDFKTDLRFQS A)[156.2484]AIGALQEASEAYLVGLFEDTN LCAIHAKRVTIMPKDIQLARRIRGERA.	2.35E-06
rep1	15318.7	15318.62	4.88E+06	sp|P84243|H33_HUMAN	.(M)[Acetyl]ARTKQTARKSTGGKAPRKQLA TKAARKSAPSTGGVKKPHRYRPGTVALRE IRRYQKSTELLIRKLPFQRLVREIAQDFKTD LRFQSAAIGA(LQE)[-41.8953]ASEAYLVGLFEDTNLCAIHAKRVT IMPKDIQLARRIRGERA.	3.64E-05
rep1	6929.277	6929.212	4.33E+06	sp|P02671|FIBA_HUMAN	R.HRHPDEAAFFDTASTGKTFPGFFSPMLG EFVSETESRGSESGIFTNTKESSSHHPGIAEF PSRG.K	6.33E-25
rep1	9355.153	9355.036	4.03E+06	sp|P68431|H31_HUMAN	Y.QKSTELLIRKLPFQRLVREIAQDFKTDLR FQSSAVMALQEACEAYLVGLFEDTNLCAI HAKRVTIMPKDIQLARRIRGERA.	1.93E-15
rep1	4004.122	4004.102	4.00E+06	sp|P02647|APOA1_HUMAN	R.LEA(LKENGGARLAE)[1.0007]YHAKATE HLSTLSEKAKPALEDL.R	0.002739
rep1	3164.737	3164.827	3.84E+06	sp|P02647|APOA1_HUMAN	R.(QGLL)[-16.9008]PVLESFKVSFLSALEEYTKKLNTQ.	7.19E-09

rep1	5789.099	5789.039	3.12E+06	sp|P02814|SMR3B_HUMAN	S.(QRGPRGPYPPGPLAPPQ)[-17.0168]PFGPGFVPPPPPPPYGPGRIPPPPPAPYGPGIFPPPPPQP.	1.58E-10
rep1	2888.526	2888.501	3.12E+06	sp|P02765|FETUA_HUMAN	R.TVVQPSVGAAAGPVVP(PCPGRIRHFKV)[149.9844].	9.02E-05
rep1	6945.24	6945.445	3.08E+06	sp|P02671|FIBA_HUMAN	R.HRHPDEAAFFDTASTGKTFPGFFS(PM)[16.2330]LGEFVSETESRGSESGIFTNTKESSSHHPGIAEFPSRG.K	8.79E-18
rep1	6182.941	6182.901	1.30E+06	sp|P01834|IGKC_HUMAN	N.SQESVTEQDSKDSTYSLSSTLTLSKADYEKHKVYACEVTHQGLSSPV(TKSFNRGEC)[-2.0110].	1.21E-11
rep1	7610.157	7610.072	4.01E+05	sp|O14791|APOL1_HUMAN	R.GVKLTDVAPVSFFLVLDVVYLVYESKHLHEGAKSETAEELKKVAQELEEKL(NILNNNYKILQADQEL)[-0.9722].	0.001701
rep2	4231.267	4231.227	1.13E+07	sp|P02647|APOA1_HUMAN	A.ARLEALKE(N)[0.9876]GGARLAEYHAKATEHLSTLSEKAKPALEDL.R	0.001312
rep2	6182.968	6182.908	1.10E+06	sp|P01834|IGKC_HUMAN	N.SQESVTEQDSKDSTYSLSSTLTLSKADYEKHK(VYACEVTHQGLSSPVTKSFNRGEC)[-2.0038].	0.00249
rep2	5982.195	5982.14	2.12E+07	sp|P02647|APOA1_HUMAN	R.THLAPYSDELRQRLAARLEALKE(N)[0.9892]GGARLAEYHAKATEHLSTLSEKAKPALEDL.R	9.62E-07
rep2	8559.763	8559.628	3.22E+07	sp|P0CG48|UBC_HUMAN	G.MQIFVKTLTGKTITLEVEPSDTIENVKAKIQDKEGIPPDQQRLIFAGKQLEDGRTLSDYNIQKESTLHLVLRLR(GGV)[-99.0574].	9.29E-22
rep2	10884.8	10884.66	7.19E+06	sp|P01040|CYTA_HUMAN	M.IPGGLSEAKPATPEIQEIVDKVKPQLEEKTNETYGKLE(AV)[16.0357]QYKTQVVAGTNYYIKVRAGDNKYMHLKVFKSLPGQNEDLVLTGYQVDKNKDDELTGF.	1.37E-08
rep2	10868.8	10868.62	5.37E+06	sp|P01040|CYTA_HUMAN	.(MI)[-131.0468]PGGLSEAKPATPEIQEIVDKVKPQLEEKTNETYGKLEAVQYKTQVVAGTNYYIKVRAGDNKYMHLKVFKSLPGQNEDLVLTGYQVDKNKDDELTGF.	0.000325

rep2	8559.725	8559.617	3.22E+07	sp|P0CG47|UBB_HUMAN	.MQIFVKTLTGKTITLEVEPSDTIENVKAKIQDKEGIPPDQQRLIFAGKQLEDGRTLSDYNIQKESTLHLVLRLRGG.M	3.23E-23
rep2	6945.311	6945.516	3.28E+06	sp|P02671|FIBA_HUMAN	R.HRHPDEAAFFDTASTGKTF(PGFFSPMLGEFVSETESRGSESGIFTNTKE)[16.3046]SSSHHPGIAEFPSRG.K	9.20E-08
rep2	6929.27	6929.212	2.10E+06	sp|P02671|FIBA_HUMAN	R.HRHPDEAAFFDTASTGKTFPGFFSPMLGEFVSETESRGSESGIFTNTKESSSHHPGIAEFPSRG.K	1.86E-22
rep2	21762.13	21762.97	1.15E+08	sp|P10412|H14_HUMAN	M.(S)[Acetyl]ETAPAAPAAPAPAEKTPVKKKARKSAGAAKRKASGPPVSELITKAVAASKERSGVSLAALKKALAAAGYDVEKNNSRIKLGLKSLVSKGTLVQTKGTGASGSFKLNKKAASGEAKPKAKKAGAAKAKKPAGAAKKPKKATGAATPKKSAKKTPKKAKKPAAAAGAKKAKSPKKAKAAKPKKAPKSPAKAKAVKPKAAKPKTAKPKAAKPKKAAAKKK.	0.000882
rep2	8210.212	8210.121	8.54E+06	sp|Q9NZT1|CALL5_HUMAN	M.(A)[Acetyl]GELTPEEEAQYKKAFSAVDTDGNGTINAQELGAALKATGKNLSEAQLRKLISEVDSDGDGEISFQEFLTAAKKARAG.L	2.54E-22
rep2	4150.209	4150.166	5.33E+07	sp|P05155|IC1_HUMAN	R.TLLVFEVQQPFLFVLWDQQHKFPVFMGRVYDPRA.	0.000414
rep2	13419.53	13419.46	9.17E+06	sp|Q5QNW6|H2B2F_HUMAN	.(M)[402.3727]PDPAKSAPAPKKGSKKAVTKVQKKDGKKRKRSRKESYSVYVYKVLKQVHPDTGISSKAMGIMNSFVNDIFERIAGEASRLAHYNKRSTITSREIQTAVRLLLPGELAKHAVSEGTKA.V	0.004439
rep2	6626.572	6626.506	4.43E+06	sp|P02654|APOC1_HUMAN	G.TPDVSSALDKLKEFGNTLEDKARELISRIKQSELSAKMREWFSETFQKVKEKLKIDS.	7.34E-21
rep2	6428.49	6428.405	1.14E+06	sp|P02654|APOC1_HUMAN	P.DVSSALDKLKEFGNTLEDKARELISRIKQSELSAKMREWFSETFQKVKEKLKIDS.	2.56E-12
rep2	3164.752	3164.842	3.81E+06	sp|P02647|APOA1_HUMAN	L.PVLESF(K)[394.3623]VSFLSALEEYTKKLNTQ.	6.09E-10
rep2	8756.559	8756.454	4.26E+07	sp|P02652|APOA2_HUMAN	R.(RQAKEPCV)[-102.0854]ESLVSQYFQTVTDYGKDLMEKV	1.10E-19

					KSPELQAEAKSYFEKSKEQLTPLIKKAGTE LVNFLSYFVELGTQPATQ.	
rep2	8685.517	8685.412	8.54E+06	sp|P02652|APOA2_HUMAN	R.(RQAK)[-173.1276]EPCVESLVSQYFQTVTDYGKDLM EKVKSPELQAEAKSYFEKSKEQLTPLIKKA GTELVNFLSYFVELGTQPATQ.	7.92E-05
rep2	8628.499	8628.389	2.46E+07	sp|P02652|APOA2_HUMAN	Q.(AK)[182.0676]EPCVESLVSQYFQTVTDY GKDLMEKVKSPELQAEAKSYFEKSKEQLT PLIKKAGTELVNFLSYFVELGTQPAT.Q	4.72E-14
rep2	6888.845	6888.745	1.17E+06	sp|P02654|APOC1_HUMAN	G.TPDVSSALDKLKEFGNTLEDKARELISRI KQSEL(SAKMREWFSE)[262.2396]TFQKVK EKLKIDS.	3.16E-14
rep2	28061.78	28061.47	1.34E+09	sp|P02647|APOA1_HUMAN	Q.DEPPQSPWDRVKDLATVYVDVLKDSGR DYVSQFEGSALGKQLNLKLLDNWDSVTST FSKLREQLGPVTQEFWDNLEKETEGLRQE MSKDLEEVKAKVQPYLDDFQKKWQEEME LYRQKVEPLRAELQEGARQKLHELQEKLS PLGEEMRDRARAHVDALRTHLAPYSDELR QRLAARLEALKENGGARLAEYHAKATEH LSTLSEKAKPALEDLRQGLLPVLESFKVSF LSALEEYTKKLNTQ.	0.000108
rep2	4815.709	4815.644	2.42E+07	sp|P81605|DCD_HUMAN	R.SSLLEKGLDGAKKAVGGLGKL(GKD)[0.0 202]AVEDLESVGKGAVHDVKDVLDSVL.	6.42E-19
rep2	14361.34	14361.19	1.35E+08	sp|P02647|APOA1_HUMAN	Q.DEPPQSPWDRVKDLATVYVDVLKDSGR DYVSQFEGSALGKQLNLKLLDNWDSVTST FSKLREQLGPVTQEFWDNLEKETEGLRQE MSKDLEEVKAKVQPYLDDFQKKWQEEME LYRQKVEPL.R	1.99E-26

3. TopPIC Suite Searching Results for Depleted Plasma TPP samples using GELFrEE

Sample	Precursor mass	Adjusted precursor mass	Feature intensity	Protein accession	Proteoform	E-value
T0	9440.72	9441	2.09E+06	sp|P02655|APOC2_HUMAN	G.(FEVQGTQQPQQDEMPSPTFLTQVKESLSSYWESAKTAAQNLYEKTYLPAVDEKLRDLYSKSTAAMSTYT)[-28.6381]GIFTDQVLSVLKGEE.	0.005441
T0	8756.471	8756.446	2.46E+07	sp|P02652|APOA2_HUMAN	R.(QAKEPC)[54.0075]VESLVSQYFQTVTDYGKDLMEKVKSPELQAEAKSYFEKSKEQLTPLIKKAGTELVNFLSYFVELGTQPATQ.	3.36E-12
T0	8685.412	8685.412	2.00E+07	sp|P02652|APOA2_HUMAN	R.(QAKE)[-17.0263]PCVESLVSQYFQTVTDYGKDLMEKVKSPELQAEAKSYFEKSKEQLTPLIKKAGTELVNFLSYFVELGTQPATQ.	9.78E-09
T0	8557.333	8557.353	9.67E+06	sp|P02652|APOA2_HUMAN	Q.(AK)[111.0320]EPCVESLVSQYFQTVTDYGKDLMEKVKSPELQAEAKSYFEKSKEQLTPLIKKAGTELVNFLSYFVELGTQPAT.Q	0.000159
T0	8013.399	8013.639	2.77E+06	sp|P02654|APOC1_HUMAN	V.(LVVVLSIVLEGPAPAQG)[-255.8322]TPDVSSALDKLKEFGNTLEDKARELISRIKQSELSAKMREWFSETFQKVKEKLKIDS.	0.000108
T0	7985.336	7985.291	3.54E+06	sp|P02654|APOC1_HUMAN	V.(VLSIVLEGPAPAQG)[27.0401]TPDVSSALDKLKEFGNTLEDKARELISRIKQSELSAKMREWFSETFQKVKEKLKIDS.	1.72E-08
T0	7747.264	7747.494	3.31E+06	sp|P02654|APOC1_HUMAN	L.(SIVLEGPAPAQG)[1.3961]TPDVSSALDKLKEFGNTLEDKARELISRIKQSELSAKMREWFSETFQKVKEKLKIDS.	0.000256
T0	7719.203	7719.208	5.86E+06	sp|P02654|APOC1_HUMAN	I.(VLEGPAPAQG)[173.2262]TPDVSSALDKLKEFGNTLEDKARELISRIKQSELSAKMREWFSETFQKVKEKLKIDS.	1.00E-06
T0	7453.03	7453.25	6.39E+06	sp|P02654|APOC1_HUMAN	V.(LEGPAPAQG)[6.3360]TPDVSSALDKLKEFGNTLEDKARELISRIKQSELSAKMREWFSETFQKVKEKLKIDS.	5.84E-05

T0	7425.006	7425.081	5.19E+06	sp|P02654|APOC1_HUMAN	V.(LEGPAPAQG)[-21.8328]TPDVSSALDKLKEFGNTLEDKARELISRIKQSELSAKMREWFSETFQKVKEKLKIDS.	7.35E-08
T0	7254.959	7255.094	3.44E+06	sp|P02654|APOC1_HUMAN	E.(GPAPAQGTP)[50.3071]DVSSALDKLKEFGNTLEDKARELISRIKQSELSAKMREWFSETFQKVKEKLKIDS.	3.11E-06
T0	7186.882	7186.792	4.80E+06	sp|P02654|APOC1_HUMAN	E.GPAPAQGTPDVSSA(L)[-17.9950]DKLKEFGNTLEDKARELISRIKQSELSAKMREWFSETFQKVKEKLKIDS.	6.72E-07
T0	7158.845	7159.055	5.74E+06	sp|P02654|APOC1_HUMAN	G.(PAPAQG)[11.2893]TPDVSSALDKLKEFGNTLEDKARELISRIKQSELSAKMREWFSETFQKVKEKLKIDS.	4.73E-10
T0	6988.783	6988.988	2.45E+06	sp|P02654|APOC1_HUMAN	P.APA(QGTP)[-61.7247]DVSSALDKLKEFGNTLEDKARELISRIKQSELSAKMREWFSETFQKVKEKLKIDS.	5.93E-05
T0	6892.679	6892.884	3.73E+06	sp|P02654|APOC1_HUMAN	A.(QG)[81.2981]TPDVSSALDKLKEFGNTLEDKARELISRIKQSELSAKMREWFSETFQKVKEKLKIDS.	4.83E-05
T0	6182.883	6182.878	1.60E+07	sp|P01834|IGKC_HUMAN	N.SQESVTEQDSKDSTYSLSSTLTLSKADYEKHKV(YACEVTHQGLSSPVTKSFNRGEC)[-2.0334].	5.30E-12
T0	3952.946	3952.946	5.30E+06	sp|Q14624|ITIH4_HUMAN	R.QAGAAGSRMNF(R)[-17.0353]PGVLSSRQLGLPGPPDVPDHAAYHPF.R	1.39E-07
T0	3478.758	3478.858	9.08E+06	sp|P02765|FETUA_HUMAN	S.(HPRKTRTVVQ)[-35.1154]PSVGAAAGPVVPPCPGRIRHFKV.	0.000258
T0	3394.735	3394.835	3.65E+07	sp|P02765|FETUA_HUMAN	H.(PRKTR)[17.9203]TVVQPSVGAAAGPVVPPCPGRIRHFKV.	2.98E-08
T0	3271.619	3271.635	8.15E+05	sp|Q14624|ITIH4_HUMAN	R.MNFRPGVLSSRQLGLPGPPDVPDHAAYHPF.R	4.75E-06
T0	2857.514	2857.514	2.06E+07	sp|P02765|FETUA_HUMAN	R.TVVQPSVGAAAGPV(V)[118.9972]PPCPGRIRHFKV.	5.09E-06
T0	2842.509	2842.504	1.53E+06	sp|P02765|FETUA_HUMAN	R.TVVQPSVGAAAGPV(V)[103.9875]PPCPGRIRHFKV.	9.84E-05

T0	2822.531	2822.611	9.56E+06	sp|P02765|FETUA_HUMAN	R.(TVVQPSV)[84.0948]GAAAGPVVPPCPGRIRHFKV.	3.69E-08
T0	2809.55	2809.545	4.36E+07	sp|P02765|FETUA_HUMAN	R.TVVQPSVGAAAGPVVP(PC)[71.0279]PGRIRHFKV.	9.95E-07
T0	2738.512	2738.517	2.89E+07	sp|P02765|FETUA_HUMAN	R.TVVQPSVGAAAGPVVPPCPGRIRHFKV.	1.11E-11
T37	9441.714	9441.994	5.16E+06	sp|P02655|APOC2_HUMAN	E.(VQGTQQPQQDEMPSPTFLTQVKESLSSYWESAKTAAQNLYEKTYLPAVDEKLRDLYSKSTAAMSTY)[248.4673]TGIFTDQVLSVLKGEE.	2.54E-06
T37	8756.511	8756.446	6.84E+07	sp|P02652|APOA2_HUMAN	R.(QAKEPCV)[54.0073]ESLVSQYFQTVTDYGKDLMEKVKSPELQAEAKSYFEKSKEQLTPLIKKAGTELVNFLSYFVELGTQPATQ.	5.51E-11
T37	8685.43	8685.41	4.95E+07	sp|P02652|APOA2_HUMAN	R.(QAKE)[-17.0289]PCVESLVSQYFQTVTDYGKDLMEKVKSPELQAEAKSYFEKSKEQLTPLIKKAGTELVNFLSYFVELGTQPATQ.	1.78E-13
T37	8628.398	8628.388	3.20E+07	sp|P02652|APOA2_HUMAN	A.(K)[253.1035]EPCVESLVSQYFQTVTDYGKDLMEKVKSPELQAEAKSYFEKSKEQLTPLIKKAGTELVNFLSYFVELGTQPAT.Q	1.25E-12
T37	8557.401	8557.351	2.11E+07	sp|P02652|APOA2_HUMAN	Q.(AK)[111.0301]EPCVESLVSQYFQTVTDYGKDLMEKVKSPELQAEAKSYFEKSKEQLTPLIKKAGTELVNFLSYFVELGTQPAT.Q	6.37E-07
T37	8223.482	8223.727	2.27E+06	sp|P02654|APOC1_HUMAN	V.(LVVVLSIVLEGPAPAQG)[-45.7450]TPDVSSALDKLKEFGNTLEDKARELISRIKQSELSAKMREWFSETFQKVKEKLKIDS.	0.001393
T37	7985.368	7985.303	2.49E+06	sp|P02654|APOC1_HUMAN	V.(VVLSIVLEGPAPAQG)[-72.0165]TPDVSSALDKLKEFGNTLEDKARELISRIKQSELSAKMREWFSETFQKVKEKLKIDS.	2.52E-07
T37	7957.337	7958.251	5.04E+06	sp|P02654|APOC1_HUMAN	V.VLSIVLEGPAPAQGTPDVSSALDKLKEFGNTLEDKARELISRIKQSELSAKMREWFSETFQKVKEKLKIDS.	3.28E-13
T37	7719.166	7719.166	4.91E+06	sp|P02654|APOC1_HUMAN	V.(LEGPA)[272.2524]PAQGTPDVSSALDKLKEFGNTLEDKARELISRIKQSELSAKMREWFSETFQKVKEKLKIDS.	4.20E-08

T37	7691.186	7691.181	8.38E+06	sp|P02654|APOC1_HUMAN	S.(IVLEGPAPAQG)[32.1153]TPDVSSALDKLKEFGNTLEDKARELISRIKQSELSAKMREWFSETFQKVKEKLKIDS.	3.11E-08
T37	7493.082	7493.302	1.11E+06	sp|P02654|APOC1_HUMAN	S.(IVLEGPAPAQGTP)[-165.7637]DVSSALDKLKEFGNTLEDKARELISRIKQSELSAKMREWFSETFQKVKEKLKIDS.	0.005866
T37	7453.036	7453.256	5.16E+06	sp|P02654|APOC1_HUMAN	I.VLEGPAPAQG(T)[-92.7260]PDVSSALDKLKEFGNTLEDKARELISRIKQSELSAKMREWFSETFQKVKEKLKIDS.	2.85E-10
T37	7425.024	7425.044	1.12E+07	sp|P02654|APOC1_HUMAN	I.(VLEGPAPAQG)[-120.9386]TPDVSSALDKLKEFGNTLEDKARELISRIKQSELSAKMREWFSETFQKVKEKLKIDS.	2.95E-13
T37	7254.927	7254.942	2.51E+06	sp|P02654|APOC1_HUMAN	E.GPAPA(QGTP)[50.1551]DVSSALDKLKEFGNTLEDKARELISRIKQSELSAKMREWFSETFQKVKEKLKIDS.	4.38E-06
T37	7226.912	7227.127	2.03E+06	sp|P02654|APOC1_HUMAN	E.GPA(PAQGTP)[22.3403]DVSSALDKLKEFGNTLEDKARELISRIKQSELSAKMREWFSETFQKVKEKLKIDS.	0.002366
T37	7186.884	7187.099	3.33E+06	sp|P02654|APOC1_HUMAN	E.(GPAPAQG)[-17.6881]TPDVSSALDKLKEFGNTLEDKARELISRIKQSELSAKMREWFSETFQKVKEKLKIDS.	1.04E-06
T37	7158.851	7159.061	1.16E+07	sp|P02654|APOC1_HUMAN	G.(PAPAQG)[11.2953]TPDVSSALDKLKEFGNTLEDKARELISRIKQSELSAKMREWFSETFQKVKEKLKIDS.	9.72E-14
T37	6988.816	6989.021	2.31E+06	sp|P02654|APOC1_HUMAN	P.APA(QGTP)[-61.6923]DVSSALDKLKEFGNTLEDKARELISRIKQSELSAKMREWFSETFQKVKEKLKIDS.	4.29E-09
T37	6960.772	6960.977	2.56E+06	sp|P02654|APOC1_HUMAN	A.(QGTP)[149.3916]DVSSALDKLKEFGNTLEDKARELISRIKQSELSAKMREWFSETFQKVKEKLKIDS.	6.71E-05

T37	6892.689	6892.894	7.43E+06	sp|P02654|APOC1_HUMAN	A.(PAQG)[-86.7821]TPDVSSALDKLKEFGNTLEDKARELISRIKQSELSAKMREWFSETFQKVKEKLKIDS.	1.71E-13
T37	6694.61	6694.81	2.11E+06	sp|P02654|APOC1_HUMAN	Q.(GTP)[11.2831]DVSSALDKLKEFGNTLEDKARELISRIKQSELSAKMREWFSETFQKVKEKLKIDS.	0.000103
T37	6626.567	6626.506	2.05E+06	sp|P02654|APOC1_HUMAN	G.TPDVSSALDKLKEFGNTLEDKARELISRIKQSELSAKMREWFSETFQKVKEKLKIDS.	6.39E-15
T37	6182.851	6182.881	1.07E+07	sp|P01834|IGKC_HUMAN	N.SQESVTEQDSKDSTYSLSSTLTLSKADYEKHKVY(ACEVTHQGLSSPVTKSFNRGEC)[-2.0303].	9.74E-12
T37	3952.945	3952.945	6.06E+06	sp|Q14624|ITIH4_HUMAN	R.(QAGAAGSRMNFR)[-17.0356]PGVLSSRQLGLPGPPDVPDHAAYHPF.R	0.000189
T37	3685.817	3685.927	5.64E+06	sp|P02765|FETUA_HUMAN	V.(SHPRKTR)[84.9218]TVVQPSVGAAAGPVVPPCPGRIRHFKV.	3.09E-05
T37	3478.758	3478.858	1.43E+07	sp|P02765|FETUA_HUMAN	V.(SHPRKTR)[-122.1477]TVVQPSVGAAAGPVVPPCPGRIRHFKV.	2.94E-07
T37	3465.771	3465.871	1.07E+08	sp|P02765|FETUA_HUMAN	V.(SHPRKTRTVVQPSV)[-135.1347]GAAAGPVVPPCPGRIRHFKV.	1.53E-06
T37	3424.747	3424.847	7.53E+06	sp|P02765|FETUA_HUMAN	H.(PRKTR)[47.9328]TVVQPSVGAAAGPVVPPCPGRIRHFKV.	0.00499
T37	3394.734	3394.834	9.70E+07	sp|P02765|FETUA_HUMAN	H.(PRKTR)[17.9202]TVVQPSVGAAAGPVVPPCPGRIRHFKV.	6.13E-11
T37	3271.633	3271.635	8.03E+05	sp|Q14624|ITIH4_HUMAN	R.MNFRPGVLSSRQLGLPGPPDVPDHAAYHPF.R	2.86E-08
T37	2888.488	2888.498	8.90E+06	sp|P02765|FETUA_HUMAN	R.TVVQPSVGAAAGP(VV)[149.9818]PPCPGRIRHFKV.	0.002807
T37	2872.499	2872.499	5.23E+06	sp|P02765|FETUA_HUMAN	R.TVVQPSVGAAAGPVVP(PC)[133.9821]PGRIRHFKV.	2.34E-09
T37	2857.523	2857.518	3.38E+07	sp|P02765|FETUA_HUMAN	R.TVVQPSVGAAAGPVVP(PC)[119.0009]PGRIRHFKV.	1.78E-09
T37	2825.546	2825.541	4.27E+06	sp|P02765|FETUA_HUMAN	R.TVVQPSVGAAAGPVV(PPC)[87.0246]PGRIRHFKV.	6.72E-05

T37	2822.532	2822.612	1.04E+07	sp|P02765|FETUA_HUMAN	R.(TVVQP)[84.0956]SVGAAAGPVVPPCPGRIRHFKV.	3.94E-08
T37	2809.55	2809.545	8.16E+07	sp|P02765|FETUA_HUMAN	R.TVVQPSVGAAAGPVVP(PC)[71.0284]PGRIRHFKV.	3.32E-09
T37	2738.513	2738.517	6.61E+07	sp|P02765|FETUA_HUMAN	R.TVVQPSVGAAAGPVVPPCPGRIRHFKV.	6.32E-13
T50	10507.11	10507.43	3.86E+06	sp|P02656|APOC3_HUMAN	.(MQPRVLLVVALLALLASARA)[-338.0709]SEAEDASLLSFMQGYMKHATKTAKDALSSVQESQVAQQARGWVTDGFSSLKDYWSTVKDKFSEFWDLDPEVRPTSAVAA.	0.003892
T50	9441.772	9442.052	7.65E+06	sp|P02655|APOC2_HUMAN	G.(FEVQGTQQPQQDEMPSPTFLTQVKESLSSYWESAKTAAQNLYEKTYLPAVDEKLRDLYSKSTAAMST)[-27.5862]YTGIFTDQVLSVLKGEE.	7.52E-08
T50	9175.61	9175.885	1.07E+07	sp|P02655|APOC2_HUMAN	G.TQQPQQDEM(PSPTFLTQVKESLSSYWESAKTAAQNLYEKTYLPAVDEKLRDLYSKSTAAMSTY)[266.5069]TGIFTDQVLSVLKGEE.	3.79E-09
T50	8909.396	8909.378	4.77E+06	sp|P02655|APOC2_HUMAN	G.TQQPQQDEMPSPTFLTQVKESLSSYWESAKTAAQNLYEKTYLPAVDEKLRDLYSKSTAAMSTYTGIFTDQVLSVLKGEE.	8.10E-10
T50	8756.514	8756.449	5.25E+07	sp|P02652|APOA2_HUMAN	R.(QAKEPC)[54.0101]VESLVSQYFQTVTDYGKDLMEKVKSPELQAEAKSYFEKSKEQLTPLIKKAGTELVNFLSYFVELGTQPATQ.	4.47E-13
T50	8685.418	8685.408	7.41E+07	sp|P02652|APOA2_HUMAN	R.(RQAK)[-173.1316]EPCVESLVSQYFQTVTDYGKDLMEKVKSPELQAEAKSYFEKSKEQLTPLIKKAGTELVNFLSYFVELGTQPATQ.	3.56E-13
T50	8628.444	8628.384	2.64E+07	sp|P02652|APOA2_HUMAN	Q.(AK)[182.0632]EPCVESLVSQYFQTVTDYGKDLMEKVKSPELQAEAKSYFEKSKEQLTPLIKKAGTELVNFLSYFVELGTQPAT.Q	2.21E-12
T50	8557.378	8557.348	3.07E+07	sp|P02652|APOA2_HUMAN	Q.(AK)[111.0265]EPCVESLVSQYFQTVTDYGKDLMEKVKSPELQAEAKSYFEKSKEQLTPLIKKAGTELVNFLSYFVELGTQPAT.Q	3.56E-11
T50	7747.233	7747.463	3.59E+06	sp|P02654|APOC1_HUMAN	V.(VLSIVLEGPAPAQG)[-210.7873]TPDVSSALDKLKEFGNTLEDKAR	0.001083

					ELISRIKQSELSAKMREWFSETFQKVKEKL KIDS.	
T50	7719.208	7719.178	6.37E+06	sp|P02654|APOC1_HUMAN	I.(VLEGPA)[173.1957]PAQGTPDVSSALDKL KEFGNTLEDKARELISRIKQSELSAKMREW FSETFQKVKEKLKIDS.	4.12E-07
T50	7691.174	7691.404	5.54E+06	sp|P02654|APOC1_HUMAN	V.(LEGPAPAQG)[244.4907]TPDVSSALDKL KEFGNTLEDKARELISRIKQSELSAKMREW FSETFQKVKEKLKIDS.	0.001968
T50	7549.153	7549.378	3.67E+06	sp|P02654|APOC1_HUMAN	I.(VLEGPAPAQGTP)[3.3963]DVSSALDKLK EFGNTLEDKARELISRIKQSELSAKMREWF SETFQKVKEKLKIDS.	9.62E-07
T50	7481.068	7481.008	4.49E+06	sp|P02654|APOC1_HUMAN	V.(LEGPAPAQG)[34.0939]TPDVSSALDKLK EFGNTLEDKARELISRIKQSELSAKMREWF SETFQKVKEKLKIDS.	0.002008
T50	7453.032	7453.252	1.03E+07	sp|P02654|APOC1_HUMAN	V.(LEGPAPAQG)[6.3378]TPDVSSALDKLKE FGNTLEDKARELISRIKQSELSAKMREWFS ETFQKVKEKLKIDS.	0.0001
T50	7425.01	7425.02	1.04E+07	sp|P02654|APOC1_HUMAN	V.(LEGPAPAQG)[-21.8934]TPDVSSALDKLKEFGNTLEDKARE LISRIKQSELSAKMREWFSETFQKVKEKLK IDS.	2.61E-09
T50	7282.996	7282.951	5.31E+06	sp|P02654|APOC1_HUMAN	L.(EGPAPAQGTP)[-50.8787]DVSSALDKLKEFGNTLEDKARELI SRIKQSELSAKMREWFSETFQKVKEKLKID S.	6.30E-08
T50	7254.962	7255.172	4.94E+06	sp|P02654|APOC1_HUMAN	E.GPA(PAQGTP)[50.3853]DVSSALDKLKEF GNTLEDKARELISRIKQSELSAKMREWFSE TFQKVKEKLKIDS.	5.69E-05
T50	7186.917	7187.132	1.13E+07	sp|P02654|APOC1_HUMAN	E.(GPAPAQG)[-17.6549]TPDVSSALDKLKEFGNTLEDKARE LISRIKQSELSAKMREWFSETFQKVKEKLK IDS.	8.71E-08
T50	7158.876	7159.086	1.62E+07	sp|P02654|APOC1_HUMAN	G.(PAPAQG)[11.3201]TPDVSSALDKLKEFG NTLEDKARELISRIKQSELSAKMREWFSET FQKVKEKLKIDS.	1.10E-15

T50	7016.84	7017.05	3.77E+06	sp|P02654|APOC1_HUMAN	P.APA(QGTP)[-33.6624]DVSSALDKLKEFGNTLEDKARELISRIKQSELSAKMREWFSETFQKVKEKLKIDS.	0.000254
T50	6988.784	6988.989	7.20E+06	sp|P02654|APOC1_HUMAN	E.(GPAPAQGTP)[-215.7982]DVSSALDKLKEFGNTLEDKARELISRIKQSELSAKMREWFSETFQKVKEKLKIDS.	2.01E-06
T50	6920.737	6920.942	5.89E+06	sp|P02654|APOC1_HUMAN	G.(PAPAQG)[-226.8241]TPDVSSALDKLKEFGNTLEDKARELISRIKQSELSAKMREWFSETFQKVKEKLKIDS.	0.000152
T50	6892.716	6892.921	1.53E+07	sp|P02654|APOC1_HUMAN	P.APA(QG)[-157.7922]TPDVSSALDKLKEFGNTLEDKARELISRIKQSELSAKMREWFSETFQKVKEKLKIDS.	4.54E-11
T50	6722.629	6722.829	4.78E+06	sp|P02654|APOC1_HUMAN	A.(QGTP)[-88.7565]DVSSALDKLKEFGNTLEDKARELISRIKQSELSAKMREWFSETFQKVKEKLKIDS.	9.01E-05
T50	6626.533	6626.506	7.61E+06	sp|P02654|APOC1_HUMAN	G.TPDVSSALDKLKEFGNTLEDKARELISRIKQSELSAKMREWFSETFQKVKEKLKIDS.	2.01E-16
T50	4415.158	4415.288	1.95E+08	sp|P02765|FETUA_HUMAN	V.SL(GSPSGEVSHPRKTR)[0.8960]TVVQPSVGAAAGPVVPPCPGRIRHFKV.	3.82E-13
T50	3952.946	3952.941	4.88E+07	sp|Q14624|ITIH4_HUMAN	R.(QAGAAGSRMNFR)[-17.0402]PGVLSSRQLGLPGPPDVPDHAAYHPF.R	0.007045
T50	3685.835	3685.945	3.47E+07	sp|P02765|FETUA_HUMAN	E.(VSHPRKTR)[-14.1291]TVVQPSVGAAAGPVVPPCPGRIRHFKV.	1.20E-09
T50	3478.757	3478.857	3.54E+07	sp|P02765|FETUA_HUMAN	S.(HPRKTR)[-35.1167]TVVQPSVGAAAGPVVPPCPGRIRHFKV.	1.15E-08
T50	3465.77	3465.87	1.69E+08	sp|P02765|FETUA_HUMAN	V.(SHPRKTRTVVQ)[-135.1351]PSVGAAAGPVVPPCPGRIRHFKV.	3.93E-06

T50	3424.748	3424.848	4.20E+07	sp|P02765|FETUA_HUMAN	V.(SHPRKTRTVVQ)[-176.1576]PSVGAAAGPVVPPCPGRIRHFKV.	8.57E-10
T50	3394.734	3394.834	3.85E+08	sp|P02765|FETUA_HUMAN	H.(PRKTR)[17.9199]TVVQPSVGAAAGPVVPPCPGRIRHFKV.	1.08E-13
T50	3271.634	3271.635	8.74E+06	sp|Q14624|ITIH4_HUMAN	R.MNFRPGVLSSRQLGLPGPPDVPDHAAYHPF.R	3.46E-07
T50	2857.515	2857.52	2.48E+07	sp|P02765|FETUA_HUMAN	R.TVVQPSVGAAAGPVVP(PC)[119.0035]PGRIRHFKV.	1.13E-07
T50	2822.53	2822.61	2.56E+07	sp|P02765|FETUA_HUMAN	R.TV(VQPSV)[84.0934]GAAAGPVVPPCPGRIRHFKV.	1.08E-07
T50	2809.548	2809.548	1.24E+08	sp|P02765|FETUA_HUMAN	R.TVVQPSVGAAAGPVVP(PC)[71.0318]PGRIRHFKV.	1.21E-08
T50	2738.512	2738.517	2.37E+08	sp|P02765|FETUA_HUMAN	R.TVVQPSVGAAAGPVVPPCPGRIRHFKV.	1.68E-13
T50	2658.257	2658.249	2.67E+07	sp|P02671|FIBA_HUMAN	A.DEAGSEADHEGTHSTKRGHAKSRPV.R	6.98E-09
T63	10156.55	10156.71	1.21E+06	sp|P62987|RL40_HUMAN	.MQIFVKTLTGKTITLEVEPSDTIENVKAKIQDKEGIPPDQQRLIFAGKQLEDGRTLSDYNIQKESTLHLVLRLRGG(IIEPS)[57.2149]LRQLAQKY.N	0.002959
T63	9441.724	9442.004	1.20E+07	sp|P02655|APOC2_HUMAN	G.(FEVQGTQQPQQDEMPSPTFLTQVKESLSSYWESAKTAAQNLYEKTYLPAVDEKLRDLYSKSTAAMST)[-27.6338]YTGIFTDQVLSVLKGEE.	2.18E-06
T63	9441.691	9441.911	1.20E+07	sp|P02654|APOC1_HUMAN	.(MRLFLSLPV)[115.8237]LVVVLSIVLEGPAPAQGTPDVSSALDKLKEFGNTLEDKARELISRIKQSELSAKMREWFSETFQKVKEKLKIDS.	0.000505
T63	9175.577	9175.852	1.50E+07	sp|P02655|APOC2_HUMAN	G.TQQPQQDEM(PSPTFLTQVKESLSSYWESAKTAAQNLYEKTYLPAVDEKLRDLYSKSTAAMSTY)[266.4733]TGIFTDQVLSVLKGEE.	4.09E-09
T63	8909.452	8909.378	6.63E+06	sp|P02655|APOC2_HUMAN	G.TQQPQQDEMPSPTFLTQVKESLSSYWESAKTAAQNLYEKTYLPAVDEKLRDLYSKSTAAMSTYTGIFTDQVLSVLKGEE.	3.70E-12
T63	8756.462	8756.437	1.72E+08	sp|P02652|APOA2_HUMAN	R.(RQAKEPC)[-102.1021]VESLVSQYFQTVTDYGKDLMEK	3.00E-23

					VKSPELQAEAKSYFEKSKEQLTPLIKKAGTELVNFLSYFVELGTQPATQ.	
T63	8685.43	8685.405	2.00E+08	sp|P02652|APOA2_HUMAN	R.(QAK)[-17.0333]EPCVESLVSQYFQTVTDYGKDLMEKVKSPELQAEAKSYFEKSKEQLTPLIKKAGTELVNFLSYFVELGTQPATQ.	8.42E-19
T63	8628.438	8628.383	8.16E+07	sp|P02652|APOA2_HUMAN	Q.(AK)[182.0616]EPCVESLVSQYFQTVTDYGKDLMEKVKSPELQAEAKSYFEKSKEQLTPLIKKAGTELVNFLSYFVELGTQPAT.Q	1.16E-16
T63	8557.376	8557.351	8.18E+07	sp|P02652|APOA2_HUMAN	A.(K)[182.0673]EPCVESLVSQYFQTVTDYGKDLMEKVKSPELQAEAKSYFEKSKEQLTPLIKKAGTELVNFLSYFVELGTQPAT.Q	4.79E-15
T63	8456.346	8456.301	5.06E+06	sp|P02652|APOA2_HUMAN	A.(K)[182.0642]EPCVESLVSQYFQTVTDYGKDLMEKVKSPELQAEAKSYFEKSKEQLTPLIKKAGTELVNFLSYFVELGTQPA.T	5.08E-05
T63	7957.333	7958.251	1.37E+07	sp|P02654|APOC1_HUMAN	V.VLSIVLEGPAPAQGTPDVSSALDKLKEFGNTLEDKARELISRIKQSELSAKMREWFSETFQKVKEKLKIDS.	3.82E-09
T63	7718.203	7718.433	4.30E+06	sp|P02654|APOC1_HUMAN	V.(LEGPAPAQG)[271.5194]TPDVSSALDKLKEFGNTLEDKARELISRIKQSELSAKMREWFSETFQKVKEKLKIDS.	5.05E-06
T63	7691.148	7691.378	2.60E+07	sp|P02654|APOC1_HUMAN	S.(IVLEGPAPAQG)[32.3123]TPDVSSALDKLKEFGNTLEDKARELISRIKQSELSAKMREWFSETFQKVKEKLKIDS.	2.04E-07
T63	7453.075	7453.295	4.84E+06	sp|P02654|APOC1_HUMAN	V.(LEGPAPAQG)[6.3815]TPDVSSALDKLKEFGNTLEDKARELISRIKQSELSAKMREWFSETFQKVKEKLKIDS.	0.00049
T63	7424.991	7425.076	3.63E+07	sp|P02654|APOC1_HUMAN	V.(LEGPAPAQG)[-21.8378]TPDVSSALDKLKEFGNTLEDKARELISRIKQSELSAKMREWFSETFQKVKEKLKIDS.	1.58E-12
T63	7254.927	7254.912	5.08E+06	sp|P02654|APOC1_HUMAN	E.(GPAPAQGTP)[50.1244]DVSSALDKLKEFGNTLEDKARELISRIKQSELSAKMREWFSETFQKVKEKLKIDS.	1.52E-06
T63	7226.917	7227.042	5.56E+06	sp|P02654|APOC1_HUMAN	V.(LEGPAPAQGTP)[-219.8721]DVSSALDKLKEFGNTLEDKAREL	2.81E-06

					ISRIKQSELSAKMREWFSETFQKVKEKLKIDS.	
T63	7186.88	7187.095	3.12E+06	sp|P02654|APOC1_HUMAN	E.(GPAPAQG)[-17.6923]TPDVSSALDKLKEFGNTLEDKARELISRIKQSELSAKMREWFSETFQKVKEKLKIDS.	1.68E-08
T63	7158.848	7159.058	3.59E+07	sp|P02654|APOC1_HUMAN	G.(PAPAQG)[11.2920]TPDVSSALDKLKEFGNTLEDKARELISRIKQSELSAKMREWFSETFQKVKEKLKIDS.	2.55E-12
T63	6988.785	6988.99	5.27E+06	sp|P02654|APOC1_HUMAN	E.(GPAPAQGTP)[-215.7974]DVSSALDKLKEFGNTLEDKARELISRIKQSELSAKMREWFSETFQKVKEKLKIDS.	4.92E-08
T63	6960.77	6960.975	6.72E+06	sp|P02654|APOC1_HUMAN	A.(PAQGTP)[-18.7005]DVSSALDKLKEFGNTLEDKARELISRIKQSELSAKMREWFSETFQKVKEKLKIDS.	5.32E-06
T63	6892.69	6892.895	2.14E+07	sp|P02654|APOC1_HUMAN	A.(PAQG)[-86.7805]TPDVSSALDKLKEFGNTLEDKARELISRIKQSELSAKMREWFSETFQKVKEKLKIDS.	8.19E-13
T63	6722.668	6722.868	2.19E+06	sp|P02654|APOC1_HUMAN	Q.(GTP)[39.3407]DVSSALDKLKEFGNTLEDKARELISRIKQSELSAKMREWFSETFQKVKEKLKIDS.	0.005414
T63	6694.601	6694.801	8.54E+06	sp|P02654|APOC1_HUMAN	Q.(GTP)[11.2738]DVSSALDKLKEFGNTLEDKARELISRIKQSELSAKMREWFSETFQKVKEKLKIDS.	1.39E-13
T63	6626.565	6626.506	6.36E+06	sp|P02654|APOC1_HUMAN	G.TPDVSSALDKLKEFGNTLEDKARELISRIKQSELSAKMREWFSETFQKVKEKLKIDS.	5.10E-16
T63	6440.957	6440.987	8.24E+06	sp|P01834|IGKC_HUMAN	Q.SGNSQESVTEQDSKDSTYSLSSTLTLSKADYEKHKV(YACEVTHQGLSSPVTKSFNRGEC)[-2.0215].	2.61E-07
T63	6428.455	6428.405	3.06E+06	sp|P02654|APOC1_HUMAN	P.DVSSALDKLKEFGNTLEDKARELISRIKQSELSAKMREWFSETFQKVKEKLKIDS.	2.56E-17

T63	6182.878	6182.883	2.62E+07	sp|P01834|IGKC_HUMAN	N.SQESVTEQDSKDSTYSLSSTLTLSKADYEKHKVYA(CEVTHQGLSSPVTKSFNRGEC)[-2.0287].	2.24E-14
T63	4415.178	4415.308	1.90E+08	sp|P02765|FETUA_HUMAN	V.SL(GSPSGEVSHPRKTR)[0.9159]TVVQPSVGAAAGPVVPPCPGRIRHFKV.	2.54E-11
T63	4415.166	4415.176	1.90E+08	sp|P02675|FIBB_HUMAN	K.(SQGV)[-104.0622]NDNEEGFFSARGHRPLDKKREEAPSLRPAPPPISGGGY.R	1.90E-06
T63	4242.099	4242.224	7.94E+07	sp|P02765|FETUA_HUMAN	L.(GSPSGEVSHPRKTR)[27.9478]TVVQPSVGAAAGPVVPPCPGRIRHFKV.	0.004424
T63	3952.945	3952.95	1.72E+07	sp|Q14624|ITIH4_HUMAN	R.QAGAAGSRMNF(R)[-17.0310]PGVLSSRQLGLPGPPDVPDHAAYHPF.R	1.08E-07
T63	3811.818	3811.928	1.38E+06	sp|Q14624|ITIH4_HUMAN	G.(ESRNRNV)[13.9893]HSGSTFFKYYLQGAKIPKPEASFSPR.R	0.00078
T63	3715.832	3715.942	4.02E+06	sp|P02765|FETUA_HUMAN	E.(VSHPRKTR)[15.8685]TVVQPSVGAAAGPVVPPCPGRIRHFKV.	0.000112
T63	3685.831	3685.941	2.85E+07	sp|P02765|FETUA_HUMAN	V.(SHPRKTR)[84.9354]TVVQPSVGAAAGPVVPPCPGRIRHFKV.	5.09E-07
T63	3493.772	3493.872	5.93E+06	sp|P02765|FETUA_HUMAN	V.(SHPRKTR)[-107.1331]TVVQPSVGAAAGPVVPPCPGRIRHFKV.	0.00993
T63	3478.755	3478.855	3.09E+07	sp|P02765|FETUA_HUMAN	V.(SHPRKTRTVVQ)[-122.1498]PSVGAAAGPVVPPCPGRIRHFKV.	2.72E-09
T63	3465.769	3465.869	2.03E+08	sp|P02765|FETUA_HUMAN	V.(SHPRKTRTVVQPSVG)[-135.1357]AAAGPVVPPCPGRIRHFKV.	8.74E-05
T63	3424.748	3424.848	3.49E+07	sp|P02765|FETUA_HUMAN	H.(PRKTRTVVQ)[47.9342]PSVGAAAGPVVPPCPGRIRHFKV.	5.76E-13
T63	3406.743	3406.843	8.78E+06	sp|P02765|FETUA_HUMAN	H.(PRKTRTVVQ)[29.9291]PSVGAAAGPVVPPCPGRIRHFKV.	0.001759
T63	3394.733	3394.833	3.02E+08	sp|P02765|FETUA_HUMAN	H.(PRKTR)[17.9189]TVVQPSVGAAAGPVVPPCPGRIRHFKV.	1.91E-12
T63	3271.623	3271.635	1.99E+06	sp|Q14624|ITIH4_HUMAN	R.MNFRPGVLSSRQLGLPGPPDVPDHAAYHPF.R	1.85E-10
T63	2872.497	2872.497	2.79E+06	sp|P02765|FETUA_HUMAN	R.TVVQPSVGAAAGPVVP(PC)[133.9802]PGRIRHFKV.	4.53E-08

T63	2857.515	2857.515	3.41E+07	sp|P02765|FETUA_HUMAN	R.TVVQPSVGAAAGPVVP(PC)[118.9979]PGRIRHFKV.	7.30E-08
T63	2837.547	2837.552	5.17E+06	sp|P02765|FETUA_HUMAN	R.TVVQPSVGAAAGPV(V)[99.0358]PPCPGRIRHFKV.	5.47E-05
T63	2822.529	2822.609	1.89E+07	sp|P02765|FETUA_HUMAN	R.TV(VQ)[84.0926]PSVGAAAGPVVPPCPGRIRHFKV.	2.21E-08
T63	2809.538	2809.548	1.65E+08	sp|P02765|FETUA_HUMAN	R.TVVQPSVGAAAGPVVP(PC)[71.0313]PGRIRHFKV.	3.28E-10
T63	2750.507	2750.542	3.27E+06	sp|P02765|FETUA_HUMAN	R.(TVVQPSVGA)[12.0250]AAGPVVPPCPGRIRHFKV.	0.000887
T63	2738.512	2738.517	1.47E+08	sp|P02765|FETUA_HUMAN	R.TVVQPSVGAAAGPVVPPCPGRIRHFKV.	1.34E-13
T63	2658.245	2658.249	3.37E+07	sp|P02671|FIBA_HUMAN	A.DEAGSEADHEGTHSTKRGHAKSRPV.R	1.31E-10
T76	10156.59	10156.52	3.55E+06	sp|P0CG47|UBB_HUMAN	.MQIFVKTLTGKTITLEVEPSDTIENVKAKIQDKEGIPPDQQRLIFAGKQLEDGRTLSDYNIQKESTLHLVLRLRGG(MQ)[35.0090]IFVKTLTGKTIT.L	2.03E-06
T76	9890.447	9890.742	5.35E+06	sp|P0CG47|UBB_HUMAN	S.(TLHLVLRLRGG)[115.3693]MQIFVKTLTGKTITLEVEPSDTIENVKAKIQDKEGIPPDQQRLIFAGKQLEDGRTLSDYNIQKESTLHLVLRLRGG.C	1.32E-06
T76	9681.648	9681.723	7.07E+07	sp|P02656|APOC3_HUMAN	V.(VALLALLASARA)[-227.2185]SEAEDASLLSFMQGYMKHATKTAKDALSSVQESQVAQQARGWVTDGFSSLKDYWSTVKDKFSEFWDLDPEVRPTSAVAA.	0.005161
T76	9640.291	9640.576	3.64E+06	sp|P0CG47|UBB_HUMAN	L.(HLVLRLRGG)[79.3345]MQIFVKTLTGKTITLEVEPSDTIENVKAKIQDKEGIPPDQQRLIFAGKQLEDGRTLSDYNIQKESTLHLVLRLRGG.C	1.20E-06
T76	9624.267	9624.247	9.48E+06	sp|P0CG47|UBB_HUMAN	L.H(LVLRLRGG)[63.0052]MQIFVKTLTGKTITLEVEPSDTIENVKAKIQDKEGIPPDQQRLIFAGKQLEDGRTLSDYNIQKESTLHLVLRLRGG.C	1.37E-10
T76	9469.766	9469.638	4.24E+06	sp|P02655|APOC2_HUMAN	G.FEVQGTQQPQQDEMPSPTFLTQVKESLSSYWESAKTAAQNLYEKTYLPAVDEKLRDLYSKSTAAMSTYTGIFTDQVLSVLKGEE.	6.62E-10

T76	9441.789	9442.069	4.20E+06	sp|P02655|APOC2_HUMAN	F.(EVQGTQQPQQDEMPSPTFLTQVKESLSSYWESAKTAAQNLYEKTYLPAVDEKLRDLYSKSTAAMST)[119.4997]YTGIFTDQVLSVLKGEE.	6.96E-05
T76	9414.474	9414.609	2.60E+07	sp|P02656|APOC3_HUMAN	L.ASARASEA(EDA)[199.1464]SLLSFMQGYMKHATKTAKDALSSVQESQVAQQARGWVTDGFSSLKDYWSTVKDKFSEFWDLDPEVRPTSAVAA.	0.000161
T76	9358.138	9358.043	8.46E+06	sp|P0CG47|UBB_HUMAN	V.(L)[146.0134]RLRGGMQIFVKTLTGKTITLEVEPSDTIENVKAKIQDKEGIPPDQQRLIFAGKQLEDGRTLSDYNIQKESTLHLVLRLRGG.C	1.20E-08
T76	9203.66	9203.935	1.98E+06	sp|P02655|APOC2_HUMAN	G.TQQPQQDEMPSPTFLTQVKESLSSYWESAKTAAQNLYEKTYLPA(VDEKLRDLYSKSTAAMSTY)[294.5562]TGIFTDQVLSVLKGEE.	6.52E-11
T76	9175.636	9175.911	1.31E+07	sp|P02655|APOC2_HUMAN	G.TQQPQQDEM(PSPTFLTQVKESLSSYWESAKTAAQNLYEKTYLPAVDEKLRDLYSKSTAAMSTY)[266.5326]TGIFTDQVLSVLKGEE.	7.90E-11
T76	9090.991	9091.261	4.85E+06	sp|P0CG47|UBB_HUMAN	.((M)[Acetyl]Q)[489.6339]IFVKTLTGKTITLEVEPSDTIENVKAKIQDKEGIPPDQQRLIFAGKQLEDGRTLSDYNIQKESTLHLVLRLRGG.M	5.24E-05
T76	8957.685	8957.585	4.22E+06	sp|P02652|APOA2_HUMAN	R.(RQAKEPCV)[99.0454]ESLVSQYFQTVTDYGKDLMEKVKSPELQAEAKSYFEKSKEQLTPLIKKAGTELVNFLSYFVELGTQPATQ.	5.49E-07
T76	8909.415	8909.378	1.19E+07	sp|P02655|APOC2_HUMAN	G.TQQPQQDEMPSPTFLTQVKESLSSYWESAKTAAQNLYEKTYLPAVDEKLRDLYSKSTAAMSTYTGIFTDQVLSVLKGEE.	5.10E-12
T76	8825.809	8825.714	1.92E+06	sp|P0CG47|UBB_HUMAN	.MQIFVKTLTGKTITLE(V)[266.0975]EPSDTIENVKAKIQDKEGIPPDQQRLIFAGKQLEDGRTLSDYNIQKESTLHLVLRLRGG.M	1.45E-09
T76	8819.411	8819.396	9.18E+07	sp|P02652|APOA2_HUMAN	R.(RQAKEPC)[-39.1438]VESLVSQYFQTVTDYGKDLMEKV	8.63E-12

					KSPELQAEAKSYFEKSKEQLTPLIKKAGTE LVNFLSYFVELGTQPATQ.	
T76	8756.463	8756.443	1.95E+08	sp|P02652|APOA2_HUMAN	R.(QAKEPC)[54.0049]VESLVSQYFQTVTDY GKDLMEKVKSPELQAEAKSYFEKSKEQLT PLIKKAGTELVNFLSYFVELGTQPATQ.	1.85E-19
T76	8685.461	8685.401	3.65E+07	sp|P02652|APOA2_HUMAN	R.RQAKEPC(VE)[-173.1387]SLVSQYFQTVTDYGKDLMEKVK SPELQAEAKSYFEKSKEQLTPLIKKAGTEL VNFLSYFVELGTQPATQ.	5.24E-08
T76	8628.435	8628.385	8.93E+07	sp|P02652|APOA2_HUMAN	Q.(AK)[182.0641]EPCVESLVSQYFQTVTDY GKDLMEKVKSPELQAEAKSYFEKSKEQLT PLIKKAGTELVNFLSYFVELGTQPAT.Q	1.16E-14
T76	8557.455	8557.35	1.09E+07	sp|P02652|APOA2_HUMAN	Q.(AK)[111.0287]EPCVESLVSQYFQTVTDY GKDLMEKVKSPELQAEAKSYFEKSKEQLT PLIKKAGTELVNFLSYFVELGTQPAT.Q	5.57E-07
T76	8281.565	8281.81	5.15E+06	sp|P02654|APOC1_HUMAN	V.(LVVVLSIVLEGPAPAQG)[12.3384]TPDV SSALDKLKEFGNTLEDKARELISRIKQSELS AKMREWFSETFQKVKEKLKIDS.	0.000181
T76	8251.499	8251.744	1.13E+07	sp|P02654|APOC1_HUMAN	V.(LVVVLSIVLEGPAPAQG)[-17.7279]TPDVSSALDKLKEFGNTLEDKARE LISRIKQSELSAKMREWFSETFQKVKEKLK IDS.	3.52E-05
T76	8223.419	8223.664	8.74E+06	sp|P02654|APOC1_HUMAN	V.(LVVVLSIVLEGPAPAQG)[-45.8076]TPDVSSALDKLKEFGNTLEDKARE LISRIKQSELSAKMREWFSETFQKVKEKLK IDS.	0.000101
T76	8013.356	8013.596	1.20E+07	sp|P02654|APOC1_HUMAN	V.(LVVVLSIVLEGPAPAQG)[-255.8754]TPDVSSALDKLKEFGNTLEDKAR ELISRIKQSELSAKMREWFSETFQKVKEKL KIDS.	1.70E-05
T76	7985.335	7985.295	2.68E+07	sp|P02654|APOC1_HUMAN	V.(VLSIVLEGPAPAQG)[27.0442]TPDVSSAL DKLKEFGNTLEDKARELISRIKQSELSAKM REWFSETFQKVKEKLKIDS.	4.29E-10
T76	7957.3	7958.251	2.38E+07	sp|P02654|APOC1_HUMAN	V.VLSIVLEGPAPAQGTPDVSSALDKLKEF GNTLEDKARELISRIKQSELSAKMREWFSE TFQKVKEKLKIDS.	3.81E-10

T76	7787.295	7787.2	2.50E+06	sp|P02654|APOC1_HUMAN	I.(VLEGPAPAQG)[241.2179]TPDVSSALDKLKEFGNTLEDKARELISRIKQSELSAKMREWFSETFQKVKEKLKIDS.	2.93E-06
T76	7747.203	7746.098	1.62E+07	sp|P02654|APOC1_HUMAN	L.SIVLEGPAPAQGTPDVSSALDKLKEFGNTLEDKARELISRIKQSELSAKMREWFSETFQKVKEKLKIDS.	3.51E-07
T76	7719.156	7719.006	6.23E+07	sp|P02654|APOC1_HUMAN	L.(SIVLEGPAPAQG)[-27.0927]TPDVSSALDKLKEFGNTLEDKARELISRIKQSELSAKMREWFSETFQKVKEKLKIDS.	3.89E-12
T76	7691.13	7691.175	5.77E+07	sp|P02654|APOC1_HUMAN	S.(IVLEGPAPAQG)[32.1089]TPDVSSALDKLKEFGNTLEDKARELISRIKQSELSAKMREWFSETFQKVKEKLKIDS.	1.33E-11
T76	7549.135	7549.36	4.47E+06	sp|P02654|APOC1_HUMAN	I.(VLEGPAPAQGTP)[3.3782]DVSSALDKLKEFGNTLEDKARELISRIKQSELSAKMREWFSETFQKVKEKLKIDS.	0.000167
T76	7521.137	7521.362	8.16E+06	sp|P02654|APOC1_HUMAN	I.(VLEGPAPAQGTP)[-24.6204]DVSSALDKLKEFGNTLEDKARELISRIKQSELSAKMREWFSETFQKVKEKLKIDS.	1.66E-06
T76	7492.102	7492.322	4.62E+06	sp|P02654|APOC1_HUMAN	V.(LEGPAPAQG)[45.4078]TPDVSSALDKLKEFGNTLEDKARELISRIKQSELSAKMREWFSETFQKVKEKLKIDS.	0.00047
T76	7482.096	7482.316	1.49E+07	sp|P02654|APOC1_HUMAN	I.(VLEGPAPAQG)[-63.6657]TPDVSSALDKLKEFGNTLEDKARELISRIKQSELSAKMREWFSETFQKVKEKLKIDS.	3.94E-06
T76	7453.002	7453.222	7.09E+07	sp|P02654|APOC1_HUMAN	V.(LEGPAPAQG)[6.3078]TPDVSSALDKLKEFGNTLEDKARELISRIKQSELSAKMREWFSETFQKVKEKLKIDS.	5.25E-14
T76	7425.021	7425.071	1.03E+08	sp|P02654|APOC1_HUMAN	V.(LEGPAPAQG)[-21.8425]TPDVSSALDKLKEFGNTLEDKARELISRIKQSELSAKMREWFSETFQKVKEKLKIDS.	7.69E-15
T76	7283.008	7282.998	6.27E+06	sp|P02654|APOC1_HUMAN	L.EGP(APAQGTP)[-50.8319]DVSSALDKLKEFGNTLEDKARELI	2.57E-09

					SRIKQSELSAKMREWFSETFQKVKEKLKIDS.	
T76	7254.958	7254.963	1.62E+07	sp|P02654|APOC1_HUMAN	E.(GPAPAQGTP)[50.1758]DVSSALDKLKEFGNTLEDKARELISRIKQSELSAKMREWFSETFQKVKEKLKIDS.	7.87E-09
T76	7226.919	7226.969	1.29E+07	sp|P02654|APOC1_HUMAN	V.(LEGPAPAQG)[-219.9448]TPDVSSALDKLKEFGNTLEDKARELISRIKQSELSAKMREWFSETFQKVKEKLKIDS.	1.40E-08
T76	7186.886	7187.031	6.25E+07	sp|P02654|APOC1_HUMAN	E.(GPAPAQG)[-17.7560]TPDVSSALDKLKEFGNTLEDKARELISRIKQSELSAKMREWFSETFQKVKEKLKIDS.	5.49E-16
T76	7158.912	7159.122	1.29E+08	sp|P02654|APOC1_HUMAN	G.(PAPAQG)[11.3565]TPDVSSALDKLKEFGNTLEDKARELISRIKQSELSAKMREWFSETFQKVKEKLKIDS.	1.85E-14
T76	6988.82	6989.025	1.93E+07	sp|P02654|APOC1_HUMAN	P.APA(QGTP)[-61.6879]DVSSALDKLKEFGNTLEDKARELISRIKQSELSAKMREWFSETFQKVKEKLKIDS.	4.14E-11
T76	6960.756	6960.726	2.23E+07	sp|P02654|APOC1_HUMAN	Q.G(TP)[277.1983]DVSSALDKLKEFGNTLEDKARELISRIKQSELSAKMREWFSETFQKVKEKLKIDS.	3.79E-13
T76	6920.712	6920.917	2.47E+07	sp|P02654|APOC1_HUMAN	Q.(G)[237.3896]TPDVSSALDKLKEFGNTLEDKARELISRIKQSELSAKMREWFSETFQKVKEKLKIDS.	3.98E-13
T76	6892.667	6892.872	1.18E+08	sp|P02654|APOC1_HUMAN	A.(PAQG)[-86.8040]TPDVSSALDKLKEFGNTLEDKARELISRIKQSELSAKMREWFSETFQKVKEKLKIDS.	1.45E-15
T76	6722.635	6722.835	1.03E+07	sp|P02654|APOC1_HUMAN	A.(PAQGTP)[-256.8408]DVSSALDKLKEFGNTLEDKARELISRIKQSELSAKMREWFSETFQKVKEKLKIDS.	9.18E-09
T76	6694.605	6694.805	2.46E+07	sp|P02654|APOC1_HUMAN	A.(QGTP)[-116.7810]DVSSALDKLKEFGNTLEDKAREL	3.72E-12

					ISRIKQSELSAKMREWFSETFQKVKEKLKIDS.	
T76	6662.952	6663.147	7.38E+07	sp|P01042|KNG1_HUMAN	L.(MKRPPGFSPFR)[11.9452]SSRIGEIKEETTVSPPHTSMAPAQDEERDSGKEQGHTRRHDWGHEKQ.R	0.005982
T76	6626.511	6626.506	4.06E+07	sp|P02654|APOC1_HUMAN	G.TPDVSSALDKLKEFGNTLEDKARELISRIKQSELSAKMREWFSETFQKVKEKLKIDS.	9.35E-23
T76	6428.443	6428.405	1.24E+07	sp|P02654|APOC1_HUMAN	P.DVSSALDKLKEFGNTLEDKARELISRIKQSELSAKMREWFSETFQKVKEKLKIDS.	1.18E-17
T76	5900.695	5900.696	9.03E+07	sp|P02671|FIBA_HUMAN	K.SSSYSKQFTSSTSYNRGDSTFESKSYKMADEAGSEADHEGTHSTKRGHAKSRPV.R	0.000969
T76	5052.749	5052.899	2.13E+06	sp|P01009|A1AT_HUMAN	A.(MFLEAIPMSI)[-11.7772]PPEVKFNKPFVFLMIEQNTKSPLFMGKVVNPTQK.	1.70E-05
T76	4888.687	4888.832	1.76E+06	sp|P01011|AACT_HUMAN	L.SALVETRTIVRFNRPFLMIIVPTDTQN(I)[266.3449]FFMSKVTNPKQA.	2.57E-08
T76	4883.694	4883.694	7.02E+05	sp|P01011|AACT_HUMAN	L.SALVETRTIVRFNRPFLMIIVPTDTQNIF(FM)[261.2072]SKVTNPKQA.	2.20E-06
T76	4786.598	4786.567	9.35E+05	sp|P01009|A1AT_HUMAN	F.LEAIPMSIPPEVKFNKPFVFLMIEQNTKSPLFMGKVVNPTQK.	8.03E-08
T76	4730.615	4730.755	2.34E+06	sp|P01011|AACT_HUMAN	A.LVETRTIVRFNRPFLMIIVPTDTQNIFF(M)[266.3377]SKVTNPKQA.	2.11E-08
T76	4707.332	4707.472	7.01E+07	sp|P00738|HPT_HUMAN	L.RTEGDGVYTLNNEKQ(WINKAVGDKLPECEAVCGKPKNPAN)[-1.8608]PVQ.R	0.000706
T76	4464.453	4464.418	1.38E+06	sp|P01011|AACT_HUMAN	A.LVETRTIVRFNRPFLMIIVPTDTQNIFFMSKVTNPKQA.	1.90E-10
T76	4416.331	4416.241	5.61E+07	sp|P05155|IC1_HUMAN	R.TLLV(FEVQQ)[266.0759]PFLFVLWDQQHKFPVFMGRVYDPRA.	0.000376
T76	4415.167	4415.172	5.53E+08	sp|P02675|FIBB_HUMAN	S.QGVN(D)[-17.0341]NEEGFFSARGHRPLDKKREEAPSLRPAPPPISGGGY.R	1.23E-06
T76	4150.17	4150.166	3.45E+07	sp|P05155|IC1_HUMAN	R.TLLVFEVQQPFLFVLWDQQHKFPVFMGRVYDPRA.	1.15E-05
T76	4089.879	4089.883	1.13E+07	sp|P02671|FIBA_HUMAN	R.GDSTFESKSYKMADEAGSEADHEGTHSTKRGHAKSRPV.R	2.90E-16

T76	3952.946	3952.946	1.99E+08	sp|Q14624|ITIH4_HUMAN	R.(QAGAAGSRMNFR)[-17.0353]PGVLSSRQLGLPGPPDVPDHAAYHPF.R	4.07E-05
T76	3811.83	3811.94	3.61E+07	sp|Q14624|ITIH4_HUMAN	G.(ESRNRNVHSGSTFFK)[14.0010]YYLQGAKIPKPEASFSPR.R	3.54E-05
T76	3756.864	3756.974	1.46E+07	sp|P02765|FETUA_HUMAN	V.(SHPRKTRTVVQ)[155.9687]PSVGAAAGPVVPPCPGRIRHFKV.	0.0053
T76	3685.821	3685.931	5.32E+06	sp|P02765|FETUA_HUMAN	V.(SHPRKTR)[84.9259]TVVQPSVGAAAGPVVPPCPGRIRHFKV.	1.83E-15
T76	3653.663	3653.669	4.62E+06	sp|P00738|HPT_HUMAN	F.AVDSGNDVTDIADDGCPKPPEIAHGYVEHSVRYQ.C	1.79E-06
T76	3594.707	3594.812	1.41E+06	sp|P02765|FETUA_HUMAN	V.(SHPRKTR)[-6.1936]TVVQPSVGAAAGPVVPPCPGRIRHFKV.	0.005292
T76	3580.794	3580.899	3.45E+06	sp|P02765|FETUA_HUMAN	V.(SHPRKTR)[-20.1059]TVVQPSVGAAAGPVVPPCPGRIRHFKV.	2.08E-06
T76	3567.806	3567.911	8.83E+06	sp|P02765|FETUA_HUMAN	V.(SHPRKTR)[-33.0941]TVVQPSVGAAAGPVVPPCPGRIRHFKV.	8.34E-05
T76	3544.71	3544.815	4.62E+07	sp|P02765|FETUA_HUMAN	S.(HPRKTR)[30.8419]TVVQPSVGAAAGPVVPPCPGRIRHFKV.	0.000331
T76	3518.792	3518.897	5.55E+05	sp|P02765|FETUA_HUMAN	V.(SHPRKTRT)[-82.1085]VVQPSVGAAAGPVVPPCPGRIRHFKV.	0.000154
T76	3514.776	3514.881	5.90E+05	sp|P02765|FETUA_HUMAN	S.(HPRKTR)[0.9074]TVVQPSVGAAAGPVVPPCPGRIRHFKV.	0.002789
T76	3478.77	3478.87	1.45E+06	sp|P02765|FETUA_HUMAN	S.(HPRKTR)[-35.1033]TVVQPSVGAAAGPVVPPCPGRIRHFKV.	1.66E-08
T76	3470.74	3470.84	1.72E+05	sp|P02765|FETUA_HUMAN	S.(HPRKTRTVVQ)[-43.1329]PSVGAAAGPVVPPCPGRIRHFKV.	1.01E-07
T76	3465.782	3465.882	1.20E+08	sp|P02765|FETUA_HUMAN	V.(SHPRKTRTVVQ)[-135.1228]PSVGAAAGPVVPPCPGRIRHFKV.	7.67E-06
T76	3424.746	3424.846	3.54E+06	sp|P02765|FETUA_HUMAN	H.(PRKTR)[47.9315]TVVQPSVGAAAGPVVPPCPGRIRHFKV.	1.92E-07

T76	3394.733	3394.833	5.98E+07	sp|P02765|FETUA_HUMAN	H.(PRKTR)[17.9187]TVVQPSVGAAAGPVVPPCPGRIRHFKV.	1.93E-13
T76	3271.635	3271.635	5.90E+07	sp|Q14624|ITIH4_HUMAN	R.MNFRPGVLSSRQLGLPGPPDVPDHAAYHPF.R	9.94E-09
T76	3254.52	3254.615	1.31E+07	sp|P02671|FIBA_HUMAN	Y.(KMADEA)[266.1933]GSEADHEGTHSTKRGHAKSRPV.R	2.13E-07
T76	3238.513	3238.517	1.35E+07	sp|P02671|FIBA_HUMAN	K.SYKMADEAGSEADHEGTHSTKRGHAKSRPV.R	4.68E-17
T76	3156.614	3156.609	7.11E+06	sp|P02766|TTHY_HUMAN	N.DSGPRRYTIAALLSPYSYSTTAVVTNPKE.	9.01E-08
T76	3026.561	3026.552	4.60E+06	sp|Q14624|ITIH4_HUMAN	N.FRPGVLSSRQLGLPGPPDVPDHAAYHPF.R	1.77E-05
T76	2961.535	2961.545	3.07E+06	sp|P02765|FETUA_HUMAN	R.TVVQPSVGAAAGPVVP(PC)[223.0285]PGRIRHFKV.	6.47E-05
T76	2938.494	2938.579	1.80E+06	sp|P02765|FETUA_HUMAN	R.TVV(Q)[200.0623]PSVGAAAGPVVPPCPGRIRHFKV.	3.14E-09
T76	2924.583	2924.668	2.18E+06	sp|P02765|FETUA_HUMAN	R.TV(VQ)[186.1515]PSVGAAAGPVVPPCPGRIRHFKV.	2.21E-06
T76	2919.256	2919.341	2.23E+04	sp|P02656|APOC3_HUMAN	Y.(W)[-61.1196]STVKDKFSEFWDLDPEVRPTSAVAA.	1.54E-05
T76	2911.578	2911.663	6.25E+06	sp|P02765|FETUA_HUMAN	R.TVVQPSVGA(AA)[173.1468]GPVVPPCPGRIRHFKV.	9.06E-07
T76	2888.498	2888.498	3.16E+07	sp|P02765|FETUA_HUMAN	R.TVVQPSVGAAAGPVVP(PC)[149.9816]PGRIRHFKV.	4.08E-08
T76	2876.327	2876.412	4.35E+07	sp|P02671|FIBA_HUMAN	K.(MADE)[16.0850]AGSEADHEGTHSTKRGHAKSRPV.R	2.43E-14
T76	2872.497	2872.497	1.65E+08	sp|P02765|FETUA_HUMAN	R.TVVQPSVGAAAGPVVPP(C)[133.9805]PGRIRHFKV.	1.45E-11
T76	2866.555	2866.57	1.01E+05	sp|P02765|FETUA_HUMAN	R.TVVQPSVGAAAGPV(V)[128.0534]PPCPGRIRHFKV.	0.002213
T76	2860.322	2860.327	4.22E+07	sp|P02671|FIBA_HUMAN	K.MADEAGSEADHEGTHSTKRGHAKSRPV.R	3.23E-18
T76	2857.509	2857.514	2.34E+07	sp|P02765|FETUA_HUMAN	R.TVVQPSVGAAAGPVVPP(C)[118.9976]PGRIRHFKV.	9.93E-10

T76	2837.547	2837.547	1.06E+07	sp|P02765|FETUA_HUMAN	R.TVVQPSVGAAAGPV(V)[99.0300]PPCPGRIRHFKV.	1.59E-06
T76	2825.544	2825.624	1.63E+06	sp|P02765|FETUA_HUMAN	R.TVV(Q)[87.1070]PSVGAAAGPVVPPCPGRIRHFKV.	0.000144
T76	2811.566	2811.551	6.47E+05	sp|P02765|FETUA_HUMAN	R.TVVQPSVGAA(A)[73.0344]GPVVPPCPGRIRHFKV.	9.04E-08
T76	2809.539	2809.549	7.68E+07	sp|P02765|FETUA_HUMAN	R.TVVQPSVGAAAGPVVP(PC)[71.0328]PGRIRHFKV.	9.15E-09
T76	2794.541	2794.521	4.05E+06	sp|P02765|FETUA_HUMAN	R.TV(VQ)[56.0048]PSVGAAAGPVVPPCPGRIRHFKV.	0.001477
T76	2786.501	2786.581	9.46E+05	sp|P02765|FETUA_HUMAN	R.TVVQPSVG(A)[48.0645]AAGPVVPPCPGRIRHFKV.	6.66E-06
T76	2738.511	2738.517	4.75E+07	sp|P02765|FETUA_HUMAN	R.TVVQPSVGAAAGPVVPPCPGRIRHFKV.	1.01E-12
T76	2658.255	2658.249	2.13E+08	sp|P02671|FIBA_HUMAN	A.DEAGSEADHEGTHSTKRGHAKSRPV.R	1.76E-17
T76	2581.332	2581.333	9.40E+06	sp|Q14624|ITIH4_HUMAN	R.NVHSGSTFFKYYLQGAKIPKPEA.S	4.34E-05
T76	2550.65	2550.725	1.09E+04	sp|P02766|TTHY_HUMAN	R.(YTIAALLSPYSYS)[62.4517]TTAVVTNPKE.	0.002159
T76	2543.214	2543.223	8.15E+06	sp|P02671|FIBA_HUMAN	D.EAGSEADHEGTHSTKRGHAKSRPV.R	2.42E-08
T76	2357.152	2357.155	2.90E+06	sp|Q14624|ITIH4_HUMAN	L.SSRQLGLPGPPDVPDHAAYHPF.R	0.000735
T76	2343.142	2343.143	1.02E+07	sp|P02671|FIBA_HUMAN	A.GSEADHEGTHSTKRGHAKSRPV.R	9.20E-13
T76	2270.121	2270.123	6.50E+06	sp|Q14624|ITIH4_HUMAN	S.SRQLGLPGPPDVPDHAAYHPF.R	0.002922
T89	14090.18	14090.3	4.63E+07	sp|P02766|TTHY_HUMAN	E.AGPTGTGESKCPLMVKVLDAVRGSPAINVAVHVFRKAADDTWEPFASGKTSESGELHGLTTEEEFVEGIYKVEID(TKSYWKALGISPFHEHAE)[266.3733]VVFTANDSGPRRYTIAALLSPYSYSTTAVVTNPKE.	0.000295
T89	13885.92	13885.91	5.36E+07	sp|P02766|TTHY_HUMAN	E.AGPTGTGESKCPLMVKV(LDAVR)[61.9820]GSPAINVAVHVFRKAADDTWEPFASGKTSESGELHGLTTEEEFVEGIYKVEIDTKSYWKALGISPFHEHAEVVFTANDSGPRRYTIAALLSPYSYSTTAVVTNPKE.	2.78E-07
T89	13824.03	13823.93	1.56E+07	sp|P02766|TTHY_HUMAN	E.AGPTGTGESKCPLMVKVLDAVRGSPAINVAVHVFRKAADDTWEPFASGKTSESGELHGLTTEEEFVEGIYKVEIDTKSYWKALGISPFHEHAEVVFTANDSGPRRYTIAALLSPYSYSTTAVVTNPKE.	0.009805

T89	13707.02	13706.9	1.71E+07	sp|P02766|TTHY_HUMAN	T.GESKCPLMVKVLDAVRGSPA(INVAVHVFRKAADDT)[367.2033]WEPFASGKTSESGELHGLTTEEEFVEGIYKVEIDTKSYWKALGISPFHEHAEVVFTANDSGPRRYTIAALLSPYSYSTTAVVTNPKE.	0.001111
T89	10422.67	10422.98	8.20E+06	sp|P0CG47|UBB_HUMAN	L.(SDYNIQKESTLHLVLRLRGGMQI)[-416.8686]FVKTLTGKTITLEVEPSDTIENVKAKIQDKEGIPPDQQRLIFAGKQLEDGRTLSDYNIQKESTLHLVLRLRGG.M	0.001738
T89	10173.52	10173.83	5.02E+06	sp|P0CG47|UBB_HUMAN	Q.KESTLHLVLRLRGGM(Q)[54.2870]IFVKTLTGKTITLEVEPSDTIENVKAKIQDKEGIPPDQQRLIFAGKQLEDGRTLSDYNIQKESTLHLVLRLRGG.C	2.57E-07
T89	10156.54	10156.53	3.84E+07	sp|P0CG47|UBB_HUMAN	K.(ESTLHLVLRLRGG)[165.0836]MQIFVKTLTGKTITLEVEPSDTIENVKAKIQDKEGIPPDQQRLIFAGKQLEDGRTLSDYNIQKESTLHLVLRLRGG.C	1.13E-11
T89	9906.391	9906.316	8.20E+06	sp|P0CG47|UBB_HUMAN	K.ESTLHLVLRLRG(GMQ)[-85.1318]IFVKTLTGKTITLEVEPSDTIENVKAKIQDKEGIPPDQQRLIFAGKQLEDGRTLSDYNIQKESTLHLVLRLRGG.C	3.11E-09
T89	9890.345	9890.305	6.07E+07	sp|P0CG47|UBB_HUMAN	K.ESTLHLVLRLRGG(M)[-101.1430]QIFVKTLTGKTITLEVEPSDTIENVKAKIQDKEGIPPDQQRLIFAGKQLEDGRTLSDYNIQKESTLHLVLRLRGG.M	4.39E-13
T89	9640.203	9640.488	1.48E+07	sp|P0CG47|UBB_HUMAN	L.(HLVLRLRGG)[79.2464]MQIFVKTLTGKTITLEVEPSDTIENVKAKIQDKEGIPPDQQRLIFAGKQLEDGRTLSDYNIQKESTLHLVLRLRGG.C	7.25E-08
T89	9624.234	9624.519	1.24E+08	sp|P0CG48|UBC_HUMAN	L.(HLVLRLRGG)[63.2774]MQIFVKTLTGKTITLEVEPSDTIENVKAKIQDKEGIPPDQQRLIFAGKQLEDGRTLSDYNIQKESTLHLVLRLRGG.V	1.46E-06
T89	9624.207	9624.167	1.24E+08	sp|P0CG47|UBB_HUMAN	L.(HLVLRLRGG)[62.9259]MQIFVKTLTGKTITLEVEPSDTIENVKAKIQDKEGIPPDQQRL	7.71E-13

					IFAGKQLEDGRTLSDYNIQKESTLHLVLRL RGG.C	
T89	9469.805	9470.085	2.94E+06	sp|P02655|APOC2_HUMAN	G.(FEVQGTQQPQQDEMPSPTFLTQVKESLS SYWESAKTAAQNLYEKTYLPAVDEKLRD LYSKSTAAMST)[0.4476]YTGIFTDQVLSVL KGEE.	5.29E-07
T89	9415.517	9415.632	3.76E+07	sp|P02656|APOC3_HUMAN	A.(LLASARA)[-25.9986]SEAEDASLLSFMQGYMKHATKTA KDALSSVQESQVAQQARGWVTDGFSSLK DYWSTVKDKFSEFWDLDPEVRPTSAVAA.	2.47E-06
T89	9374.156	9374.436	1.87E+07	sp|P0CG47|UBB_HUMAN	L.(VLRLRGG)[63.3372]MQIFVKTLTGKTIT LEVEPSDTIENVKAKIQDKEGIPPDQQRLIF AGKQLEDGRTLSDYNIQKESTLHLVLRLR GG.C	5.51E-09
T89	9358.011	9358.061	1.44E+08	sp|P0CG47|UBB_HUMAN	L.(VLRLRGG)[46.9623]MQIFVKTLTGKTIT LEVEPSDTIENVKAKIQDKEGIPPDQQRLIF AGKQLEDGRTLSDYNIQKESTLHLVLRLR GG.M	7.26E-14
T89	9175.634	9175.909	4.97E+06	sp|P02655|APOC2_HUMAN	G.TQQPQQDEM(PSPTFLTQVKESLSSYWE SAKTAAQNLYEKTYLPAVDEKLRDLYSKS TAAMST)[266.5305]YTGIFTDQVLSVLKGE E.	6.35E-09
T89	9107.925	9107.885	1.63E+07	sp|P0CG47|UBB_HUMAN	R.(LRGG)[165.0405]MQIFVKTLTGKTITLEV EPSDTIENVKAKIQDKEGIPPDQQRLIFAGK QLEDGRTLSDYNIQKESTLHLVLRLRGG.C	1.05E-10
T89	9091.917	9092.187	1.17E+08	sp|P0CG47|UBB_HUMAN	.((M)[Acetyl]QIFVKTLTGKTITLEVE)[490.56 02]PSDTIENVKAKIQDKEGIPPDQQRLIFAG KQLEDGRTLSDYNIQKESTLHLVLRLRGG. M	5.37E-24
T89	8909.45	8909.378	4.45E+06	sp|P02655|APOC2_HUMAN	G.TQQPQQDEMPSPTFLTQVKESLSSYWES AKTAAQNLYEKTYLPAVDEKLRDLYSKST AAMSTYTGIFTDQVLSVLKGEE.	5.22E-05
T89	8861.469	8861.404	3.97E+07	sp|P02652|APOA2_HUMAN	V.(RRQA)[-153.2367]KEPCVESLVSQYFQTVTDYGKDL MEKVKSPELQAEAKSYFEKSKEQLTPLIKK AGTELVNFLSYFVELGTQPATQ.	2.21E-10

T89	8840.777	8840.847	1.28E+07	sp|P0CG47|UBB_HUMAN	.(M)[281.2302]QIFVKTLTGKTITLEVEPSDTIENVKAKIQDKEGIPPDQQRLIFAGKQLEDGRTLSDYNIQKESTLHLVLRLRGG.M	1.52E-11
T89	8835.457	8835.382	3.49E+07	sp|P02652|APOA2_HUMAN	R.(RQAKEPCV)[-23.1571]ESLVSQYFQTVTDYGKDLMEKVKSPELQAEAKSYFEKSKEQLTPLIKKAGTELVNFLSYFVELGTQPATQ.	1.20E-16
T89	8826.766	8827.026	7.62E+07	sp|P62979|RS27A_HUMAN	.MQI(FVKTLTGKTITLEVEPSDTIENVKAKIQDKEGIPPDQQRLIFAGKQLED)[267.4095]GRTLSDYNIQKESTLHLVLRLRGG.A	1.90E-05
T89	8824.771	8824.701	7.62E+07	sp|P0CG47|UBB_HUMAN	.MQIFVKTLTGKTITLEV(E)[265.0843]PSDTIENVKAKIQDKEGIPPDQQRLIFAGKQLEDGRTLSDYNIQKESTLHLVLRLRGG.M	4.48E-18
T89	8819.398	8819.393	3.83E+08	sp|P02652|APOA2_HUMAN	R.(RQAKEPC)[-39.1466]VESLVSQYFQTVTDYGKDLMEKVKSPELQAEAKSYFEKSKEQLTPLIKKAGTELVNFLSYFVELGTQPATQ.	1.74E-25
T89	8758.289	8759.218	1.55E+06	sp|P02656|APOC3_HUMAN	A.SEAEDASLLSFMQGYMKHATKTAKDALSSVQESQVAQQARGWVTDGFSSLKDYWSTVKDKFSEFWDLDPEVRPTSAVAA.	0.003794
T89	8756.457	8756.442	2.98E+08	sp|P02652|APOA2_HUMAN	R.(QAKEPC)[54.0032]VESLVSQYFQTVTDYGKDLMEKVKSPELQAEAKSYFEKSKEQLTPLIKKAGTELVNFLSYFVELGTQPATQ.	1.93E-24
T89	8733.413	8733.343	1.09E+07	sp|P02652|APOA2_HUMAN	R.(QAKEPCV)[158.9629]ESLVSQYFQTVTDYGKDLMEKVKSPELQAEAKSYFEKSKEQLTPLIKKAGTELVNFLSYFVELGTQPAT.Q	4.18E-06
T89	8691.359	8691.334	1.47E+08	sp|P02652|APOA2_HUMAN	R.(QAKEPCV)[116.9542]ESLVSQYFQTVTDYGKDLMEKVKSPELQAEAKSYFEKSKEQLTPLIKKAGTELVNFLSYFVELGTQPAT.Q	6.85E-10
T89	8685.435	8685.405	4.41E+06	sp|P02652|APOA2_HUMAN	Q.(AK)[111.0256]EPCVESLVSQYFQTVTDYGKDLMEKVKSPELQAEAKSYFEKSKEQLTPLIKKAGTELVNFLSYFVELGTQPATQ.	8.08E-07
T89	8651.499	8651.419	1.94E+07	sp|P02652|APOA2_HUMAN	K.(EPCV)[276.1713]ESLVSQYFQTVTDYGKDLMEKVKSPELQAEAKSYFEKSKEQLTPLIKKAGTELVNFLSYFVELGTQPATQ.	3.21E-16

T89	8628.417	8628.387	1.29E+08	sp|P02652|APOA2_HUMAN	Q.(AKE)[182.0655]PCVESLVSQYFQTVTDYGKDLMEKVKSPELQAEAKSYFEKSKEQLTPLIKKAGTELVNFLSYFVELGTQPAT.Q	5.69E-14
T89	8575.609	8575.609	5.05E+06	sp|P0CG47|UBB_HUMAN	.(MQ)[15.9924]IFVKTLTGKTITLEVEPSDTIENVKAKIQDKEGIPPDQQRLIFAGKQLEDGRTLSDYNIQKESTLHLVLRLRGG.M	8.32E-15
T89	8558.589	8559.617	2.66E+07	sp|P0CG47|UBB_HUMAN	.MQIFVKTLTGKTITLEVEPSDTIENVKAKIQDKEGIPPDQQRLIFAGKQLEDGRTLSDYNIQKESTLHLVLRLRGG.M	2.22E-21
T89	8557.433	8557.353	7.42E+06	sp|P02652|APOA2_HUMAN	Q.(AK)[111.0317]EPCVESLVSQYFQTVTDYGKDLMEKVKSPELQAEAKSYFEKSKEQLTPLIKKAGTELVNFLSYFVELGTQPAT.Q	0.000214
T89	7747.227	7747.457	3.71E+07	sp|P02654|APOC1_HUMAN	L.(SIVLEGPAPAQG)[1.3587]TPDVSSALDKLKEFGNTLEDKARELISRIKQSELSAKMREWFSETFQKVKEKLKIDS.	3.98E-07
T89	7719.176	7719.406	4.36E+07	sp|P02654|APOC1_HUMAN	L.(SIVLEGPAPAQG)[-26.6925]TPDVSSALDKLKEFGNTLEDKARELISRIKQSELSAKMREWFSETFQKVKEKLKIDS.	1.01E-07
T89	7549.12	7549.345	1.11E+07	sp|P02654|APOC1_HUMAN	I.(VLEGPAPAQGTP)[3.3627]DVSSALDKLKEFGNTLEDKARELISRIKQSELSAKMREWFSETFQKVKEKLKIDS.	1.58E-08
T89	7521.1	7521.045	1.14E+07	sp|P02654|APOC1_HUMAN	I.(VLEGPAPAQGTP)[-24.9373]DVSSALDKLKEFGNTLEDKARELISRIKQSELSAKMREWFSETFQKVKEKLKIDS.	1.14E-07
T89	7481.033	7481.028	7.05E+07	sp|P02654|APOC1_HUMAN	L.(EGPAPAQG)[147.1988]TPDVSSALDKLKEFGNTLEDKARELISRIKQSELSAKMREWFSETFQKVKEKLKIDS.	1.15E-15
T89	7452.999	7453.219	1.13E+08	sp|P02654|APOC1_HUMAN	V.(LEGPAPAQG)[6.3050]TPDVSSALDKLKEFGNTLEDKARELISRIKQSELSAKMREWFSETFQKVKEKLKIDS.	5.46E-14
T89	7424.968	7425.013	5.72E+07	sp|P02654|APOC1_HUMAN	V.(LEGPAPAQG)[-21.9009]TPDVSSALDKLKEFGNTLEDKARELISRIKQSELSAKMREWFSETFQKVKEKLKIDS.	5.20E-09

T89	7282.964	7282.994	1.59E+07	sp|P02654|APOC1_HUMAN	L.EGP(APAQGTP)[-50.8357]DVSSALDKLKEFGNTLEDKARELISRIKQSELSAKMREWFSETFQKVKEKLKIDS.	1.06E-08
T89	7254.981	7254.876	2.56E+07	sp|P02654|APOC1_HUMAN	E.(GPAPAQGTP)[50.0889]DVSSALDKLKEFGNTLEDKARELISRIKQSELSAKMREWFSETFQKVKEKLKIDS.	2.49E-10
T89	7214.868	7215.083	5.28E+07	sp|P02654|APOC1_HUMAN	V.(LEGPAPAQG)[-231.8303]TPDVSSALDKLKEFGNTLEDKARELISRIKQSELSAKMREWFSETFQKVKEKLKIDS.	1.68E-14
T89	7186.828	7186.948	1.77E+08	sp|P02654|APOC1_HUMAN	E.(GPAPAQG)[-17.8390]TPDVSSALDKLKEFGNTLEDKARELISRIKQSELSAKMREWFSETFQKVKEKLKIDS.	8.45E-17
T89	7158.879	7159.089	1.59E+08	sp|P02654|APOC1_HUMAN	G.(PAPAQG)[11.3232]TPDVSSALDKLKEFGNTLEDKARELISRIKQSELSAKMREWFSETFQKVKEKLKIDS.	3.57E-15
T89	7016.832	7016.787	9.78E+06	sp|P02654|APOC1_HUMAN	P.(APAQGTP)[-33.9261]DVSSALDKLKEFGNTLEDKARELISRIKQSELSAKMREWFSETFQKVKEKLKIDS.	0.001403
T89	6988.793	6988.998	3.65E+07	sp|P02654|APOC1_HUMAN	E.(GPAPAQGTP)[-215.7895]DVSSALDKLKEFGNTLEDKARELISRIKQSELSAKMREWFSETFQKVKEKLKIDS.	6.20E-15
T89	6960.752	6960.957	2.55E+07	sp|P02654|APOC1_HUMAN	E.(GPAPAQGTP)[-243.8300]DVSSALDKLKEFGNTLEDKARELISRIKQSELSAKMREWFSETFQKVKEKLKIDS.	2.16E-08
T89	6920.745	6920.95	1.28E+08	sp|P02654|APOC1_HUMAN	Q.(G)[237.4232]TPDVSSALDKLKEFGNTLEDKARELISRIKQSELSAKMREWFSETFQKVKEKLKIDS.	1.66E-14
T89	6892.658	6892.863	2.09E+08	sp|P02654|APOC1_HUMAN	Q.(G)[209.3358]TPDVSSALDKLKEFGNTLEDKARELISRIKQSELSAKMREWFSETFQKVKEKLKIDS.	1.73E-13

T89	6753.193	6753.168	6.05E+07	sp|P01834|IGKC_HUMAN	N.ALQSGNSQESVTEQDSKDSTYSLSSTLTLSKADYEKHKV(YACEVTHQGLSSPVTKSFNRGEC)[-2.0199].	0.002085
T89	6722.648	6722.848	2.09E+07	sp|P02654|APOC1_HUMAN	A.(QGTP)[-88.7383]DVSSALDKLKEFGNTLEDKARELISRIKQSELSAKMREWFSETFQKVKEKLKIDS.	8.08E-09
T89	6694.595	6694.795	3.39E+07	sp|P02654|APOC1_HUMAN	Q.(GTP)[11.2681]DVSSALDKLKEFGNTLEDKARELISRIKQSELSAKMREWFSETFQKVKEKLKIDS.	3.19E-11
T89	6678.971	6679.171	4.44E+07	sp|P01042|KNG1_HUMAN	R.SSRIGEIKEETTVSPPHTSMAPAQDEERDSGKEQGHTRRHDWGHEKQ(RKHNLGHGHKH)[26.9590].E	0.007439
T89	6662.952	6663.082	4.81E+07	sp|P01042|KNG1_HUMAN	L.(MKRPPGFSPFR)[11.8803]SSRIGEIKEETTVSPPHTSMAPAQDEERDSGKEQGHTRRHDWGHEKQ.R	1.19E-07
T89	6626.565	6626.506	1.44E+08	sp|P02654|APOC1_HUMAN	G.TPDVSSALDKLKEFGNTLEDKARELISRIKQSELSAKMREWFSETFQKVKEKLKIDS.	2.45E-23
T89	6440.983	6440.973	1.22E+08	sp|P01834|IGKC_HUMAN	Q.SGNSQESVTEQDSKDSTYSLSSTLTLSKADYEKHKVY(ACEVTHQGLSSPVTKSFNRGEC)[-2.0353].	0.000218
T89	6428.469	6428.405	1.64E+07	sp|P02654|APOC1_HUMAN	P.DVSSALDKLKEFGNTLEDKARELISRIKQSELSAKMREWFSETFQKVKEKLKIDS.	2.43E-14
T89	6354.006	6353.936	5.69E+07	sp|P01834|IGKC_HUMAN	S.GNSQESVTEQDSKDSTYSLSSTLTLSKADYEKHKV(YACEVTHQGLSSPVTKSFNRGEC)[-2.0406].	1.21E-06
T89	6196.924	6196.899	1.34E+08	sp|P01834|IGKC_HUMAN	N.SQESVTEQDSKDSTYSLSSTLTLSKADYEKHK(VYACEVTHQGLSS)[11.9873]PVTKSFNRGEC.	6.65E-14
T89	6182.934	6182.889	3.71E+08	sp|P01834|IGKC_HUMAN	N.SQESVTEQDSKDSTYSLSSTLTLSKADYEKHKVY(ACEVTHQGLSSPVTKSFNRGEC)[-2.0224].	9.09E-16
T89	5916.712	5916.887	1.08E+08	sp|P02671|FIBA_HUMAN	K.(SS)[16.1911]SYSKQFTSSTSYNRGDSTFESKSYKMADEAGSEADHEGTHSTKRGHAKSRPV.R	1.07E-10

T89	5900.72	5900.696	1.14E+08	sp|P02671|FIBA_HUMAN	K.SSSYSKQFTSSTSYNRGDSTFESKSYKMADEAGSEADHEGTHSTKRGHAKSRPV.R	5.01E-26
T89	4960.487	4960.486	1.45E+07	sp|P62328|TYB4_HUMAN	M.(S)[Acetyl]DKPDMAEIEKFDKSKLKKTETQEKNPLPSKETIEQEKQAGES.	2.15E-08
T89	4888.702	4888.847	1.11E+06	sp|P01011|AACT_HUMAN	L.SALVETRTIVRFNRPFLMIIVPTDTQNIF(FM)[266.3599]SKVTNPKQA.	2.52E-07
T89	4815.67	4815.623	3.61E+06	sp|P81605|DCD_HUMAN	R.SSLLEKGLDGAKKAVGGLGKLGKDAVEDLESVGKGAVHDVKDVLDSVL.	1.91E-20
T89	4787.223	4787.271	2.05E+07	sp|A0M8Q6|IGLC7_HUMAN	N.NKYAASSYLSLTPEQWKSHRSYSCRVTHEGSTVEKTVAPAECS.	0.000516
T89	4721.396	4721.536	2.45E+04	sp|P02655|APOC2_HUMAN	Y.(EKTYLPAVDEKLRDLYSKSTAAMSTY)[25.1529]TGIFTDQVLSVLKGEE.	0.00035
T89	4707.353	4707.493	3.17E+07	sp|P00738|HPT_HUMAN	L.RTEGDGVYTLNNEKQWINKAVGDKL(PECEAVCGKPKNPAN)[-1.8403]PVQ.R	2.27E-07
T89	4686.667	4686.807	6.86E+05	sp|P05154|IPSP_HUMAN	T.(GTIFTFR)[-23.7778]SARLNSQRLVFNRPFLMFIVDNNILFLGKVNRP.	1.82E-05
T89	4416.374	4416.504	5.57E+07	sp|P05155|IC1_HUMAN	R.TLLVFE(VQQ)[266.3382]PFLFVLWDQQHKFPVFMGRVYDPRA.	9.66E-05
T89	4416.354	4416.484	5.57E+07	sp|P05154|IPSP_HUMAN	I.(FTFR)[-22.9478]SARLNSQRLVFNRPFLMFIVDNNILFLGKVNRP.	0.005728
T89	4415.184	4415.174	3.58E+08	sp|P02675|FIBB_HUMAN	K.SQGVN(D)[-104.0644]NEEGFFSARGHRPLDKKREEAPSLRPAPPPISGGGY.R	1.04E-07
T89	4290.085	4290.17	4.39E+06	sp|P02671|FIBA_HUMAN	N.(RGDSTFESKSYKM)[44.1855]ADEAGSEADHEGTHSTKRGHAKSRPV.R	0.00477
T89	4239.94	4240.065	1.73E+05	sp|P02765|FETUA_HUMAN	S.LGSPSGEVSHPRK(TR)[-87.2952]TVVQPSVGAAAGPVVPPCPGRIRHFKV.	0.007317
T89	4154.34	4154.46	2.61E+06	sp|P05154|IPSP_HUMAN	R.SARLNSQRLVFNRPFLMFI(V)[266.3136]DNNILFLGKVNRP.	6.89E-09
T89	4150.203	4150.323	5.65E+07	sp|P05154|IPSP_HUMAN	R.SARLNSQRLVFNRPFLMFIVDNN(I)[262.1772]LFLGKVNRP.	1.11E-08
T89	4150.195	4150.166	5.65E+07	sp|P05155|IC1_HUMAN	R.TLLVFEVQQPFLFVLWDQQHKFPVFMGRVYDPRA.	2.07E-06

T89	4106.871	4106.991	3.19E+05	sp|P02671|FIBA_HUMAN	R.(GDSTFESKSYKMADE)[17.1073]AGSEADHEGTHSTKRGHAKSRPV.R	3.93E-09
T89	4089.885	4089.883	2.16E+07	sp|P02671|FIBA_HUMAN	R.GDSTFESKSYKMADEAGSEADHEGTHSTKRGHAKSRPV.R	1.76E-11
T89	4048.893	4049.013	3.78E+05	sp|P02671|FIBA_HUMAN	G.(DSTFESKSY)[16.1505]KMADEAGSEADHEGTHSTKRGHAKSRPV.R	2.66E-06
T89	3968.976	3968.941	1.27E+08	sp|Q14624|ITIH4_HUMAN	R.(QAGAAGSRMNFR)[-1.0397]PGVLSSRQLGLPGPPDVPDHAAYHPF.R	0.00215
T89	3952.977	3952.947	1.03E+08	sp|Q14624|ITIH4_HUMAN	R.(QAGAAGSRMNFR)[-17.0336]PGVLSSRQLGLPGPPDVPDHAAYHPF.R	3.82E-05
T89	3888.184	3888.146	3.84E+06	sp|P05154|IPSP_HUMAN	R.SARLNSQRLVFNRPFLMFIVDNNILFLGKVNRP.	3.60E-12
T89	3811.858	3811.968	3.39E+07	sp|Q14624|ITIH4_HUMAN	G.(ESRNRNVH)[14.0293]SGSTFFKYYLQGAKIPKPEASFSPR.R	4.28E-05
T89	3685.847	3685.957	7.34E+06	sp|P02765|FETUA_HUMAN	V.(SHPRKTR)[84.9520]TVVQPSVGAAAGPVVPPCPGRIRHFKV.	6.69E-07
T89	3652.698	3652.683	1.12E+07	sp|P00738|HPT_HUMAN	F.AVDSGNDVTDIADDGCPKPPEIAHGYVEH(SVRYQC)[-103.9956].K	7.44E-05
T89	3641.487	3641.592	6.91E+05	sp|P02766|TTHY_HUMAN	V.(VFTANDSGPRRYTIAALLSPYSY)[-47.2821]STTAVVTNPKE.	0.001355
T89	3580.808	3580.913	5.08E+06	sp|P02765|FETUA_HUMAN	V.(SHPRKTR)[-20.0923]TVVQPSVGAAAGPVVPPCPGRIRHFKV.	0.002072
T89	3544.724	3544.829	5.04E+07	sp|P02671|FIBA_HUMAN	F.(ESKSYKMA)[-37.8582]DEAGSEADHEGTHSTKRGHAKSRPV.R	0.002288
T89	3544.716	3544.821	5.04E+07	sp|P02765|FETUA_HUMAN	S.(HPRKTRTVVQ)[30.8474]PSVGAAAGPVVPPCPGRIRHFKV.	0.009707
T89	3522.8	3522.905	1.34E+06	sp|P02765|FETUA_HUMAN	V.(SHPRKTR)[-78.1007]TVVQPSVGAAAGPVVPPCPGRIRHFKV.	2.94E-05
T89	3513.749	3513.854	1.74E+07	sp|P02765|FETUA_HUMAN	S.(HPRKTR)[-0.1193]TVVQPSVGAAAGPVVPPCPGRIRHFKV.	0.001137

T89	3481.764	3481.864	1.48E+05	sp|P02765|FETUA_HUMAN	S.(HPRKTRTVVQ)[-32.1089]PSVGAAAGPVVPPCPGRIRHFKV.	6.06E-06
T89	3394.747	3394.847	5.33E+07	sp|P02765|FETUA_HUMAN	H.(PRKTR)[17.9324]TVVQPSVGAAAGPVVPPCPGRIRHFKV.	2.48E-10
T89	3387.708	3387.808	1.04E+06	sp|P02765|FETUA_HUMAN	H.(PRKTRTVVQ)[10.8941]PSVGAAAGPVVPPCPGRIRHFKV.	9.00E-08
T89	3271.659	3271.635	3.59E+07	sp|Q14624|ITIH4_HUMAN	R.MNFRPGVLSSRQLGLPGPPDVPDHAAYHPF.R	8.61E-09
T89	3254.507	3254.602	1.70E+07	sp|P02671|FIBA_HUMAN	Y.(KMADE)[266.1804]AGSEADHEGTHSTKRGHAKSRPV.R	9.91E-09
T89	3238.512	3238.517	1.14E+07	sp|P02671|FIBA_HUMAN	K.SYKMADEAGSEADHEGTHSTKRGHAKSRPV.R	3.67E-09
T89	3156.638	3156.609	9.54E+06	sp|P02766|TTHY_HUMAN	N.DSGPRRYTIAALLSPYSYSTTAVVTNPKE.	4.07E-08
T89	3155.614	3155.619	1.08E+07	sp|Q14624|ITIH4_HUMAN	R.NVHSGSTFFKYYLQGAKIPKPEASFSPR.R	0.001123
T89	3009.483	3009.573	6.53E+04	sp|P02656|APOC3_HUMAN	D.YWSTVKDKFSE(F)[-133.9513]WDLDPEVRPTSAVAA.	0.000325
T89	2914.521	2914.516	2.28E+07	sp|P02765|FETUA_HUMAN	R.TVVQPSVGAAAGPVV(PPCPGRIRHFKV)[175.9998].	0.001579
T89	2888.485	2888.495	1.87E+07	sp|P02765|FETUA_HUMAN	R.TVVQPSVGAAAGPVVP(PC)[149.9783]PGRIRHFKV.	8.88E-09
T89	2876.316	2876.401	1.38E+07	sp|P02671|FIBA_HUMAN	K.(MADE)[16.0736]AGSEADHEGTHSTKRGHAKSRPV.R	5.40E-13
T89	2872.508	2872.593	4.53E+07	sp|P02671|FIBA_HUMAN	K.(MADE)[12.2663]AGSEADHEGTHSTKRGHAKSRPV.R	0.002386
T89	2872.496	2872.501	4.53E+07	sp|P02765|FETUA_HUMAN	R.TVVQPSVGAAAGPVVP(PCPGRIR)[133.9842]HFKV.	5.45E-09
T89	2860.33	2860.327	3.26E+07	sp|P02671|FIBA_HUMAN	K.MADEAGSEADHEGTHSTKRGHAKSRPV.R	2.22E-19
T89	2837.547	2837.547	8.16E+06	sp|P02765|FETUA_HUMAN	R.TVVQPSVGAAAGPV(V)[99.0301]PPCPGRIRHFKV.	1.96E-06
T89	2825.534	2825.554	3.57E+05	sp|P02765|FETUA_HUMAN	R.TVVQPSVGAAAGPV(V)[87.0378]PPCPGRIRHFKV.	0.009335
T89	2809.55	2809.545	3.39E+07	sp|P02765|FETUA_HUMAN	R.TVVQPSVGAAAGPVVP(PC)[71.0280]PGRIRHFKV.	7.95E-10

T89	2738.52	2738.517	1.34E+07	sp|P02765|FETUA_HUMAN	R.TVVQPSVGAAAGPVVPPCPGRIRHFKV.	2.28E-11
T89	2723.383	2723.382	1.74E+07	sp|Q14624|ITIH4_HUMAN	R.PGVLSSRQLGLPGPPDVPDHAAYHPF.R	8.23E-05
T89	2692.537	2692.527	8.86E+05	sp|P02765|FETUA_HUMAN	R.TVVQPSVGAAAGPVVP(PC)[-45.9894]PGRIRHFKV.	2.48E-07
T89	2658.264	2658.249	1.82E+08	sp|P02671|FIBA_HUMAN	A.DEAGSEADHEGTHSTKRGHAKSRPV.R	1.30E-15
T89	2594.265	2594.259	8.85E+06	sp|P02671|FIBA_HUMAN	T.ADSGEGDFLAEGGGVRGPRVVERHQ.S	1.00E-07
T89	2559.181	2559.181	4.41E+06	sp|P02671|FIBA_HUMAN	A.DEAGSEADHEGTHSTKRGHAKSRP.V	2.15E-07
T89	2543.222	2543.223	3.80E+06	sp|P02671|FIBA_HUMAN	D.EAGSEADHEGTHSTKRGHAKSRPV.R	2.21E-06
T89	2421.133	2421.203	1.44E+07	sp|P02671|FIBA_HUMAN	E.(A)[7.0230]GSEADHEGTHSTKRGHAKSRPV.R	9.23E-08
T89	2377.212	2377.203	2.37E+07	sp|P0C0L4|CO4A_HUMAN	K.DDPDAPLQPVTPLQLFEGRRN.R	0.009695
T89	2357.16	2357.155	6.86E+06	sp|Q14624|ITIH4_HUMAN	L.SSRQLGLPGPPDVPDHAAYHPF.R	0.005534
T89	2343.138	2343.143	4.54E+06	sp|P02671|FIBA_HUMAN	A.GSEADHEGTHSTKRGHAKSRPV.R	7.70E-11
T89	2335.139	2335.209	2.69E+06	sp|P02671|FIBA_HUMAN	S.(EADH)[136.1192]EGTHSTKRGHAKSRPV.R	0.001003
T89	2270.12	2270.123	1.56E+07	sp|Q14624|ITIH4_HUMAN	S.SRQLGLPGPPDVPDHAAYHPF.R	6.15E-05
T89	2026.986	2026.99	5.87E+06	sp|Q14624|ITIH4_HUMAN	R.QLGLPGPPDVPDHAAYHPF.R	0.002132
T89	1031.429	1031.459	3.66E+03	sp|P02766|TTHY_HUMAN	S.(T)[-27.1015]TAVVTNPKE.	0.000169